POLITECNICO DI TORINO

Master of Science course
in *Automotive Engineering*

Thesis

The impact of vehicle auxiliary systems on battery electric vehicle design and performance

Mentors
Prof. Ezio Spessa
Prof. Daniela Misul
Prof. Roberto Finesso
Prof. Vittorio Ravello

Company mentors
Ing. Alessandro Piu
Ing. Diego Caporali

Candidate
Prisco Ferrentino
S232076

A.A.2017/2018

CONTENTS

ABSTRACT

This thesis comes up as collaboration between the Politecnico di Torino and FCA-CRF, in order to analyze how the real-world conditions impact on a Battery Electric Vehicle (BEV) design and performance. The vehicle considered is an A-segment vehicle. In this abstract the logical thread behind the work is shown.

Internal combustion engines (ICE) have dominated the scene of propulsion systems for passenger vehicles for almost all the twentieth century. Indeed the ICE is able to guarantee good performances, versatility, controllability, and refilling simplicity. All those properties improved as the engine technologies got better: nowadays the ICE has reached a high degree of maturity, with possibility of improvement limited to few areas.

With the rise of the new century, environmental conscience grew stronger and ICEs were acknowledged to be highly pollutant (especially in terms of particulate matter, NOx and smog). Also, they are a major CO_2 emitter, and, therefore, one of the causes of global warming. Governments of countries all around the world enforced laws in order to limit pollution and CO_2 emission. To top that off, oil resources are believed to be running out by the end of the century.

In these conditions, fleet electrification came out as one of the possible solutions. Fleet electrification comprehends both hybrid-electric architectures, which means ICE and electric powertrains working together, and full-electric architectures, where only the electric propulsion system is present. Hybrid-electric vehicles are a short-term partial solution to the problems. Instead full-electric vehicles, and in particular BEVs, are the only complete solution in the long-term.

BEVs have the simplest propulsion system, made by an electrochemical storage system (battery), a power electronics device (inverter), an electric motor and by the rest of the transmission which, usually, doesn't even need a gearbox. BEVs can guarantee zero tank-to-wheel (TTW) emissions, high performance, efficiency, control and low noise. The main open points are, instead, the battery (in terms of cost, weight, life, environmental impact) and the lack of infrastructures for recharging. However, range anxiety is probably the most important drawback limiting the diffusion of BEVs.

In this scenario, the aim of this thesis is to investigate what is the impact of auxiliary systems on the vehicle autonomy when the car is in a real driving condition. This situation is strongly different compared to the actual European CO_2 type-approval tests based on standard cycles: the New European Driving Cycle (NEDC) and the Worldwide harmonized Light vehicles Test Cycle (WLTC), whose procedures provide strict guidance regarding the conditions of dynamometer tests and road load (motion resistance), gear shifting, ambient temperature and car weight, but no specification about auxiliary systems activation, in particular the ones related to the cabin comfort.

The methodology developed in this thesis to perform the energetic assessment is based on a MATLAB program including sub-models for the vehicle (resistance, transmission, motor and inverter, battery) and for its auxiliaries (air conditioning, both in heating and cooling mode, lights, battery management system, generic accessories, etc.). Indeed, in order to maximize the range, it is extremely important

to tackle all the energy wastes. Also, it is important to develop a test mission which is representative of the real world driving, which is often very different with respect to type-approval conditions. The test mission will be characterized by many runs with different speed profiles, ambient temperature, number of passengers, daily hour, initial SOC of the battery. The main output of the program is the energy consumption, which is the conversion factor between range and battery energy capacity.

In order to get results comparable with the data available by the company, the model is fitted on a real vehicle and a calibration procedure is conducted for the vehicle cabin thermal model, in order to tune the model results with respect to data available from real world. The program is, later on, run in standard conditions over NEDC and FTP driving cycles in order to test the correct functioning of the models and to check the program ability to replicate experimental outcomes.

In addition to that, an optimization of the transmission is carried out, in order to get the best configuration for type-approval driving and real-world driving. In particular, both the cases of single-speed transmission and two-speed gearbox conditions are analyzed, in order to understand what the convenience of one solution over the other is.

Afterwards, a simulation on the realistic mission is conducted and the results are compared to type-approval ones, showing, as expected, a consistently higher energy consumption. In particular, the most critical components and conditions causing those energy wastes are detected. Also, it is evaluated the effect of the battery limit for incoming currents (charging) on the regenerative braking capability of lowering the BEV energy consumption.

1. THE COMPONENTS OF A BATTERY ELECTRIC VEHICLE

1.1 INTRODUCTION

A Battery Electric Vehicle (BEV) is an electric vehicle whose storage system is an electrochemical accumulator (the battery).

BEV powertrain is made by four main components: battery, inverter, electric motor, transmission. The battery is the energy storage system of the vehicle, able to supply electric power to the motor in order to make it work and playing a major role in defining the vehicle range. However, the electricity produced by a battery is of the DC type, while most of the electric machines equipped by a BEV work with AC supply. That is the first reason why a power electronic device (inverter) is adopted. Power electronics also play a fundamental role in the machine control, since those devices are able to convert not only current type, but also its characteristics, such as voltage amplitude and frequency. That is the reason why, even when the vehicle is equipped with DC e-machine, a power electronics device is always present. The transmission is the mechanical element transferring the torque generated by the motor to the wheels. It is made by a gearbox (optional), by a final speed reduction device and, when necessary, by a differential.

The number of components of a BEV is much higher than the four main ones, since nowadays it’s impossible to sell a vehicle without some accessories which are now standards. This is the case of the cabin cooling/heating systems, essential for passenger comfort, or the case of the Electric Power Steering (EPS), able to reduce driver effort on the driving wheel. Finally, many secondary components are present, like in all other vehicles. Among those there are the 12V battery (with its DC/DC converter for the connection to the High Voltage circuit), the 12V accessories (wipers, electric windows, etc.), the Electric Control Unit, the lights.

This chapter aims at giving a short description of the components’ task and an overview of the main technologies adopted.

1.2 BATTERY

The electrical battery is the energy storage device of the vehicle, being equivalent in this task to the fuel tank in a conventional Internal Combustion Engine Vehicle (ICEV) and determining the vehicle range. However, due to its peculiar characteristics, the battery is much more critical than a fuel tank, because it also affects directly the performance of the car.

It is assumed conventionally that the first battery was described and built by Alessandro Volta in 1800, consisting in a stack of alternating plates made of copper and zinc separated by salty paper discs. Although the Italian physicist did not understand the chemical reactions behind the voltage generation of his "pile", in less than 40 years the process became clearer and clearer and the major invention of the Daniell cell was made. The Daniell cell is the prototype for all the modern batteries. It is made by:

a) Two semi-cells with two electrodes (anode and cathode);
b) Two chemical solutions in the semi-cells;
c) A separator.

The solution is formed by positive and negative ions. At the anode an oxidation reaction happens, which means that the electrode will release some additional positive ions in the solution, charging itself negatively. At the cathode, a reduction reaction happens, which means that some of the positive ions will accumulate on the electrode, charging it positively. When an electric load closes the circuit between anode and cathode, electrons are able to pass from one electrode to the other, providing a DC current, and the reactions can go on until the pile is exhausted. The charge balance in each half-cell is allowed thanks to the migration of the negative ions present in it through the separator. A pile is exhausted when one of the reactants is too poor in concentration, so that there's no more potential for the reactions to happen. The Daniell cell is made by a zinc anode and a copper cathode, submerged in zinc sulphate ($ZnSO_4$) and copper sulphate ($CuSO_4$), respectively. The separator is a salt bridge, which allows the flow of the sole SO_4^- ion between the half-cells.

Each element and each molecule is characterized by its ability to generate an electric potential during an oxidation reaction; this ability is called electromotive force (*emf*) potential and is measured in $Volts$. The reference case is the one of the hydrogen which is assumed to have a null potential when reacting with oxygen to form water. By convention, the cathode will have a positive *emf* potential, while the anode will have a negative *emf* potential, and the total one of the cell is given by the subtraction of the two. If an increase of battery voltage is needed, it's sufficient to put many cells in series. Table 1 lists the *emf* potential for some metallic materials; however, cells elements can be also of the non-metallic type.

Newest batteries, such as the nowadays spread Lithium-Ion battery, can be very different with respect to the Daniell scheme: for example the separator could be solid (salt), or the ions dissolved in it can have more than one oxidation state, etc. However the way voltage arises at the electrode has the same nature.

METAL	ELECTRODE *EMF* POTENTIAL [V]
Gold	$+1.40$
Platinum	$+1.20$
Palladium	$+0.83$
Silver	$+0.80$
Copper	$+0.34$
Hydrogen	$+0.00$ (REF)
Lead	-0.22
Nickel	-0.25
Cobalt	-0.28
Zinc	-0.76
Manganese	-1.05
Potassium	-2.92

Table 1. Electrode potential for some metals.

In the years passing by, many chemical formulations for the battery were proposed, each with its advantages and disadvantages. Indeed it must be noted that voltage is not the only desirable feature, since many characteristics are important when choosing the technology of a battery:

a) *Energy density* and *specific energy*: they determine how much energy for a given volume or weight can be stored. Of course, referring to automotive batteries, an increase of both the parameters is sought after, since volumes impact on the roomability and weight on the vehicle dynamics. The main typologies of batteries adopted for automotive traction, together with their specific density, are listed in Table 2;
b) Cost: it depends not only on the cost of the materials (electrodes, solution), but also on the cost of the battery engineering and on the cost of the containment structure, which depends itself on the nature of the reactions and on the intrinsic safety of the battery. For the automotive application, the *cost-for-Watthour* of usable stored energy is of primary importance, since it determines the trade-off between range and vehicle initial cost;
c) Life of the battery: it involves many different chemical effects, such as self-discharging, corrosion, overcharging, memory effect, physical component changes and the dependency of its characteristics on environmental conditions, especially the temperature. The battery used in a BEV should have a life at least as long as the one of the car, especially if its cost is not negligible, such as the cost of a normal 12V battery for conventional cars. Moreover, the life-time should be as much independent as possible from the effect previously mentioned, since the mission of a car is variable;
d) Safety issues: they concern the toxicity of some materials used in the battery, which makes leakages and disposal at the end of life a very critical (and expensive) matter. Moreover, the danger of explosion is to be considered for the chemistry of some batteries;
e) Rechargeability: it involves the ability of the battery to reverse its reaction when a reverse current is imposed at the electrodes. If that’s not possible, the battery is

called “primary”, while rechargeable batteries are called “secondary”. Even for secondary batteries, there’s always an irreversible fraction of reactions during the battery operation: those lead, cycle after cycle, to the diminution of the battery performance and capacity. This is critical in the automotive world, since “range anxiety” is one of the main concerns regarding BEVs.

CHEMISTRY	MAXIMUM SPECIFIC ENERGY
Nickel-Cadmium	$120\ kJ/kg$
Lead-acid	$140\ kJ/kg$
Nickel-Metal Hydride	$360\ kJ/kg$
Nickel-Zinc	$360\ kJ/kg$
Silver-Zinc	$460\ kJ/kg$
Lithium-Iron-Phosphate	$360\ kJ/kg$
Lithium-ion	$460\ kJ/kg$

Table 2. Chemistry of the main batteries for automotive traction purposes and their maximum specific energy with best available technology.

Lead-acid batteries are widespread in the automotive world, where they’re applied as the small 12V battery powering electric auxiliaries, such as pumps, starter motor, wipers, electric windows, radio, etc.

When, instead, a large amount of energy is needed, the choice goes on batteries with high specific energy to limit the weight increase, such as Nickel-Metal-Hydride, Lithium-Iron-Phosphate, Lithium-Ion. Those are applied, in the automotive world, as main energy storage device in hybrids and electric vehicles. In particular, for BEVs the maximum energy is required and the constraint on the specific energy is stronger, which makes Lithium-Ion the only possible solution. At the moment, almost all BEVs on market mount a Li-Ion battery.

However, batteries for traction purpose must guarantee not only a good specific energy, in order to comply with the desired range, but also a good specific power, so that the battery can deliver enough power to the motor to fulfill the driver needs. Usually, for each of the battery’s chemistries, we can try to maximize the specific energy, in spite of the specific power, and vice-versa, as shown on the Ragone Plot (Figure 1). Therefore, the choice of the chemistry for a BEV will be a compromise between the two needs, while the maximization of one of the two is not possible.

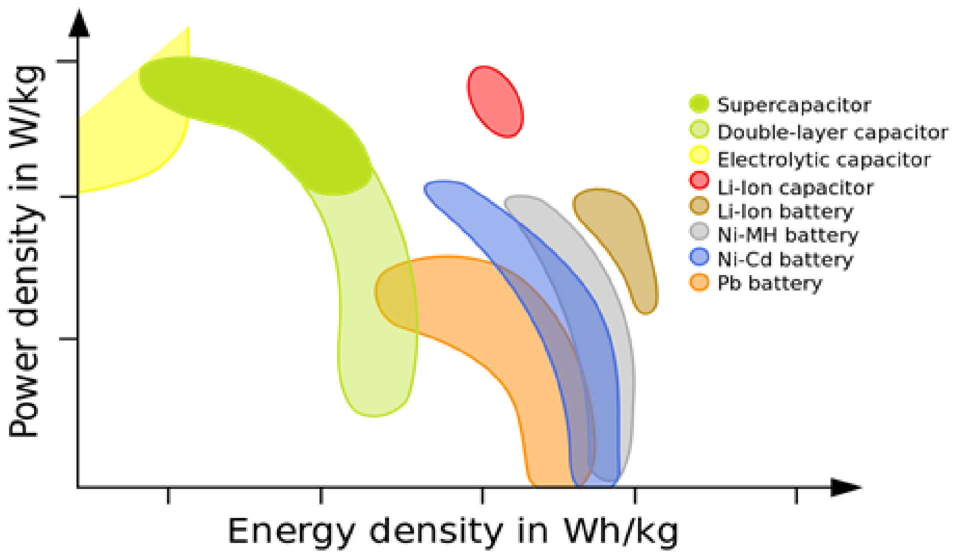

Figure 1. Ragone Plot. Axes are deliberately without values since they constantly change as technology progresses.

1.3 MOTOR

An electric motor is a machine able to transform electrical power into mechanical power by means of Lorentz or reluctance forces. All the electric motors are reversible machines, which means that their way of operation can be reversed and they can be used as electric generators, transforming mechanical power into electrical one. That's why these devices are more properly called electric machines (*e-machines*).

Electric machines include a vast variety of different solutions whose working principle can be quite different. A first classification can be made according to the type of current which must feed them, either direct or alternate current. Since all batteries deliver direct current, AC e-machines will need an inverter, which is a device that turns current from direct to alternate. Even inside the same class, we can find very different machines, as highlighted by the scheme proposed in Figure 2.

Between the end of the nineteenth and the beginning of the twentieth century, electric vehicles had their golden age, since the electric technology was, at that time, superior to the petrol one. DC motors were used, due to the maturity of this technology and to the fact that power electronics were not discovered yet. However the limits of DC motors are numerous, so that nowadays the AC motor has replaced almost completely the DC one in vehicular application, except for some really small vehicles like golf carts or forklifts. In particular, in the last years the approaches were different, such as PM synchronous motors, induction motors or synchronous reluctance motors. Nowadays the tendency is towards hybrid solutions in order to improve all the characteristics of the motor: for example, synchronous reluctance machines can have permanent magnets buried in the rotor to improve the peak torque of the machine.

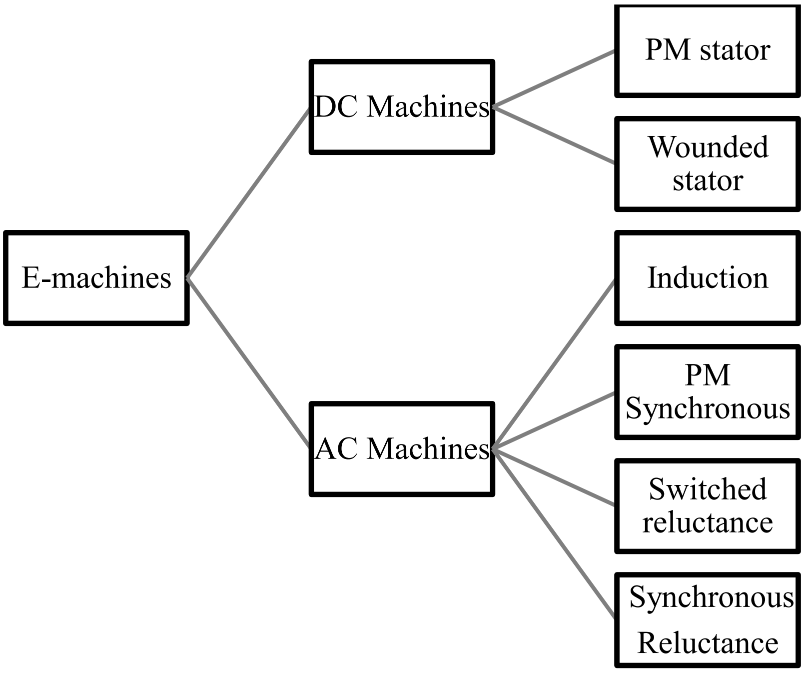

Figure 2. Classification of electric machines

The operating principles and salient characteristics of the main machines adopted are explained in the following.

1.3.1 DIRECT CURRENT ELECTRIC MACHINES

DC e-machines are simpler than AC ones, since they don't need an inverter and can be controlled by means of low efficiency by-passable resistor or with lower cost power electronics. That's why they have been discovered and applied before the other type. The DC e-machines are made by:

- a stator, which generates a fixed magnetic field by means of magnetic poles (the simplest machine has two poles). The magnetic field can either be generated by poles made of Permanent Magnets or by excitation windings placed at the poles. The second type adds a new degree of freedom for control, which is the excitation current and, thus, the control of the magnetic field intensity. However the principle of operation of the machine remains the same, making the DC e-machine class more homogeneous than the AC one.
- a rotor, made by a winding with current fed from outside. The electric lines, when moving inside the magnetic field, will be subjected to Lorentz forces, which generate the useful torque of the machine.
- a commutation system. In fact Lorentz forces are in the form $\bar{F} = l\bar{\imath} \wedge \bar{B}$, and they will cancel out, with no useful torque, when the winding is in a plane perpendicular to the magnetic field: even if the winding goes on a little bit by inertia, the torque induced will bring it back to this rest position. The commutation system guarantees that, at this point of the revolution, the current will change its sense inside the winding, so that the new rest position will be

180° away and the revolution can go on. The commutation system is made more difficult by the fact that the current must be transmitted from a stationary to a rotating coil. The solution is a cylindrical collector alternating conductive lamellae (connected to the windings) and insulating lamellae. The current will be transmitted to the windings through the collector by means of low-wear carbon brushes pressed on the collector by a spring system. The position of the brushes axis with respect to the stator magnetic field axis is important so to guarantee the proper current inversion in the coils. The commutation principle is clarified in Figure 3.

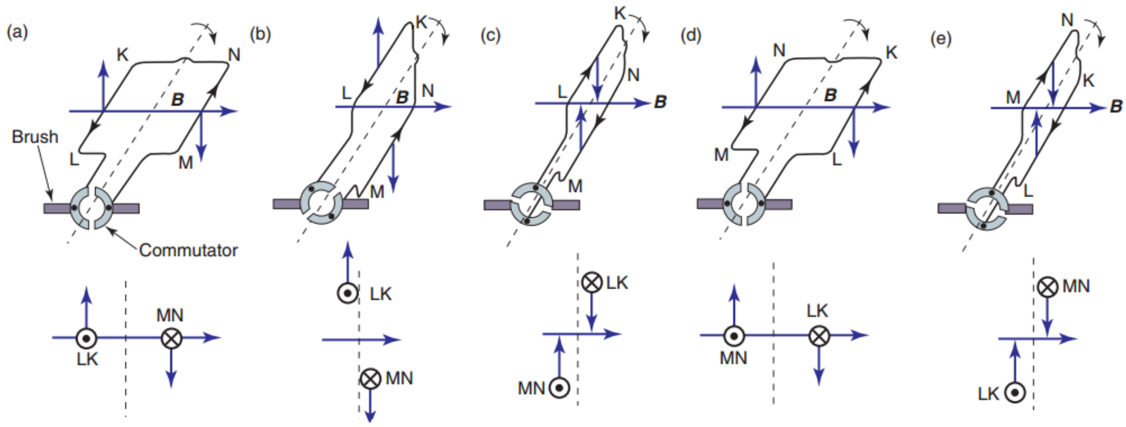

Figure 3. Working principle of the commutation system and of the DC motor: (a) Maximum torque plane, (b) Approaching no torque plane, (c) Commutation with reversal of current, (d) Maximum torque plane 180° shifted with respect to the first one, (e) Approaching again commutation plane. *Source: DuxCollege*

For what concerns the case of DC machine with wounded stator, depending on how the stator and rotor circuits are connected, we can have the possibility of:

a) separately excited: different sources for stator and rotor;
b) series excited: stator and rotor circuits are connected in series, thus sharing the same current;
c) parallel excited: the parallel connection makes the stator and rotor circuits share their voltage;
d) mixed series-parallel: with the possibility of having both the situations.

Series and separately excited machines are the most widespread. Indeed series excited DC machines show the highest peak torque of all, while separately excited machines have the highest degree of freedom in control, since it can be actuated either on the rotor or the stator separately.

The main limits of the DC machines are intrinsic of the commutation mechanism, which, in addition to its complexity, also produces wear of the brushes, limits the maximum rotor speed (up to 6000rpm) and the maximum transient power. During commutation, sparkles can appear between brushes and collector, with potential hazards. Finally, the friction between brushes and collector lowers the efficiency of these machines in comparison to AC ones where mechanical access to the rotor is not necessary.

1.3.2 ALTERNATING CURRENT ELECTRIC MACHINES

AC machines are supplied by alternating voltage/current. They are usually more expensive than DC machines: this is counterbalanced by higher performances, as will be explained later. The speed of AC machines is related in some way to the supply voltage/current frequency and so the control by means of power electronics (inverters) is mandatory. The AC machines class is quite inhomogeneous, with many different machines. Namely we have, as shown already in Figure 2:

a) induction machines;
b) permanent magnet synchronous machines;
c) switched reluctance machines;
d) synchronous reluctance machines.

Their principle of work will be briefly analyzed, especially referring to the motor mode of operation. However AC machines, like all electric machines, are reversible, which means that they can be used also as generators.

Induction motor

The induction motor, also called *asynchronous*, is one of the most applied AC machines in the engineering world, thanks to its good characteristics. The name “induction” refers to the electromagnetic induction phenomenon, which is exploited in order to make the current flow into the rotor without the need of the brush/collector system (like in DC motors).

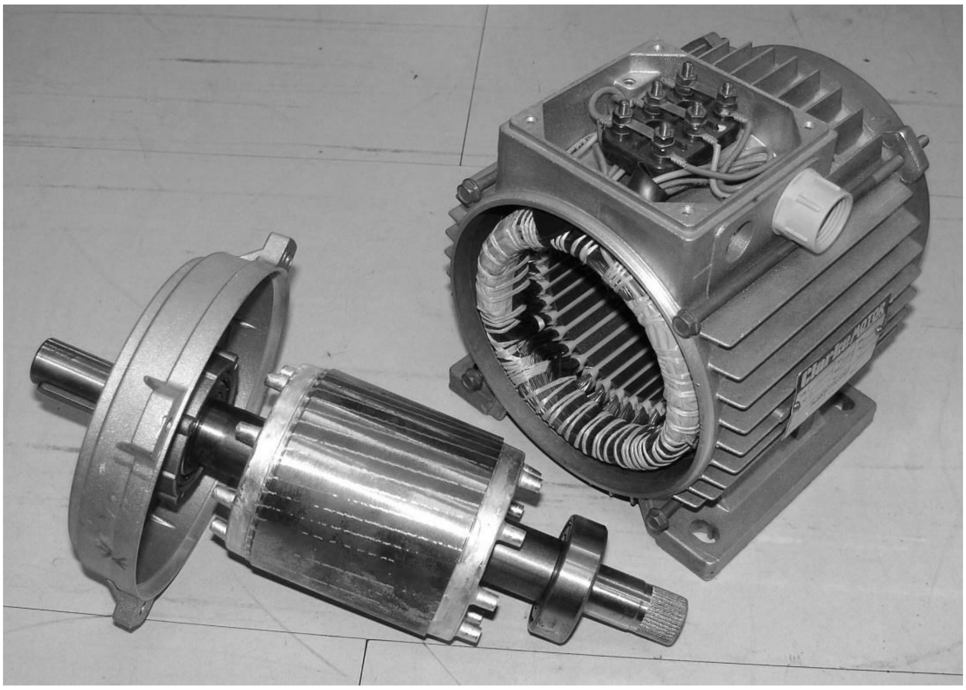

Figure 4. Induction motor with “squirrel-cage” rotor and distributed winding stator

The stator of an induction motor can either be made by concentrated or distributed windings. In the first case, typically, three couples of windings, with radial axis, geometrically 120° apart one from the other are fed by a three-phase current. This configuration results in three magnetic fields which are directed along three lines 120° one from the other, pulsating with same frequency and shifted in time by an equivalent angle of 120°. Summing together these three fields, what is obtained is a magnetic field with constant amplitude (1.5 times the one of each winding) but rotating in the space with a speed:

$$\Omega_s[\mathrm{rpm}] = \frac{60}{\mathrm{pp}} \mathrm{f}[\mathrm{Hz}]$$

where pp is the number of pair poles of each phase, f is the frequency of the supply voltage/current, and Ω_s is the synchronous speed. In the distributed windings case, instead, the conductors are arranged in slots cut axially along the whole surface of the stator, such as to maximize the number of coils for each phase. Also in this case three groups of windings are fed by a three-phase current in order to generate a magnetic field rotating at synchronous speed.

The rotor is made either by windings or by solid conductive bars (like a *squirrel-cage)*, forming closed coils. They will "see" the magnetic field vary with respect to them, and a current will therefore be induced by the Faraday law. This, however, could only happen when the speed of the rotor is different with respect to the synchronous speed: in this specific case, in fact, the magnetic field variation with respect to the rotor goes to zero. This is the reason why induction motors are also called asynchronous. The current induced in the rotor will interact with the magnetic field providing a force which, in turns, generates the traction torque. Since the machine works based on different speeds of rotor and rotating magnetic field, the slip ratio s is defined:

$$\mathrm{s} = \frac{\Omega_\mathrm{s} - \Omega_\mathrm{rot}}{\Omega_\mathrm{s}}$$

The torque of the machine will be a function of the slip ratio, as shown in Figure 5, which plots the characteristic curve of an induction motor.

It can be seen that:

- for $s = 0$ $(\Omega_{rot} = \Omega_s)$ we have no torque, as we already discussed;
- for $s = 1$ $(\Omega_{rot} = 0)$ we have a non null stall-torque, which makes induction motors self-starting.

The behavior shown in Figure 5 can be mathematically verified if an equivalent circuit of the motor is analyzed, such as the one in Figure 6. This scheme refers to a steady state conditions and is identical to the electrical scheme of a transformer: this is due to the fact that the induction motor is very similar to a transformer, being its operation based on a varying magnetic flux which concatenates two sets of coils. However in a transformer both the sides are concatenated by the magnetic field with the same frequency. In an induction motor, instead, the rotor will "see" a magnetic field which is at a frequency called "slip frequency":

$$f_{slip} = \frac{pp}{60}(\Omega_\mathrm{s} - \Omega_{rot})$$

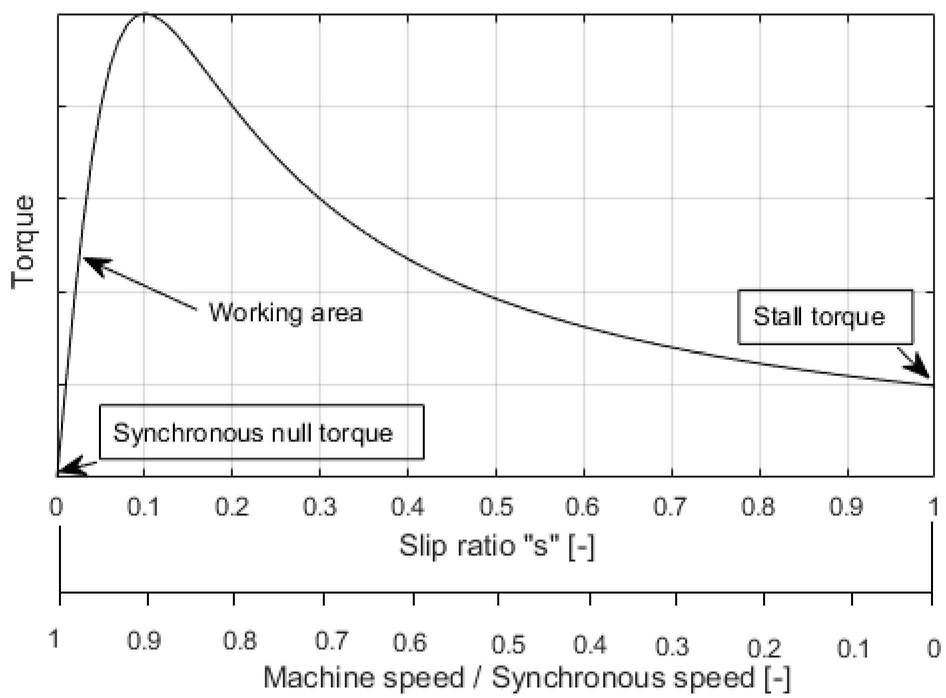

Figure 5. Induction motor characteristic curve

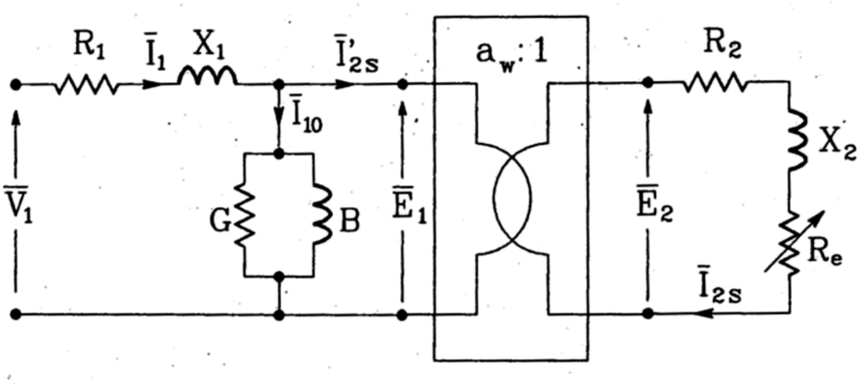

Figure 6. Induction motor equivalent circuit. *Source: G. Fabbricatore, Elettrotecnica e Applicazioni, 1994*

So, when approaching the study of the equivalent transformer, we should remember the different frequencies of the two sides, because this impacts on the losses, which depend on the frequency. This is why induction motors always work in the descending part of their characteristic curve at small slips (and small frequency of the current inducted in the rotor). Another reason for that is that the descending part of the curve is stable, being its derivative opposite in sign with respect to the load curve at their intersection.

The mathematical study of the equivalent circuit is beyond the scope of this discussion. However its main results, which are the variation of the characteristic when varying some operating parameters, are shown in Figure 7.

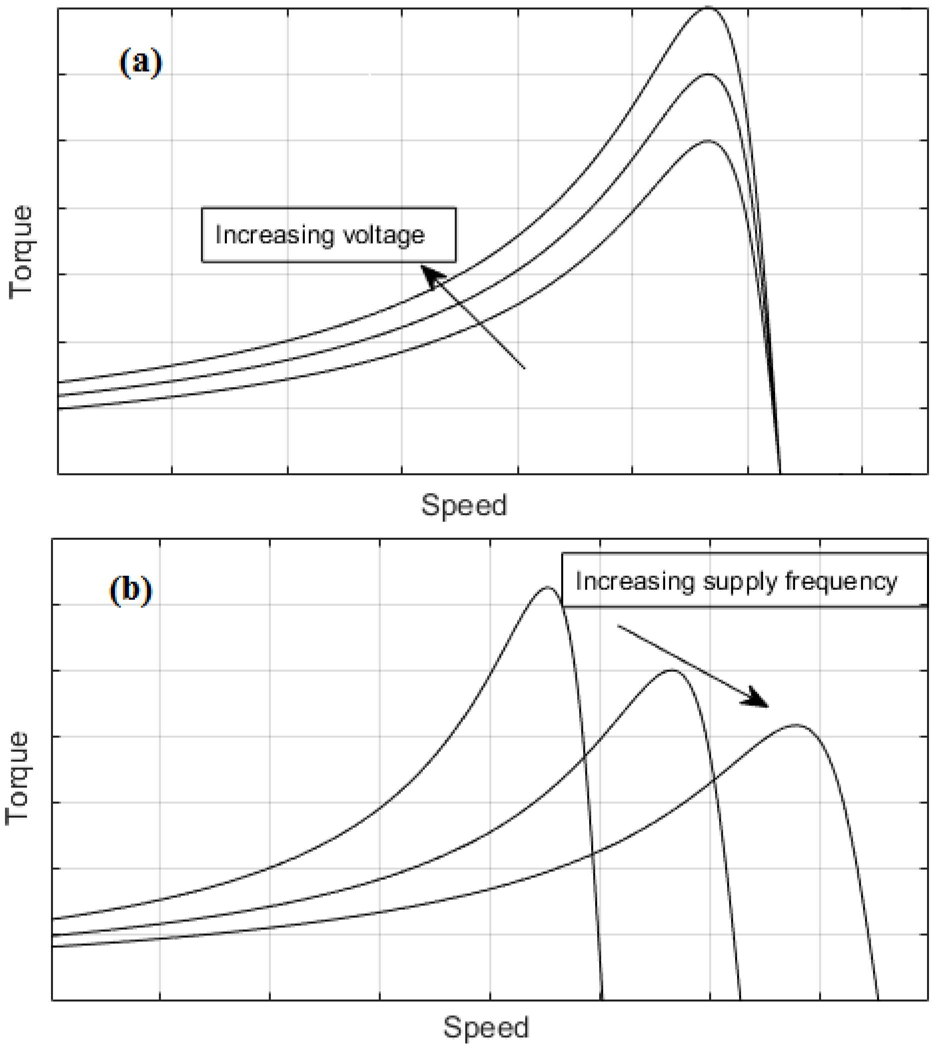

Figure 7. Induction motor characteristic curve dependence on (a) supply voltage amplitude and (b) supply frequency

The induction motor map is the classical one of all electric motors (Figure 8) and is obtained by means of the following control over the inverter:

- in the constant torque region, the supply voltage and frequency are proportionally increased from zero to base speed. Mathematically it can be demonstrated that the torque depends directly over the magnetic flux which, in turn, is proportional to square of the ratio voltage/frequency. Thus constant torque is obtained.
- in the constant power region, the voltage amplitude is kept constant while frequency is proportionally increased with speed. This makes the magnetic flux and the torque dropping with the square of the speed, while the power can be kept constant.

Sometimes, when really high speeds with low loads are to be achieved, a third region appears, where voltage and frequency are fixed but a lower current is provided to the stator to avoid a fast increase in rotor losses: the flux is then weakened more in this region.

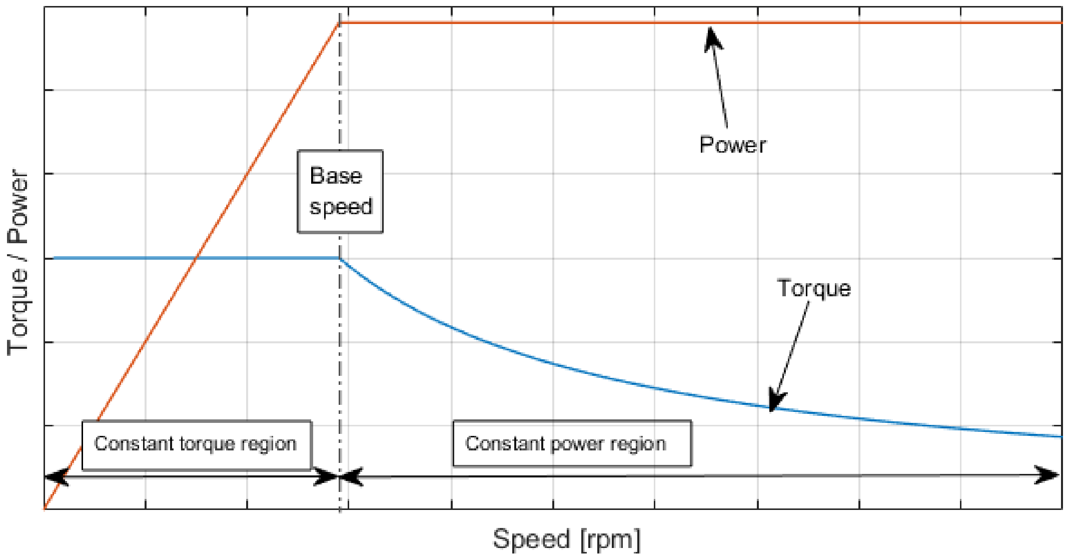

Figure 8. E-machine torque and power working curves

Induction motors have a high electromechanical and control robustness. They have good (but not outstanding) specific torque and power, good overload capability and efficiency (in the range 0.87-0.96), high flux weakening range and max speed. The induction motor has acceptable performance for all the characteristics necessary in a motor for vehicular application with no great flaws: so it is applied quite often.

Permanent Magnet Synchronous motor

The permanent magnet synchronous motor, also called *brushless*, is one of the most performing motors for vehicular application, as will be shown. A synchronous machine is called like that because it will rotate at a rate which is exactly proportional to the supply frequency. In particular, it will rotate at the synchronous speed already defined for the induction motor: this is due to the fact that, unlike induction motors, synchronous machines don't need any slip of the rotor with respect to the excitation magnetic field, being their working principle not based on the induction of a current in the rotor.

In a permanent magnet synchronous machine, in particular, the rotor will be made by permanent magnets, while the stator is similar to the one of an induction machine, producing a rotating magnetic field. The rotor will try to align its magnetic field with the stator rotating one, thus resulting in a rotation at synchronous speed. The permanent magnets position in the rotor determines its characteristics:

- *surface mounted permanent magnet* (SMPM), which makes the machines cheaper because they're easier to be built. They also have smaller cogging torque because the distance between the magnet and the excitation coils is smaller. Cogging torque is the torque that derives from the interaction of magnets and stator slots, also known as “no-current” torque. It is highly undesirable because it can cause jerkiness during the operation;

- *internally mounted permanent magnet* (IMPM) which are replacing the first solution thanks to the smaller inverter sizing, due to the possibility of taking advantage of reluctance torque, and to the higher speeds which can be reached, due to the fact that the magnets are safely stored inside the rotor.

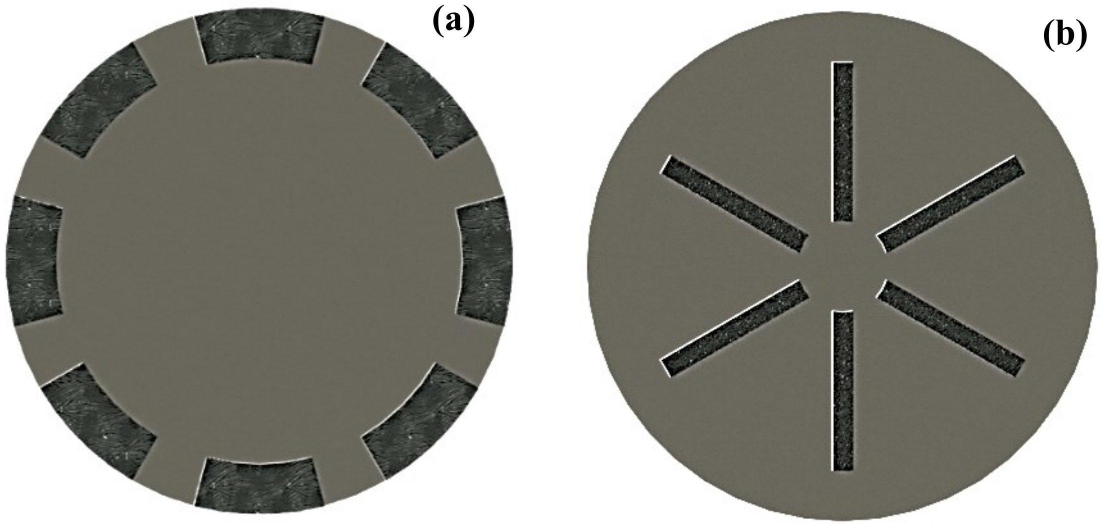

Figure 9. Cut-off view of rotor configurations for (a) SMPM and (b) IMPM synchronous machines. The darkest parts represent the magnets.

Permanent magnet machines can also have quite different stator winding layouts which bring the following classification:

- *brushless AC machines*, which is a PM synchronous machine with the stator windings scheme equivalent to the one of an induction motor (distributed axially mounted windings in slots);
- *brushless DC machines* (BLDC), which is a PM synchronous machine where the stator is made by concentrated coils, each with its axis radially directed. The current supply is DC, but thanks to an inverter, the coils can also be supplied by an AC current. The inverter, or the power electronics device, is controlled such as to provide a rotating magnetic field. Of course, using directly DC source implies higher ripple.

AC brushless have lower torque ripple, but the position sensors are more complex. DC brushless, since the stator coils are more “discrete”, presents higher torque ripple, but it can use Hall sensors, which are less complex.

PM synchronous motors present several advantages. Indeed they have high efficiency, since their rotor is made by magnets and have no flowing currents nor will it need brushes. This is also an advantage in terms of rotor cooling, whose requirements are much reduced with respect to the case of wounded rotors. Also, when rare-earth PM are employed (such as $NdFeB$), their high flux density maximizes the specific torque of these machines, which makes them also compact. Last but not least, the absence of brushes minimizes the wear. For all that reasons PM motors are widespread in vehicular application. However there're also some intrinsic limits to these machines, and in particular, the presence of the magnets on the rotor limits the maximum speed for safety reasons (especially in the case of SMPM). Rare-earth magnets are also very expensive because of their scarce abundance: this makes the motors more expensive than other solutions. Finally, the absence of control in PM makes the electronic flux-weakening mandatory, but with limited constant power range and low efficiency. To decouple at best flux-torque, sometimes we could find also wounded rotor synchronous machines, where the rotor is similar to the one of a DC machine. However the added complexity (both mechanical and electrical) usually doesn't justify this solution.

Switched Reluctance motor

Switched reluctance motor (SRM) is a type of electric machine whose working principle is based on the exploitation of forces related to the magnetic reluctance. The current is supplied to the stator coils, which are concentrated and always in couples diametrically opposed (stator salient poles), so that each couple is able to generate a magnetic field in the direction of its axis. The stator scheme is similar to the one of BLDC machines. The rotor is made by a ferromagnetic material, so that it will be easily magnetized by the stator magnetic field. It will also have a toothed shape (rotor salient poles), so that a reluctance torque is generated when its teeth try to align with the axis of the active magnetic field, in order to minimize the air gap. After the alignment, another couple of stator poles will be excited and the rotor will again try to align with it. In order not to have a single equilibrium position for all the different stator poles, the number of stator salient poles is always greater and not a multiple of the ones in the rotor. The most common configuration is 6/4 or 8/6 poles (the first number referring to the stator, the second to the rotor). The switching instant is determined on the basis of the rotor position, whose information is collected by a sensor.

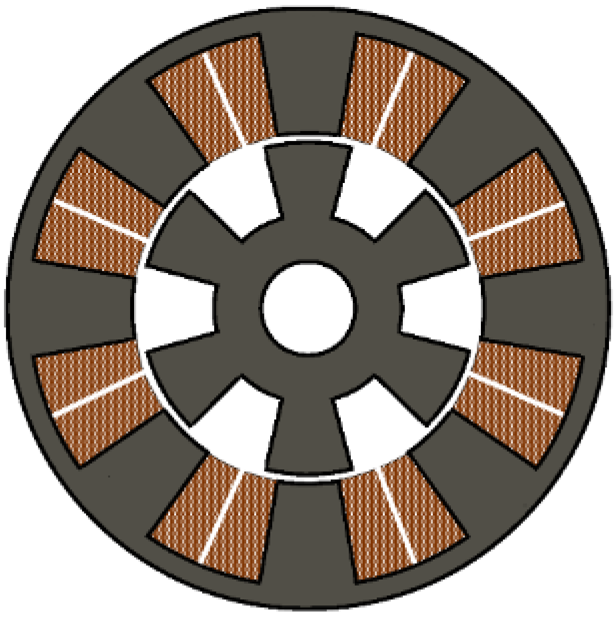

Figure 10. Switched reluctance motor cut-off view.

The working principle described above would be quite rough and present a huge torque ripple. Actually the control of the poles is slightly more sophisticated, involving for example a partial excitation overlap of following electromagnetic poles, so that the reluctance torque is smoother.

The absence of PMs or windings makes the structure of the SRM robust (even at very high speeds), easy to be manufactured and cheap. However the machine should be manufactured with a really small air-gap, such as to maximize the reluctance torque. Also, since there’s no Joule loss in the rotor or frictions due to brushes, the efficiency is very high. However, the SRM has a number of drawbacks: due to the continuous magnetization of the electromagnetic poles the reactive power of this machine is quite high, with an impact on the power electronic sizing. Moreover the magnetic utilization of the machine is low, since it works with one active pair pole per time. Finally, the discrete control of the concentrated stator coils generates the highest torque ripple of all the machines. Noise is a concern too.

Synchronous Reluctance motor

This machine tries to combine the advantages of a reluctance machine with the smooth functioning of a synchronous one. The stator is the same of a synchronous machine, so with distributed windings generating a rotating magnetic field. The rotor, instead, present anisotropy in its geometry thanks to holes that induce a predefined axis of minimum reluctance. Thus, once magnetized, the rotor will always follow the rotating magnetic field at the same speed (synchronous working).

This type of machine has lower ripple, vibration and noise with respect to the switched reluctance and can achieve higher specific torque than the induction one (but never as high as a PM synchronous). The average efficiency is quite high, due to absence of friction and Joule losses in the rotor. Also, the rotor lamination helps to reduce the stray currents in it. It is slightly more difficult to be manufactured with respect to the switched reluctance, but the manufacturability, cost and reliability are still better than many other machines.

1.4 POWER ELECTRONICS AND INVERTER

Power electronics refers to the electronic devices and their control structure used in order to adapt the energy source characteristics to those required by the electric machine. These devices are essential for the correct working and the control of the electric machines. The main power electronics devices are DC/DC converters, adapting voltage amplitude between a DC source and a DC utilizer, and the DC/AC converter (also called inverter), making current/voltage turn from DC to AC and vice versa. The electronics building blocks are semiconductor switches, based on the Field Effect studied by J.E. Lilienfield and applied starting from ‘50s. Prior to this discovery, DC/AC conversion was done with rotating converters, made of a DC machine running an AC synchronous generator. Another way was the one of mercury vapors devices, which was unreliable, expensive and cumbersome. The control, instead, was entrusted to slow and inefficient mechanical switches, or to dissipative by-passable resistors.

All the semiconductor devices are to be considered as switches able to make current pass in given conditions. Ideal hypotheses contemplate the current to be exactly null in OFF conditions, while in ON conditions the voltage drop is null. However, in real life those conditions are never found to be true. In this work a complete analysis of all the devices, their operating characteristics and of their non-ideal effect, it's not presented. However, it should be noted that losses happen in all working modes (conduction, switching, off). The main semiconductor devices applied in automotive applications are:

- Power diodes, which are non-controllable devices acting as an ON switch when the current is in a given direction, and going OFF when the current changes sign.
- Metal Oxide Semiconductor Field Effect Transistor (MOSFET), it's a fully controllable device, whose state depends on a low-voltage signal provided to its control terminals.
- Insulated Gate Bipolar Transistor (IGBT), it's similar to the MOSFET in the practical operation, even if it's made with a different technology.

For what concerns the control, the ability to control the switch is indispensible, also at very high speeds. MOSFETs and IGBTs are the chosen solutions. MOSFETs allow very high switching frequency (from 10 to more than $100kHz$), at the cost of a high conduction resistance for high powers: therefore, they're applied in low voltage applications (lower than $100V$). IGBTs switching frequencies are at least one order of magnitude lower than MOSFETs ones, but their limited resistance allows them to be used for high power applications (voltage higher than $100V$), such as electric or full hybrid electric vehicles. Diodes are anyway used, most of the time coupled with MOSFTETs or IGBTs, when an inversion of the current has to be avoided in a given branch of a circuit.

Inverter

Figure 11 shows the electrical scheme of a three-phase inverter. In a BEV it has great importance, since it is essential for the conversion of energy from the DC source (battery), to the motor which, most of the times, is of the AC type. Moreover, it is also fundamental for the control of the same. A three-phase inverter is made by three "legs" each of which is made by a couple of controllable devices (T1-T2, T3-T4 and T5-T6). Each leg is controlled such as to have only one of the devices in conduction, while the other is kept off: this is done to avoid short-circuiting the battery. Appropriately controlling the legs' switches through modulation[1], the inverter circuit is able to turn the input voltage/current from a DC type, to an AC one with some ripple, which is a disturbance of the ideal voltage/current profile. The ripple is usually a negative feature and is reduced by means of passive filters (inductors or capacitors) or increasing the switching frequency. It also depends on the type of modulation adopted.

[1] *Modulation* is the technique that translates an initial signal into a "carrier" one that contains the same information, but it's easier to be transmitted. In an inverter it is used to give the appropriate timing of

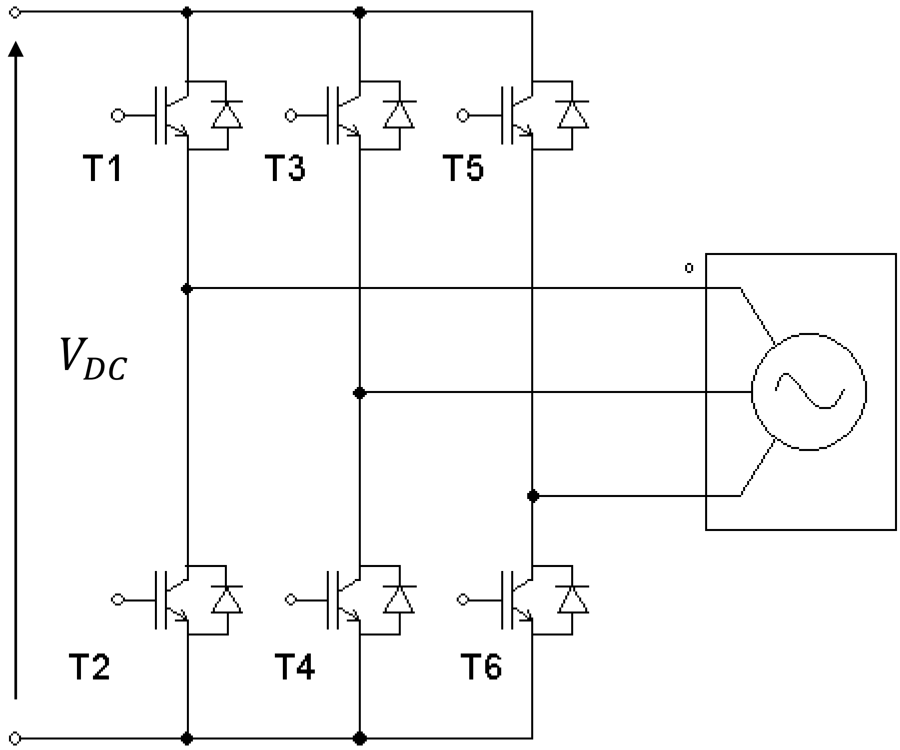

Figure 11. Inverter electrical scheme

Inverters have a high number of switches operating at high frequency and, therefore, produce a lot of heat. This implies that power losses can be not negligible with respect to the managed power, impacting on the total electric drivetrain efficiency. Moreover, the heat should be dissipated, and this poses the problem of inverter cooling. The latest tendency is to integrate the inverter with the motor case, so that a single cooling circuitry can be used for both. That is also why, most of the times, efficiency maps of the electric motors already include the losses of the inverter.

DC/DC converters

DC/DC converters are controllable devices with two sides, both of which work in direct current: the converter job is to adapt the voltage ratio between the two sides. *Buck* and *boost* converters are mono-directional devices used respectively to reduce or increase the voltage level between input and output. The voltage ratio is a function of the duty cycle[2] applied to the switch present in the circuit. The buck-boost converter, represented in Figure 12a, is a mix of the other two: depending always on the duty cycle, it can either bring up or down the voltage level, as can be observed in Figure 12b. Moreover it is, intrinsically, bidirectional: this is important in automotive applications, where current can flow either in one sense or in the other, depending whether the battery is providing power or being recharged.

[2] The duty cycle is defined as the ratio between the conduction time of a switch and the sum of the conduction time and interdiction time.

In a conventional vehicle the DC/DC converter is applied between the $12V$ battery and the low voltage (usually $\sim 5V$) electric accessories. In an electrified vehicle, instead, another DC/DC converter is needed between the High Voltage (HV) side of the traction battery ($> 200V$) and the Low Voltage (LV) side of the 12V battery and loads. This converter has to be, by regulations and for safety reasons, galvanically insulated (which means that contact from outside with the circuitry should be interdicted).

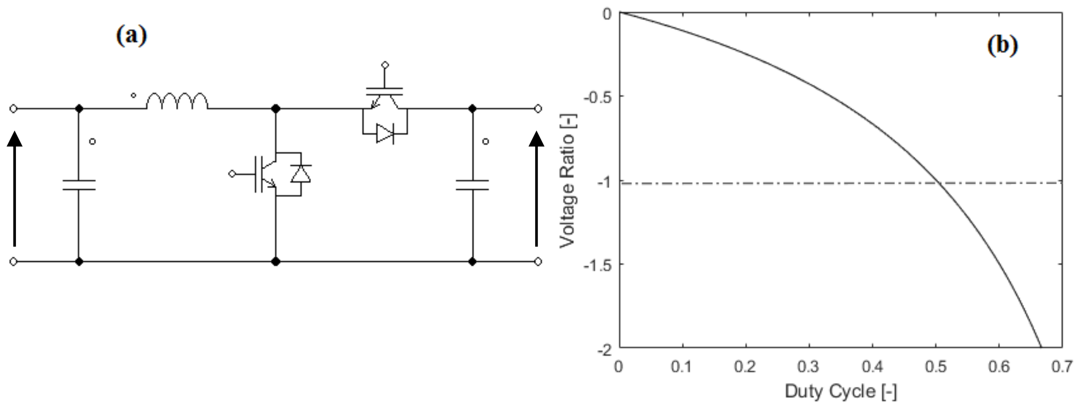

Figure 12. Bidirectional buck-boost converter (a), and the voltage ratio between input and output as a function of the duty cycle (b).

1.5 TRANSMISSION

The transmission of an electric vehicle is usually quite simple. Indeed the motor working characteristic, in terms of power and torque, is really close to the ideal one, with a good availability of torque at low speeds and with constant power at higher speeds, as already shown in Figure 8. This makes the presence of a gearbox not necessary: the only reason for the adoption of a gearbox would be to make the motor works as close as possible to its high efficiency areas. However, while for conventional vehicles gearbox is indispensible, for BEV it is a plus and usually is not equipped: currently all the electric vehicles on the market, from the small Renault Tweezy to the luxury Tesla Model S, don’t have a gearbox. This is done in order to save on costs, complexity, weight, roominess and transmission mechanical efficiency. Therefore, the transmission is usually composed just by a final drive and by the differential.

1.6 BEV AUXILIARIES

BEVs, like all vehicles at these days, present a number of auxiliaries and accessories. Those are all electric, thanks to the availability of electric power, while for conventional vehicles the power for the accessories is sometimes directly taken from the engine shaft. This implies that the auxiliaries of a BEV have higher cost, but also better performances, better control and easier packaging capability. The main auxiliaries, with a short description, are reported in the following.

Air conditioning

Air conditioning is present virtually on all vehicle sold, since passenger thermal comfort has become a must in the latest years. Usually, two systems are present, one for cabin cooling and the other for cabin heating.

For what concerns cabin cooling, the design is exactly similar to the cooling cycle of a conventional vehicle and based on the Refrigeration Cycle:

a) a compressor increases the refrigeration fluid (gas) pressure, up to the point at which it starts to condensate;
b) inside the radiator the gas turns into liquid and releases heat to the external environment;
c) an expansion valve allows the liquid pressure to drop;
d) the fluid will then start to turn into gas in the evaporator, adsorbing heat from the environment (the evaporator communicates with the passenger cabin) and cooling it down.

The compressor is always electric, while for conventional vehicles the compressor is most of the times driven by the engine shaft, with poor performance and control capabilities.

For what concerns cabin heating, BEV are disadvantaged with respect to conventional vehicles. In fact, while working, an ICE releases large amounts of heat, which is taken off by the engine coolant, whose working range is $90 \div 100°C$. In cold conditions, instead of rejecting this heat in the environment through the radiator, part of it can be directed towards the passenger cabin, heating it. In BEV the powertrain is much more efficient, such that the heat rejected is inadequate to heat up the cabin, and therefore the heating requirements must be fulfilled entirely by a dedicated system. The easiest solution is to use a resistor that, due to the Joule effect, becomes hot and releases heat. In order to limit the current adsorbed by this component, a Positive Thermal Coefficient resistor is adopted, whose resistance increases as temperature increase. The other solution would be to adopt a thermodynamic cycle such as the refrigeration one, called *heat pump*. This method is much more efficient and allows reducing the power adsorbed from the battery. The main problem arises from its cost, which is several times higher than the PTC resistor solution.

Electric Power Steering

The Electric Power Steering (EPS) allows reducing the effort of the driver on the driving wheels by supporting its action with an additional torque provided by a small electric motor. The motor can be either placed on the steering column or directly on the steering rack, with similar performances. The working, real-time, algorithm of the system is:

- a sensor reads the torque applied by the driver on the steering wheel;
- a “boost curve” determines the target motor torque based on the driver torque;
- a PID controller acting on the motor seeks the target torque.

The EPS, with respect to the hydraulic solution commonly applied on ICEVs, ensures lower consumptions, longer durability, easier packaging, and easier calibration. Usually, it is actuated the most in city driving conditions, where the speeds are lower and the steering angles larger. Anyway, the nominal power of the motor is in the range $200 \div 400W$ and its consumption on everyday working is negligible with respect to the other power requirements of the vehicle, such as the traction motor one or the air conditioning one. The worst case scenario sets the maximum value of energy adsorbed by the EPS motor 5% of the total energy on the cycle [1].

Battery conditioning system

The battery conditioning system is necessary for two reasons: to make the battery work in its optimal temperature range, and to make the temperature uniform between the cells of the battery.

Each battery has an optimal temperature working range which, for Lithium-Ion technologies, is approximately $20 \div 40°C$, where the internal resistance has usually a minimum. If the battery temperature goes above the maximum allowed temperature, its performance starts to decay and, if not controlled, thermal runaway could happen. Therefore in these conditions battery cooling should be active. Also at low temperatures the battery performance are limited by decrease of chemical reactions rate, which increases internal resistance and decreases battery capacity. Therefore battery heating is necessary in those conditions. For both the cases of heating and cooling, the conditioning system is usually done with a liquid fluid passing through jackets cut off in the battery case. However some applications with natural or forced air cooling can be found on the market, with lower performances with respect to the liquid counterpart.

Moreover, batteries work without problems only when all cells have same voltage level, or at least the differences are contained in a really small gap. Temperature differences between the cells are to be avoided, since they have a direct impact on voltage non-homogeneity. Those latters could impair the functioning of the battery, and even lead to battery damaging.

Generic accessories

Among the generic accessories, can be classified many devices that have less importance in terms of adsorbed energy and whose typology doesn't differ from their counterparts used on ICEVs, such as lights, stereo, infotainment, windows, locks, etc.

2. REASONS FOR THE DESIRABILITY OF A BEV

2.1 INTRODUCTION

This chapter will analyze the major reasons for which BEVs are attractive vehicle solutions for substituting the vehicles equipped with an Internal Combustion Engine (ICE). Those reasons may be summarized in three points:

1. Electric vehicles have zero tail-pipe emissions, so they're perfect for city-centers and urbanized areas subjected to severe pollution phenomena;
2. Electric vehicles have usually a lower impact on the Greenhouse effect and the consequent global warming;
3. Electric vehicles will be the natural solution to the oil depletion in the next century.

Those presented are all external forces. Anyway, BEVs have also merits and other appealing characteristic intrinsic to their powertrain, such as low noise level, high on board efficiency, high performances and low operational cost.

Together, external forces are moving the car manufacturers towards the introduction of many electric cars and prototypes. However, even if the customers are charmed by the BEVs' superior features and green footprint, the market response to the manufacturers' offer is still slow and the share of electric cars sold is still negligible with respect to the one of conventional vehicles. This is essentially due to the high purchasing price, which doesn't allow a fair competition between a BEV and an ICEV of the same segment. Another critical point is the limited range of these vehicles, which, even if it is enough for every-day urban driving, causes the so-called "range anxiety" on the driver. Other drawbacks that can be listed are the long charging times, the increased weight, and the battery environmental impact. It's easy to understand that most of the problems are related to the battery, which is the main limiting technology to the diffusion of BEVs on large scale.

This chapter will present the main advantages, classified as external and internal ones, and disadvantages of the BEV solution. The conclusion is a market analysis of the electric car, studying the main trends in terms of technologies and achieved range and energy consumption.

2.2 EXTERNAL ADVANTAGES

2.2.1 POLLUTION

A compound can cause pollution that can be classified, according to its scale, into:

- *Global air pollution*, when the compound is long-living, thus affecting air quality on a global scale regardless of the emission location. The principal examples would be Greenhouse gases and ozone layer depleting gases (such as CFCs).
- *Local* or *regional air pollution*, when the compound is not very stable and tends to fade away quite quickly: thus it affects mainly the area where it is emitted. The principal examples are particulate matter, nitrogen oxides and ozone.

A summary of the most interesting pollutants is given in Table 3.

COMPOUND	DESCRIPTION	PRODUCTION
Particulate matter (PM)	It's a complex aerosol system. Ultimately it is mostly made by carbonaceous nuclei over which organic compounds, nitrogen oxides, metal oxides are condensated. Its concentration in the air causes respiratory tract irritation and a prolonged exposition could be linked with tumor outbrake.	It is produced by combustion, both the one in vehicular engines (especially diesel) and the ones in thermal plants and domestic facilities.
Carbon monoxide (CO)	Odorless, colorless gas. It fixes to hemoglobin more easily than oxygen, thus limiting fresh air transfer from the lungs to other body parts. High concentration of CO leads to asphyxia.	It is produced by the incomplete combustion of hydrocarbons under lack of oxygen: these conditions are found especially on vehicular engines, which are the main responsibles of CO pollution.
Nitrogen oxides (NOx)	They are toxic compounds and respiratory tract irritants. They also contribute to secondary pollution phenomena, such as acid rains and photochemical smog.	It is produced when a combustion happens at high temperatures (>1900K) and with availability of oxygen. In these conditions Nitrogen reacts with oxygen giving NO and NO_2. Diesel engines are one of the main NOx polluters due to their particular combustion.
Sulphur dioxide (SO_2)	Colorless, rotten-egg smelling gas. It is irritant to eyes, throat and respiratory systems. It also contributes to acid rains.	It is produced by combustion of a fuel with sulphur impurities. Vehicular emission of SO_2 is very small, due to the laws enforcing ultra-low sulphur fuels (less than 10 ppm).
Ozone (O_3)	Highly reactive and oxidizing gas, smelling and blue-coloured.	Produced by a complex reaction chain involving volatile organic compounds and nitrogen oxides, when activated by solar radiation energy.
Benzene	Ring-shaped liquid hydrocarbon. It has proven to be mutagenic and a possible cause of leukemia.	It is present in gasoline fuel as anti-knock agent, with a maximum permitted quantity of 1%. It is also produced during combustion starting from others aromatic hydrocarbons.

Table 3. Summary of main car pollutants characteristics

Carbon monoxide, sulphur dioxide and benzene concentrations are usually well below the limit values that scientific community gives as reference for avoiding health effects, thanks to the legislation that, over time, brought a significant improvement in fuel quality and combustion control. Instead, the other pollutants present concentrations that can easily overcome safety limits [4], especially in areas that have favorable characteristics for their accumulation, such as depressed zones protected from the winds.

Of course BEVs don't burn any fuel for traction, and therefore the pollutant emission is null in the usage place of the vehicle. This is especially important in city centers, where peak concentrations of pollutants are usually registered, also due to the large and concentrated traffic. That is the reason why many cities are limiting the traffic in their very centers and allowing just low-emission vehicles circulation.

2.2.2 GREENHOUSE GAS REGULATION

As said, CO_2 is not a pollutant. Instead, it is, together with other elements such as methane (CH_4) and chlorofluorocarbons (CFCs), a Greenhouse gas (GHG). GHGs form an opaque shield for the low-frequency radiation outgoing from earth to space, while they're transparent to the high-frequency incoming solar radiation: the net result is an increase in the total thermal energy of the earth environment, and consequently an increase in temperature. CO_2 alone accounts for over 50% of relative contribution to the greenhouse effect. A correlation has therefore been proposed by scientists between CO_2 global concentration in the atmosphere and temperature anomalies of the earth, as shown in Figure 13.

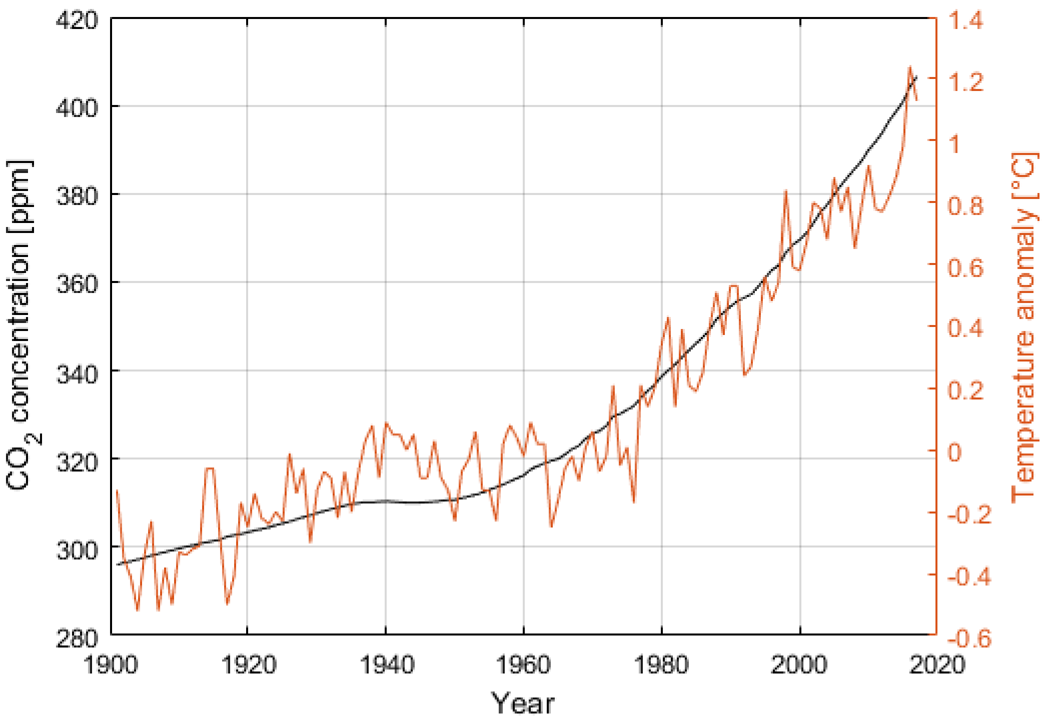

Figure 13. Relation between CO_2 concentration and temperature anomaly. *Data: NOOA and NASA GISS*

The increase in earth temperature is responsible for land desertification, glacial ice melting, sea level raise, intensification of severe weather phenomena, such as tornadoes and floods. In October 2016, CO_2 concentration reached the record-level of 400 ppm. Many scientists would argue that the world is near to a non-return point. For that reason governments are getting more and more involved in plans for limiting global warming. The latest commitment is the Paris Agreement, signed by all world states as of November 2017[3]. The Paris Agreement has the following aims:

> “*(a) Holding the increase in the global average temperature to well below 2 °C above pre-industrial levels and to pursue efforts to limit the temperature increase to 1.5 °C above pre-industrial levels, recognizing that this would significantly reduce the risks and impacts of climate change;*
>
> *(b) Increasing the ability to adapt to the adverse impacts of climate change and foster climate resilience and low greenhouse gas emissions development, in a manner that does not threaten food production;*
>
> *(c) Making finance flows consistent with a pathway towards low greenhouse gas emissions and climate-resilient development.*”

The agreement is general, for all sectors, and does not include fines for countries which will not respect their targets (which are also auto-imposed). However, in the automotive sector regulations limiting the CO_2 emissions (or, equivalently, fuel consumption) are being adopted for at least 20 years.

European regulation

At the end of ‘90s the ACEA (European Automobile Manufacturers’ Association) committed on a voluntary basis to reduce CO_2 emission targeting $140\ g/km\ CO_2$ emission to be reached, on an average fleet basis, in 2008. A second step should’ve been placed at $120\ g/km$ in 2012. The commitment produced some benefits, especially in the early years, but was not sufficient to get the hoped results. So European Commission, as part of the ECCP (European Climate Change Programme), set new targets. Those are $130 g/km$ for 2015 and $95\ g/km$ for 2020, with fines for the non-complying manufacturers.

American regulation

Also in USA we can find limits, although less severe. National Highway Traffic Safety Administration (NHTSA), an agency of the Department of Transportation,

[3] except for USA, which has claimed to withdraw.

adopted in 1975 the CAFE (Corporate Average Fuel Economy) standards, which were limiting fuel consumption to $27.5\,mpg$, equivalent to around $205\,g/km$ of CO_2 emitted. Actual limits are the MY2016 equivalent to $155\,g/km$, while future target is $101\,g/km$ in MY2025.

It can be understood that the long-term targets, both European and American, are quite challenging and for sure not reachable with full conventional ICE based fleet. Electrification, in all its forms, is the only possible way to reach the targets:

- Mild and micro hybrids technologies allow a non-negligible reduction in fuel consumption and CO_2 emissions.
- Plug-in hybrids technologies (PHEV) allow a substantial reduction in fuel consumption and CO_2 emissions.
- Full electric vehicle technologies allow null emission.

Moreover, regulations are pushing the introduction of electrification, by means of suited rules. As a first example, under European legislation a plug-in hybrid vehicle able to run at least one complete NEDC cycle in pure EV mode will be counted for an emission level equivalent to [5]:

$$CO_{2,PHEV} = \frac{25}{25 + km_{EV}} CO_{2,HEV}$$

where $CO_{2,HEV}$ is the amount of CO_2 emitted over the driving cycle in hybrid-mode and km_{EV} is the pure-electric range of the vehicle. This means that a PHEV able to run for 25km in pure EV mode, will be considered as if it had emitted half of the CO_2 registered on the cycle run in HEV mode. A second example refers to EVs, which, under the CAFE program, are awarded with a multiplier [6] that started at 2.5 in 2016 and will still be 1.5 in 2021. PHEV will be awarded with a multiplier too, yet smaller. This means that electrified vehicles will have a strong impact in lowering the average fleet emission.

The regulations are based on a simple Tank-to-wheel approach, which could be misleading. If we consider a Well-to-wheel approach, BEV could result to be not much better than PHEVs or even ICEVs, since its total CO_2 emission depends strongly on how the energy is produced. A BEV running in France, where the energy mix is based in great part on nuclear power will be much "greener" than a BEV running in China, where the energy mix is based on coal. However, not considering these extreme cases, a BEV emits usually less total CO_2 than all other vehicles. Also, it will get better and better as energy mix will move towards renewable and nuclear energy source in the next future, as shown in Figure 14.

2.2.3 OIL SHORTAGES

According to the majority of scientific studies, we've already extracted about half of the global oil reserves, which will therefore end at the beginning of the next century. Figure 14 refers to a forecast by US Department of Energy. It shows that, by the end of the century, we will lack of the nowadays energy backbone (gas and oil), while the total energy demand will continue to grow (due mainly to the increasing world population and of new energy request by fast-developing countries).

Electric vehicles, either with Battery or Fuel Cell storage system, will then be the only solution in that not-so-far scenario. This explains why OEMs are rushing to develop and present electric vehicles even if the demand is very poor at the moment and still will be in the short-medium term (up to 2040).

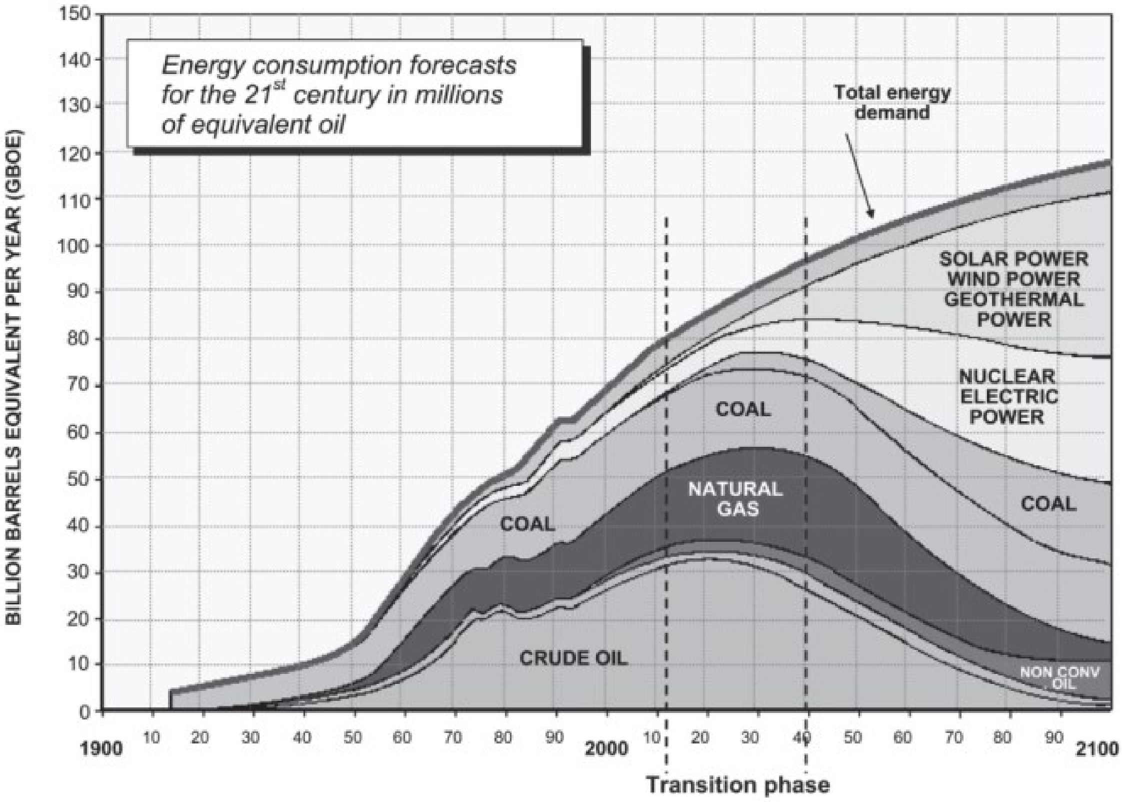

Figure 14. Energy resources estimated future trend. *Source: US Department of Energy*

2.3 INTERNAL ADVANTAGES

The main advantages due to the battery electric vehicle powertrain adoption are analyzed in the following.

Noise level

The main sources of noise emission in a BEV are the tire-road interaction, the powertrain, the brakes and the aerodynamics. Tire-road interaction noise is due mainly to the tread impact on the road surface and on the fluid-dynamic effects of air trapped between two threads. Aerodynamic noise is due to the vortices generated by the vehicle shape when running through air, mainly localized at the lateral mirrors and rear windows areas. Both those noise sources are dominating at high speeds and are equivalent for ICEVs and BEVs. At low speeds, powertrain sound is, instead, the main noise component. Electric motors are rotating machines, thus being balanced and generating less vibrations, and do not rely on combustion, which creates the typical noise. Therefore, at low speeds, it's easy to expect a huge reduction in noise when passing from conventional to electric vehicle [7]. This helps to reduce slow city traffic noise. However, concerns about pedestrian safety are emerging, since people could scarcely hear an electric vehicle approaching. Some solutions with an external noise generator for those occasions are being studied.

On-board efficiency

On-board efficiency refers to the ratio between the mechanical energy at the wheels used for traction purposes and the energy stored in the vehicle, namely the chemical energy of the fuel in an ICEV and the electrical energy of the battery in a BEV. This ratio is inclement towards conventional vehicles: indeed, the internal combustion engine is an extremely inefficient machine, with consistent heat dissipation and frictions. Moreover, the gearbox, which is always present, adds another source of mechanical power dissipation. BEVs' motors dissipations are only due to frictions, which are limited since e-machines are natively rotating machines, and to the Joule and parasitic losses. As an example, the NEDC energy consumption of the 2017 Volkswagen e-Golf is $127\ Wh/km$, compared with the best-in-class gasoline Golf 7, whose energy consumption is $408\ Wh/km$[4].

Anyway, these comparisons are not complete, since, considering a Well-to-Tank approach, the energy consumption of fuel extraction and distribution is much lower as compared to the energy consumption when producing electricity starting from non-renewable sources such as coal or oil. As explained in Chapter 2.2.1, the total energy consumption of a BEV at Well-to-Wheel level depends strongly on how the energy is produced, and could be comparable to that of a conventional vehicle if renewable energies are not in the production mix of the country where BEV is running.

Performance

Performances of electric vehicles are, in general, superior to the conventional ones, especially for what concerns acceleration. This is due to the fact that the electric motors usually have larger power-to-weight ratios and ideal performance curves, with availability of torque at low speeds. Moreover, the simplification of the transmission, due to the possible absence of a gearbox, increases the powertrain efficiency and response times.

Operating cost

Still referring to the two Golfs examples, the *cost-per-km* of the electric one is $0.03\ €/km$, while that of the gasoline one is $0.08\ €/km$[5]. In terms of an annual mission

[4] based on a declared consumption on NEDC declared consumption of $4.9\ l/100km$, considering the gasoline lower heating value as $LHV = 12.06\ kWh/kg$ and the gasoline density $\rho_{gas} = 0.737\ kg/l$.
[5] based on an electricity cost of $0.241\ €/kWh$ and on a gasoline cost of $1.7€/l$.

of $25000\ km$, the annual costs would be, respectively, 750 € and 2000 €. BEVs allow substantial savings in terms of operating cost: however it's easy to understand that this conclusion cannot be generalized, since the amount of saving depends on the relative price of electricity and gasoline.

2.4 DISADVANTAGES

In the following the main disadvantages of a BEV will be listed. All of them are due to the same component, which is the electric battery, the real weak point of the BEVs.

High purchasing price

BEVs are more expensive than their equivalent ICEVs, with the prices that can be easily doubled. This is essentially attributable to the battery, whose cost is dropping but it's still quite high. Indeed, in 2012 the US Energy Department estimated a *cost-per-Wh* which was in the order of magnitude of $1000\ \$/kWh$ [8], while in 2016 many data agreed on a cost dropped to around $273\ \$/kWh$ [9]. Tesla, which is the market leader in battery cost, claims to be already at around 190 $/kWh [10]. The trend is clearly falling down, but costs are still too high for having a real competition with ICEVs. Indeed, assuming an average energy consumption of $200\ Wh/km$ and a desired range of at least $200\ km$, the battery capacity should be at least $40\ kWh$. With the optimistic cost declared by Tesla, the battery price of this simple example is around $8000\ \$$.

Moreover, when considering battery cost, most of the time data are referred simply to the finished cost of the battery. However, the electrochemical storage device brings added costs: for example, a BEV should be, generally, redesigned from scratch since battery integration with the chassis is essential to keep packaging acceptable; moreover, battery recycling at the end of life is usually not negligible, and should be taken into account.

Range anxiety

"Range anxiety" refers to the driver's fear of not reaching its destination with the energy available on-board. This is practically absent in ICEVs for many reasons: their range can easily go up to $1000km$ thanks to the high energy content of the fuel, the infrastructure network for refueling are widespread and the refueling times are contained (usually less than 5 minutes).

Instead, most of BEVs' range is lower than $150km$ and, to make things worse, the range is much more depending on ambient conditions, driving style and auxiliaries' utilization with respect to the ICEVs. This is due to the fact that the electric vehicle on-board efficiency is quite high, so the most of the installed energy is used for traction and every load increase acts directly on the range.

Range anxiety is often claimed to be one of the main limiting factors to the diffusion of electric vehicles. However, this is also helped by misconceptions of the consumers with respect to the range that they believe to travel daily [11]. Indeed, BEVs range is fully compatible at least with every-day city driving, which is the most diffused condition. Instead, a much more important issue should be related to the low availability of charging stations, whose capillary distribution could mitigate a lot this problem.

Charging time

This issue is related to the fact that power transfer from the electric grid to the battery has to be limited for at least two reasons. The first one is related to the battery stressing linked to high power transfers: batteries undergo undesired and irreversible reactions when stressed with high currents, especially during the recharging phase. That is why all the batteries show a limit to the incoming currents, controlled by BMS. Therefore, in order to limit battery depletion of performances or reduction in life-cycles, normal charging has to be done with currents as low as possible, in compatibility with recharging time requirements. Fast charging is available for many cars sold nowadays, and allows charging most of the battery capacity (usually between 80 and 90%) in short times. This has not to be done regularly in order to avoid battery wear: however battery manufacturers are pushing to create batteries able to resist to these charging cycles. This poses the second problem: in order to deliver certain energy to the battery, the smaller the amount of time, the higher the power required. As a reference, $30\ kWh$ to be delivered in half an hour require a power subtracted to the grid of about $60\ kW$. This would be quite challenging if the electric share of the total vehicular fleet will start being non-negligible.

Vehicle weight

The weight of a BEV powertrain is smaller than the one of an ICEV, since electric motors dispose of higher power densities with respect to engines and the transmission of an EV is simplified. However the total weight of a BEV total vehicle is much higher, being impacted by the battery. As an example, a $460\ kJ/kg$ battery with rated capacity of 40 kWh would weight more or less $300\ kg$. In addition to that, battery conditioning systems and restraining system should be considered. The weight increase reduces vehicle dynamic performances and increases energy consumption.

Environmental impact

Virtually all the batteries equipped by BEVs are based on a different shade of the same basic chemistry, which is the Lithium-Ion one. Lithium, however, is not a common metal (it is only the 25th most abundant element in Earth's crust) and the main reserves are concentrated in South America, followed by China and USA.

Lithium is highly reactive and is, therefore, found in rocks, from which it should be mined and separated. Both those operations have a non-null environmental impact. Indeed, mining requires the usage of great amounts of water, which are usually taken from clean sources near to the extraction areas. Moreover, among the separation methods, the most used one in non-advanced countries uses cheap and toxic elements such as PVC [12]. Finally, also the environmental impact at the battery end-of-life should be accounted for, since batteries contain toxic elements and heavy metals, which could cause pollution in the discharge site. Therefore batteries recycling should be addressed, also in order to recover lithium which could be subjected to shortages in the next future. However the cost of battery recycling is, at the moment, not economically profitable.

2.5 MARKET ANALYSIS

The characteristics of the main BEVs sold (as of the beginning of 2018) are registered and compared in order to understand market trends. All of this is shown in Table 4.

CAR	MOTOR	TRANSMISSION	RANGE	CHARGE TIME	STARTING PRICE
Fiat 500e	SMPM Synchronous	Single Speed	140 km	<4h	$34000
Tesla Model S	Induction	Single Speed	500 km	<9.5h	$70000
Chevrolet Bolt	IMPM Synchronous	Single Speed	380 km	<9.5h	$37000
Volkswagen e-Golf	PM Synchronous	Single Speed	200 km	<6h	$31000
BMW i3	Hybrid (IPM+ Reluctance)	Single Speed	180 km	<5h	$45000
Nissan Leaf	IMPM Synchronous	Single Speed	170 km	<4h	$31000

Table 4. BEV market analysis

The following considerations can be made, confirming many affirmations made in the previous chapters of this thesis:

- Concerning the type of motor adopted, there's not a clear trend, with different manufacturers following different approaches. However, the IPM synchronous machine, especially in hybrid solutions, seems to be the most efficient one, as explained also in Chapter 1.3.2. To support this thesis, one could argue that BMW i3 is the one, among the list, having the smallest EPA rated fuel economy (172 Wh/km), even if the result is also influenced by the small size of the car.
- All the electric vehicles analyzed in the table are not equipped with a gearbox, while they all count on a single speed reduction ratio. This implicitly tells that, probably, the increase in efficiency that can be obtained by a gearbox is not

compensated by the additional costs and complexity. This issue will be addressed in the following of this work, supported by simulation results.

- Usually the manufacturers propose different batteries size with different estimated range. Therefore the ranges reported in the table are only referred to a particular configuration of the vehicle and work as an order of magnitude. However, it is interesting to note that the most sold electric vehicle, which is the Nissan Leaf with ~300'000 units, is among the ones with the smallest range. This is mainly due to its early access to the market and to the low price. Also, this helps to understand that range anxiety can be easily overcome, while the price of the BEV remains the principal element steering the market.
- The recharging times are scaled with the battery capacity. However, for all the cars in the list fast-charging is available, with different potentialities.
- The price is largely dependent on the vehicle segment and on the battery capacity. However, in all the cases, it is largely higher than the price of a similar segment ICEV.

3. MODEL OF VEHICLE AND REAL MISSION

3.1 INTRODUCTION

One of the main working areas of this thesis has been the development of a program, written entirely in Matlab® code, whose objective is to simulate the longitudinal working of a BEV running in given conditions. In particular, the program is based on a kinematic approach, calculating the required power for motion starting from the speed profile. The building blocks of the program are the models of each piece of the vehicle, from the main powertrain component ones to the auxiliaries. Also, a model for a realistic mission has been created, in order to make the program able to give real-world predictions of the energy consumption of the vehicle.

The resistance model has experimental nature, being based on the application of coast-down coefficients for calculating the resistant forces acting on the vehicle at a given speed. The transmission model is simply obtained by applying speed-reduction laws and considering a constant mechanical efficiency. The electric motor is considered by application of an efficiency map, based on the machine torque and speed. Finally, the battery is modeled as a simple battery-resistance circuit, allowing the evaluation of the State of Charge (SOC). All those models are slightly different if referred to the case of regenerative braking.

Auxiliaries modeling is extremely important in order to evaluate their impact on the real-driving energy consumption. The most consuming auxiliary is by far the air conditioning system: its model includes a cabin thermal model and a fixed COP model differentiated for the cases of cooling and heating. Also the action of battery heating system in cold condition has been modeled based on experimental data. Other, less relevant, models include those of the lights and of the generic auxiliaries.

Finally, a realistic mission has been generated. It is made by 1000 cycles, each of which with its own speed profile, number of passengers, ambient temperature, daytime, initial SOC of the battery.

This chapter will give an insight of the solutions adopted for all the models. In certain cases discarded solutions will also be shown, although with few details.

3.2 RESISTANCE MODEL

3.2.1 LONGITUDINAL DYNAMICS EQUATION

The resistance model is able to calculate what the required power at the wheels is for each operating condition. Indeed, the longitudinal dynamics equation (in terms of force and power) can be written as:

$$F_{traction} - F_{res} = M_{eq}\frac{dV}{dt} \tag{1}$$

$$P_{traction} - P_{res} = M_{eq}V\frac{dV}{dt} \tag{2}$$

where $F_{traction}$ is the traction force, F_{res} is the sum of all the resistance forces and M_{eq} is the equivalent mass of the vehicle, which takes into account both the translational inertias and the inertia of rotating components. The resistant forces are mainly:

- Rolling resistance;
- Aerodynamic drag;
- Slope resistance.

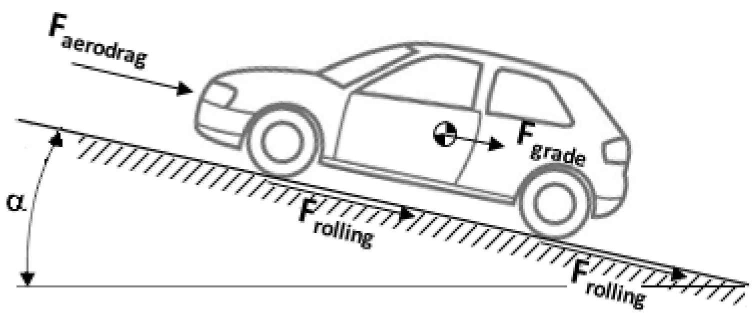

Figure 15. Forces acting in the longitudinal motion of the vehicle

This is shown in Figure 15. The traction force at the wheels can be written rearranging Eq. 1:

$$F_{traction} = F_{res} + M_{eq}\frac{dV}{dt} \tag{3}$$

Since the traction force (and power) depends directly on the speed profile over time, it is common to define this approach as "kinematic". The kinematic approach reverses the real power flow from the energy storage system to the wheels; instead, it is supposed that the vehicle is exactly able to follow a certain speed profile which determines the power required at the wheels. Then, going upstream of the powertrain, the power required at the motor can be calculated. The kinematic approach opposes to the dynamic approach, which instead, starts by providing a certain motor power and, going downstream of the powertrain, on the basis of the actual vehicle speed, calculates the acceleration of the vehicle. In order to follow the desired speed profile, a controller on the power delivered is needed, based on the error in following the speed profile. This controller usually tries to replicate the human reaction to the power delivery control when following a route. The dynamic approach is closer to the real working operation of the vehicle, but it’s more complex than the kinematic one and its performances are only slightly superior, depending strongly on the accuracy of the driver control model. This is the reason for choosing, in this work, a kinematic approach over a dynamic one.

Equivalent mass

The equivalent mass of the vehicle is defined as the mass of a body that moves linearly at the same speed of the vehicle and has the same kinetic energy. The equivalent mass will be such as to verify the equation:

$$\frac{1}{2}M_{eq}V^2 = \frac{1}{2}MV^2 + \frac{1}{2}(4J_w)\omega_w^2 + \frac{1}{2}J_m\omega_m^2 \tag{4}$$

where ω_w and ω_m are the rotational speeds of wheels and motor respectively and J_w and J_m the relative inertias. Only the inertias of wheels and electric motor are considered, while the one of the final drive is neglected.

At this stage, remembering that:

$$\begin{cases} \omega_w = \dfrac{V}{r_d} \\ \omega_m = \dfrac{V}{r_d}\,\tau_{t,i} \end{cases} \tag{5}$$

where $\tau_{t,i}$ is the reduction ratio of the engaged gear “i”, it is easy to demonstrate that:

$$M_{eq} = M + 4\frac{J_w}{r_d^2} + \frac{J_m}{r_d^2}\tau_{t,i}^2 \tag{6}$$

All the parameters in the latter equation are known powertrain parameters, except for the wheel inertia, which depends on the manufacturer of the wheel. However, it is common practice to consider the moment of inertia approximately proportional to the tire rolling radius. In this thesis it is hypothesized that the moment of inertia of a single wheel is calculated as:

$$J_w = 10r_d - 2.2 \tag{7}$$

where the rolling radius r_d is expressed in meters and the moment of inertia in kgm^2.

For the vehicle considered in this thesis the equivalent mass results to be

$$M_{eq} = 1.037 \cdot M$$

that is greater by 3.7%[6] than the test mass. This factor can be considered constant only when no gearbox is applied, otherwise it would change as a function of the engaged gear.

Rolling resistance

The rolling resistance is due to energy dissipation occurring at the tire/ground contact area when a wheel is rolling: energy is dissipated because, when the part of tire deformed[7] by the contact pressure springs back after leaving the contact area, it will be dampened by the tire itself, which is made of rubber. With reference to Figure 16, it can be seen that, when the wheel is rolling, the contact pressure is higher in the front part of the wheel: this produces a force with a small arm that results, in turn, in a resisting torque at the wheel. The torque is discharged at the wheel hub as a force opposing motion, the rolling resistance force, which has the following mathematical expression:

$$F_r = \frac{-F_z \Delta x + M_f}{r_d} \tag{8}$$

where M_f is the moment at the wheel hub due to the wheel aerodynamic drag and to the bearings friction, F_z is the total vertical force obtained by integration of the pressure distribution and Δx is the arm of F_z.

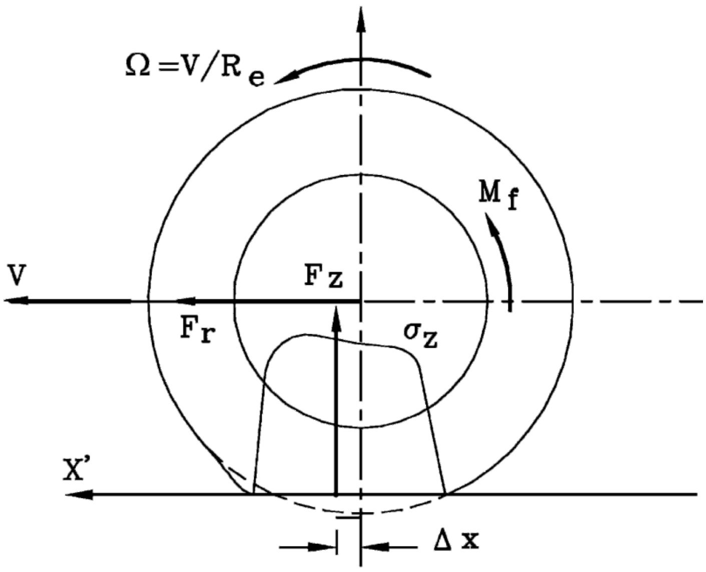

Figure 16. Contact pressure distribution of a wheel under traction torque

[6] A factor ranging between 3% and 5% is common for passenger cars application.

[7] Actually some energy could be dissipated in the ground too if it were compliant. Under the assumption that ground is always concrete, its deformation can be neglected and so will be the part of rolling resistance due to the dissipation in the ground.

However, all the parameters in Eq. 8 are difficult to be determined, so it is commonly assumed that the rolling resistance is simply proportional to the vertical force acting on the wheel, with a proportionality coefficient called "rolling coefficient" f_{roll}. At vehicle level the total rolling resistance is:

$$F_{rolling} = f_{roll} M g cos(\alpha) \tag{9}$$

where α is the slope angle. The rolling coefficient main dependence is versus speed. Usually a polynomial expression of the type $f_{roll} = \sum f_i V^i$ is adopted: in particular, the second order polynomial usually matches with a good approximation experimental data.

$$f_{roll} = f_0 + f_2 V^2 \tag{10}$$

Other parameters affecting rolling resistance are the tire structure and material, the wear, the operating temperature, the inflating pressure and vertical force, the tire size, the type of road and the angles of sideslip and camber.

Aerodynamic drag

Every object moving inside a fluid is subjected to aerodynamic forces due to the effects that it produces on the fluid: this is also true for a vehicle moving through air. If the fluid had no viscosity, no energy would be dissipated in the movement, which means that the distribution of pressure around the vehicle would compensate in all directions with no net effect. However all fluids have a certain degree of viscosity, which causes the following two effects[8]:

- Direct friction caused by tangential forces. Indeed, while air is at standstill away from the vehicle surface, it will move at the same vehicle speed in a thin layer adjacent to its surface, causing different air layers to slide on each other. Due to viscosity this sliding results in a drag on the vehicle;
- The pressure distribution caused by the presence of the moving vehicle in the air will not balance itself due to energy dissipation: this means that aerodynamic forces and moments in all directions could arise. In particular, the most important is the force along the vehicle moving direction, which is called aerodynamic drag or shape drag. Indeed, when the vehicle moves it will push the air in front of it and part of the air cannot move out of the way, thus creating a high pressure stagnation point. Instead behind the vehicle a low pressure wake area is present, caused by the fact that air cannot fill instantaneously the space left empty by the vehicle forward motion. The net effect is force opposing motion.

It is difficult to consider all the contributions to the drag and a common approach is the experimental one. It has been observed that the total aerodynamic drag force is proportional to the dynamic pressure $p_d = \frac{1}{2}\rho V_r^2$ and to the vehicle frontal surface area A_f:

[8] Actually in some special applications, such as aeronautical ones, a third effect of the pressure distribution contributes to the total drag, which is called induced drag. It is caused by the fact that, in order to generate lift, some energy has to be spent. In fact, a wing works by generating a delta pressure between its bottom and top: this difference in pressure causes dissipating vortexes in the fluid after the wing has left it.

$$F_{aerodrag} = \frac{1}{2}\rho_{air} V_r^2 A_f C_D \tag{11}$$

where ρ_{air} is the air density, V_r is the vehicle speed relative to the wind (if the wind speed is null it corresponds to the vehicle speed) and C_D is the drag coefficient, which characterizes each vehicle. In particular, the drag coefficient depends on:

- The vehicle external shape, which is especially influencing the wake dimension and detachment point;
- The drag due to the wheel rotation, which creates a very chaotic fluid flow on the vehicle side and in the wheel compartment and thus energy dissipation. Some solutions are implemented to reduce this component of the drag, such as the wheel streamlining or the smoothening of wheel compartment (Lokari®);
- The internal flows, which consist mainly in the one passing through the radiator for cooling purposes and the one going in the passenger compartment, both chaotic and generating drag. BEVs, from this point of view, are more efficient than ICEVs, since the aperture on the front is smaller, being the cooling requirements reduced.

The reduction of drag coefficient is especially important for high-speed and competition vehicles, while for cars driving in urban environment its value has less importance. This is because the aerodynamic drag force depends on square of the speed, and, therefore, it becomes prevalent at high speeds. In particular, it is common to compare the laws of rolling and aerodynamic resistant forces on the same plot, as in Figure **17**, in order to individuate the so-called "characteristic speed", which is the speed at which rolling resistance and aerodynamic resistance attain the same value. Aerodynamic drag becomes prevalent after this speed. Analytically:

$$V_{char} = \sqrt{\frac{f_0 Mgcos(\alpha)}{f_2 Mgcos(\alpha) + \frac{1}{2}\rho C_D A_f}} \tag{12}$$

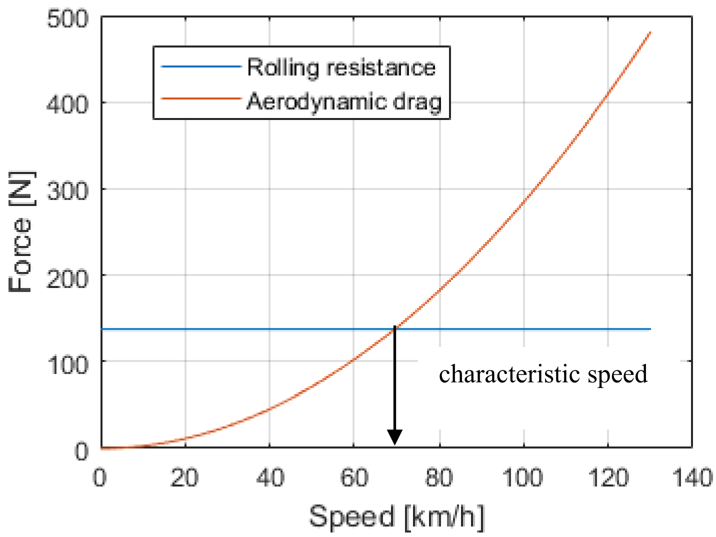

Figure 17. Characteristic speed

As a reference, a vehicle traveling on level ground, with $M = 1400kg, f_0 = 0.01, f_2 = 0, C_D = 0.3, A_f = 2m^2$, has a characteristic speed of $V_{char} = 70\ km/h$.

Slope resistance

When a vehicle is travelling on a slope, its weight will have two components: one of these, scaled by the cosine of the grade angle, is perpendicular to the ground and represents the vertical force acting on the wheels; the other one, scaled by the sine, is in the vehicle moving direction, either supporting or opposing the motion, depending on the descending or climbing grade. This force is expressed by

$$F_{grade} = Mgsin(\alpha) \tag{13}$$

In this work all routes will be considered on flat roads, so, from now on, this component will always be neglected.

3.2.2 COAST-DOWN FORCE

Expanding the total resistant force, it is possible to write down:

$$F_{res} = \frac{1}{2}\rho V^2 A_f C_D + (f_0 + f_2 V^2)Mg = F_0 + F_1 V + F_2 V^2 \tag{14}$$

where slope has been considered absent and

$$\begin{cases} F_0 = f_0 Mg \\ F_1 = 0 \\ F_2 = \frac{1}{2}\rho A_f C_D + f_2 Mg \end{cases}$$

Actually, this form of the resistant force is adopted frequently as, instead of calculating theoretically all the parameters, just $F_0, F_1$and F_2 are determined through experimental test, using the so-called *coast-down method*.

The test consists in accelerating the vehicle to speeds up to $130\ km/h$, after which, if a gearbox is present, it is placed in neutral position, and the vehicle is let decelerate naturally[9]. In these conditions the vehicle deceleration will be directly linked to the action of the resistant forces described before[10], and Eq.1 becomes:

$$-F_{res} = -(F_0 + F_1 V + F_2 V^2) = M_{eq}\frac{dV}{dt} \tag{15}$$

---

[9] There are at least two standards, EEC and SAE, which are slightly different, describing in detail how to conduct the test and to extrapolate the coast-down coefficients from the experimental results.

[10] Actually other resisting actions should be considered, such as the residual brake action F_{brk} (which is due to misassembly) and the frictions in the driveline downstream of the motor $F_{driveline}$ (in particular in the final drive and in the bearings supporting the shafts). Indeed the traction force at the wheels is not exactly equal to the one at the motor, being $F_{traction} = F_{motor} - F_{driveline} - F_{brk}$. In the coast-down approach $F_{motor} = 0$, while the others are non-null.

The measurement of the vehicle speed as a function of time is enough to determine, through regression of the data, the coefficients F_0, F_1 and F_2. In this work, experimental values of the coast-down coefficients are used. However, as it is easy to understand, the values obtained are exact only when considering the same conditions of the test, in particular in terms of running mass, while an error is made if the running mass is different from the test one. In order to correct this error, the F_0 coefficient will be corrected depending on the running mass.

$$F_{0,corr} = F_0 \frac{M_{run}}{M_{test}} \tag{16}$$

3.3 VEHICLE CABIN THERMAL MODEL

The vehicle cabin thermal model is necessary in order to estimate the heating or cooling requirement for passenger comfort when air conditioning is working. Passenger comfort is a matter subject to many studies and requires a thermofluidodynamic design of the air conditioning flows: indeed, the temperature distribution is not homogeneous inside the cabin, and can vary a lot depending on the location. For example, the passengers head areas are usually more interested by heating/cooling flows with respect to the feet area, and, therefore, the temperatures of these two areas will be quite different [14]. In this thesis passenger comfort is not studied in detail and, therefore, temperature distribution study is not interesting. Instead, taking into account literature research [15,16], the vehicle cabin is modeled as a concentrated parameters body, which means that the entire cabin is assumed to have the same thermodynamic properties and, in particular, the same temperature. This simplification is possible since the main objectives of the cabin thermal model are the air conditioning thermal loads and the average cabin temperature, while the actual temperature distribution inside the cabin is not needed.

The equation governing the heat exchange is:

$$TM \frac{dT_{cab}}{dt} = \sum \dot{Q}_{load} \tag{17}$$

where TM is the thermal mass of the cabin, dT_{cab}/dt is the temperature variation and $\sum \dot{Q}_{load}$ is the summation of all the thermal loads acting on the cabin. The thermal loads are:

- Ambient load;
- Internal load;
- Metabolic load;
- Solar load;
- Ventilation load;
- Conditioning load.

Thermal mass

TM is the thermal mass of the cabin, expressed in $J/°C$. It represents the thermal inertia of the system, opposing temperature changes. Indeed, we can see from Eq. 17 that, given a certain constant thermal load, the higher the thermal mass, the smaller the temperature change. The thermal mass is made up of two main components: the cabin air and the objects in the passenger compartments.

$$TM = c_{p,a}\rho_a V_{cab} + DTM \tag{18}$$

The air thermal mass can be easily determined once the volume of the cabin is estimated, since the air density and specific heat are known. The thermal inertia of other objects inside the passenger compartments (such as seats, plastic covers, dashboard), called Deep Thermal Mass (DTM), is much more difficult to be determined. Indeed, those objects are made by many different materials whose weight is often unspecified. Moreover, the objects to be considered in the DTM are those which will attain the same temperature of the cabin, contributing to its inertia: however, no object inside the cabin will reach exactly the same temperature as that of the air, so some of these will contribute more and some less to the total extent of the thermal inertia.

Usually the air inertia is quite small with respect to the total cabin one. To make an example, a small A-class vehicle with $V_{cab} = 3.5\ m^3$, if air properties are considered to be $\rho_a = 1{,}2\ kg/m^3$ and $c_p = 1005\ J/kgK$, will have $c_{p,a}\rho_a V_{cab} = 4200\ J/K$. DTM can reach a value even ten times larger. The total thermal inertia, as found during the literature research stage of this work, lies in the range $TM = 7 \div 70\ J/K$ [17,18].

Ambient load

The ambient load is the thermal load due to the difference in temperature between the air inside the cabin and the one outside it. This generates a heat flow through the walls of the compartment. In order to have an analytical expression, the thermal resistance approach is considered. This approach consists in writing all the heat exchanges in the form:

$$\dot{Q} = \frac{1}{R_{therm}}\Delta T \tag{19}$$

The resistance is then specified:

- $R_{conv} = 1/hA$ in the case of heat exchanged by convection, where $h\ [W/m^2K]$ is the convection coefficient and $A\ [m^2]$ the heat exchange area;
- $R_{cond} = s/kA$ in the case of heat exchanged by conduction through solids, where $s\ [m]$ is the thickness of the solid layer, $k\ [W/mK]$ its thermal conductivity and $A\ [m^2]$ the heat exchange area.

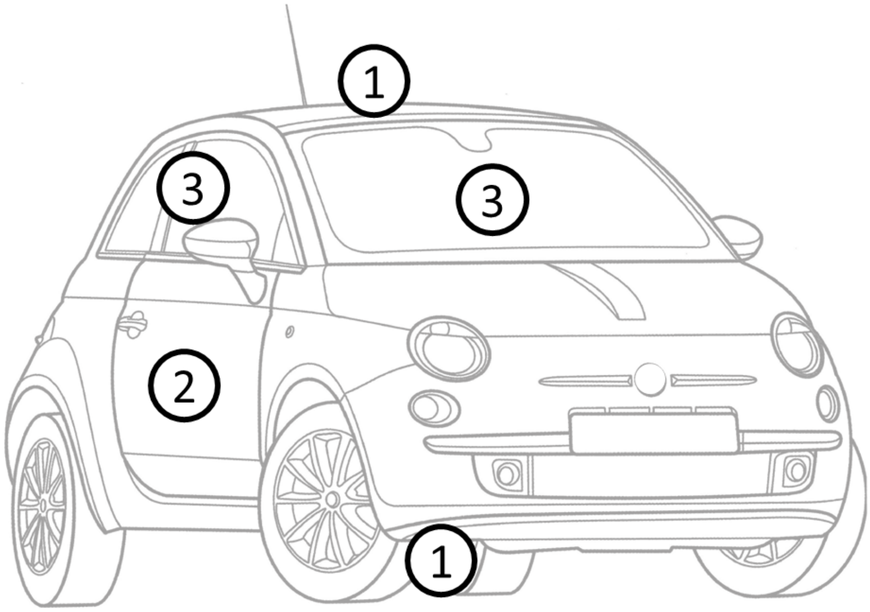

Figure 18. The wall types of a vehicle cabin.

In this thesis the vehicle compartment is considered to be contained by three main "walls" types, represented in Figure 18:

1. Roof and underbody. These two walls are made of two metal layers sandwiching one insulating layer.
2. Doors. Door structure is quite complex, being made of metal layer, plastic covers and insulating materials. To simplify an equivalent single-layer door model, developed by Möller and Sörensen [19], has been adopted.
3. Windscreen and windows. This type of wall is made by a single layer of glass.

Table 5 shows all the resistances associated to the three wall types.

#	Component	Conduction resistance	Convection resistance	Total conductibility
1	Roof and underbody	$R_{cd,1} = \frac{s_{m1}}{k_{m1}A_1} + \frac{s_{is1}}{k_{is1}A_1}$	$R_{cv,1} = \frac{1}{hA_1}$	$C_1 = \frac{1}{R_{cd,1}} + \frac{1}{R_{cv,1}}$
2	Doors	$R_{cd,2} = \frac{s_{eq.2}}{k_{eq,2}\, A_2}$	$R_{cv,2} = \frac{1}{hA_2}$	$C_2 = \frac{1}{R_{cd,2}} + \frac{1}{R_{cv,2}}$
3	Windscreen and windows	$R_{cd,2} = \frac{s_{g,3}}{k_{g,3}\, A_3}$	$R_{cv,3} = \frac{1}{hA_3}$	$C_3 = \frac{1}{R_{cd,3}} + \frac{1}{R_{cv,3}}$

Table 5. Thermal resistances and conductibility of the main wall types of the vehicle cabin

The values adopted for all the parameters featuring in the previous Table 5 are either estimated or adopted based on literature research outcomes. The convection heat exchange coefficient has been found to be a function of the relative speed between the walls and the air:

$$h = 0.6 + 6.64\sqrt{V} \tag{20}$$

The ambient load will result from the summation of the heat exchanged through the three walls:

$$\dot{Q}_{amb} = (C_1 + C_2 + C_3)(T_{cab} - T_{amb}) \tag{21}$$

Internal load

The internal thermal load is due to all those components which, during their functioning, will heat up and, possibly, exchange heat with the passenger compartment. This load cannot usually be neglected for ICE based vehicles. Their engine, operating at high temperatures, is usually positioned close to the firewall separating passenger compartment and engine compartment and part of the heat rejected can flow through it. Moreover, hot exhaust gases pass through pipes which are just below the vehicle cabin, and a small fraction of heat can be exchanged also in this case. This thesis, however, is focused on a BEV, whose motor rejects much less heat with respect to a petrol motor, so that its thermal load on the cabin can be neglected. Instead, a BEV usually has a battery positioned just below the cabin: the battery operates at temperatures in the range $20 - 40°C$. This could cause a certain load on the cabin. However, for simplicity, also this load has been neglected. Therefore, no internal loads will be considered.

Metabolic load

Metabolic load is due to the sensible (due to a difference in temperature) and latent (due to phase transition) heat generated by a human being. Usually this load depends on many factors, such as the age of the passenger, the dressing and its activity (driving, resting, etc.). In literature many different works can be found, approaching this issue [15]. The most detailed one estimates the thermal flux generated by the driver and by the passenger. The first one is higher ($85\ W/m^2$), due to activity and concentration while driving, while the second one is sensibly lower ($50\ W/m^2$), as the passenger is just resting. The actual loads are then calculated multiplying the flux by the bodies' areas, which can be expressed with the Du-Bois formula:

$$A_{body} = 0.202\ W^{0.425} H^{0.725} \tag{22}$$

where W and H are respectively weight and height.

In literature are also common some approaches that take into account just an average heat generated by each passenger. Usually this average value is

$$\dot{Q}_{met} = 100\ W/pass$$

The values obtained with the two approaches are close to each other. In this thesis, for simplicity, the second formulation is adopted.

Solar load

This load is due to the solar radiation which can heat up the passenger compartment in three ways:

1. Direct radiation: it's the part of solar radiation which directly hits the vehicle surface.
2. Diffuse radiation: it's the part of solar radiation which hits the vehicle surface after being diffused through clouds or fog.
3. Reflected radiation: it's the part of solar radiation which hits the vehicle surface after being reflected by the ground.

The formulations of these loads can be found in literature [20] and are complex functions of vehicle radiation area and transparency, ground reflectivity, daily hour, position and orientation of the car on the globe. This makes the rigorous implementation of the formulae beyond the scope of the thesis. Instead a simplification is made, considering a single constant radiation load.

Ventilation load

HVAC systems work cooling down or heating up the cabin air, which is continuously recirculated. Indeed, conditioning new air coming from outside all the time would be too expensive in terms of energy. However, this causes accumulation of the CO_2 emitted by passengers while breathing. In order to avoid unpleasant levels of carbon dioxide, a small ventilation of air from outside is allowed. The enthalpy of this air will be different from the one already conditioned inside the cabin and, then, will bring a certain ventilation thermal load, which can be quantified in:

$$\dot{Q}_{ven} = \dot{m}_{ven}(h_{amb} - h_{cab}) \tag{23}$$

where $\dot{m}_{ven}$ is the air-mass flux, h_{amb} and h_{cab} are the enthalpies of ambient and cabin air respectively. Their formulation is the following:

$$h = 1006 \cdot T + (2.501 \cdot 10^6 + 1770 \cdot T)X \tag{24}$$

where all the temperatures are expressed in degree $K$and X is the humidity factor, which is expressed as:

$$X = 0{,}62198 \frac{\varphi p_s}{100 p_{amb} - \varphi p_s} \tag{25}$$

In this expression φ is the relative humidity, p_{amb} is the ambient pressure and p_s is the water saturation pressure at the actual ambient temperature. This last value can be either read from a water-properties table or calculated with semi-empirical correlations, such as the Antoine equation:

$$\log_{10} p_s = 8.0713 - \frac{1730.63}{233.426 + T} \tag{26}$$

A fixed ventilation strategy with $\dot{m}_{ven} = 0.01 kg/s$ has been adopted in this work.

Conditioning load

The conditioning load is the one caused by the air conditioning system in order to heat up or cool down the cabin. The formulation of this load depends mainly on its working strategy. In this work it has been assumed that the conditioning load is controlled through a PI controller in order to reach an objective temperature T_{obj}. The formulation will, then, be:

$$\dot{Q}_{AC} = k_P(T - T_{obj}) + k_I \int (T - T_{obj}))dt \quad (27)$$

The proportional and integrative coefficients should be different when considering heating or cooling modes: indeed, the vehicle considered is assumed to be provided with an HVAC system for cooling and with a PTC resistor for heating. The coefficients need to be calibrated based on conditioning performance requirements.

3.4 HVAC AND PTC MODELS

Once the thermal conditioning load is calculated, it is necessary to understand how this load will translate to an electrical load on the battery.

The air conditioning system for cooling purposes is based on the classic air-conditioning scheme, made of compressor, radiator, evaporator and expansion valve. It was explored the possibility of having a complete thermodynamic model of the cycle: however, the lack of data and the increased complexity made this possibility unfeasible. Instead, a simple model with fixed Coefficient of Performance (COP), has been adopted. COP, in a thermodynamic cycle, is defined as the ratio between the useful thermal power and the spent mechanical power. In the case of the HVAC:

$$COP = \frac{\dot{Q}_{evap}}{P_{comp}} \quad (28)$$

where $\dot{Q}_{evap}$ is the thermal load at the evaporator, which corresponds to the previous conditioning load $\dot{Q}_{AC}$, and P_{comp} is the power required at the compressor. Literature research has provided an average COP in the range $2 \div 3$ [21]. The actual value is calculated through calibration of the simulation over real-world data.

The heating system, instead, is made by a PTC resistor, which is a particular resistor which increases its resistance with temperature in order to limit the current adsorbed. It works exploiting the Joule effect:

$$\dot{Q}_{heat} = R_{PTC} I^2 \quad (29)$$

Being its operational principle based on energy dissipation, in this case the COP is smaller than unity. Also in this case, the actual value is calculated after calibration of the thermal model.

3.5 TRANSMISSION MODEL

The transmission is adopted in order to adapt the electric motor operating points, in terms of torque and speed, to the road requirements. Since an electric motor for vehicular applications can spin at speeds up to $15000\ rpm,$ a reduction of the speed to the wheels is necessary, with a consequent increase of torque. The speed reduction is, generically, obtained in two stages:

1. A gearbox stage, where the reduction ratio can either be discretely or continuously variable depending on the type of gearbox adopted;
2. A final drive stage, which is usually implemented together with the differential that brings the torque from the transmission shaft to the wheels.

The reduction ratios of the two stages are written as follows:

$$\begin{cases} \tau_{gbx,i} = \dfrac{\omega_{mot}}{\omega_{gbx,i}} \\ \tau_{fin} = \dfrac{\omega_{gbx,i}}{\omega_{wheels}} \end{cases} \tag{30}$$

where ω_m is the motor speed, $\omega_{gbx,i}$ is the gearbox output speed and ω_w is the speed of the wheels. The total reduction ratio is then written as:

$$\tau_{t,i} = \frac{\omega_{mot}}{\omega_{wheels}} = \tau_{gbx,i}\tau_{fin} \tag{31}$$

Since a kinematic approach is adopted, the wheel speed is fixed by the speed profile of the cycle by the relation

$$\omega_w = \frac{V}{r_d} \tag{32}$$

and Eq. (31), can be reversed to obtain the motor speed:

$$\omega_{mot} = \omega_w \tau_{t,i} \tag{33}$$

The transmission model also takes into account friction and aerodynamic losses in the gears, bearings and so on. Usually this type of losses depends on the transmission shaft speed and transmitted torque. However, a simplification has been introduced, considering constant transmission efficiency in the range $\eta_{tra} = 0.91 \div 0.95$ for all the transmitted torques and speeds. Thus, the power to be delivered by the electric machine, is related with the one required at the wheels by the relation:

$$P_{em} = \frac{P_{traction}}{\eta_{tra}} \tag{34}$$

In conclusion, the torque to be delivered by the electric machine is:

$$T_{em} = \frac{P_{em}}{\omega_{mot}} \tag{35}$$

3.6 ELECTRIC MACHINE AND INVERTER MODEL

The electric machine is made by a SMPM synchronous machine, with an integrated inverter. An estimated machine efficiency map is used, as shown in Figure 19.

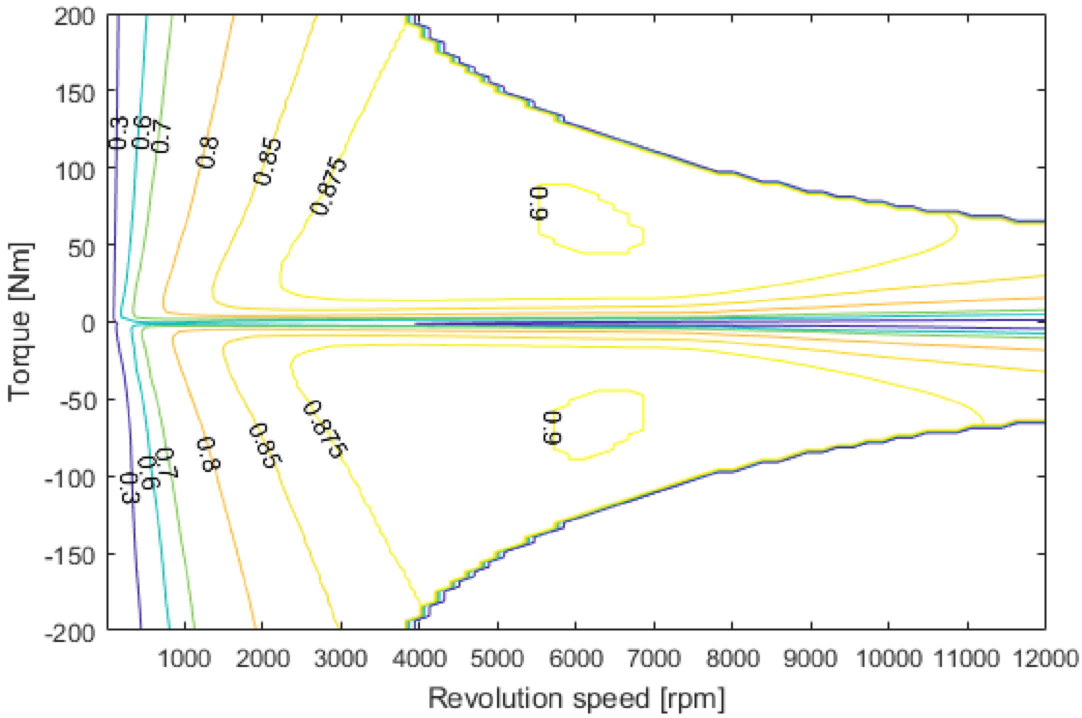

Figure 19. E-machine and inverter efficiency map

Table 6 reports the machine main specifications.

Base speed	$4000 rpm$
Maximum speed	$12000 rpm$
Maximum torque	$200\ Nm$
Maximum power	$85\ kW$

Table 6. E-machine main specifications

It is clear that, by entering the map with the machine torque and speed, its efficiency can be obtained. The electric power to be delivered by the battery is then simply obtained as:

$$P_{batt} = \frac{P_{em}}{\eta_{em}} \tag{36}$$

3.7 BATTERY MODEL AND BATTERY MANAGEMENT SYSTEM

The battery considered in this work is a Lithium-Ion battery. The cell model is a simple electric circuit with a voltage generator, representing the open circuit voltage (OCV) $E_{0,cell}$, and a resistor, representing the internal resistance $R_{int,cell}$. The circuit is shown in Figure 20. Both the OCV and the internal resistance are modeled as a function of the SOC only, based on experimental data.

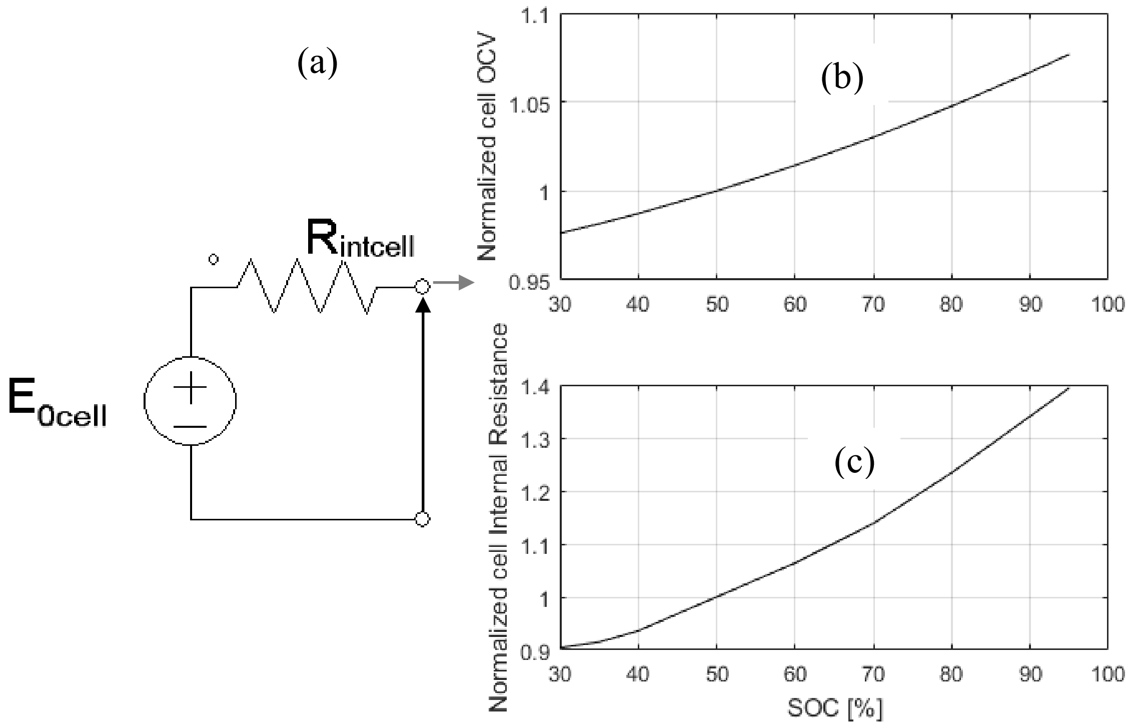

Figure 20. Battery model: (a) electrical scheme, (b) normalized cell OCV and internal resistance variation with SOC

It is assumed that all the cells are put in series and that the OCV and internal resistance at battery level are just the sum of all the cells ones. At a given instant of time, if the SOC is known, also E_0 and R_{int} of the battery are known. The power going out of the battery can be written as:

$$P_{batt} = (E_0 - R_{int}I)I \tag{37}$$

This is a second order equation, which can be solved in the variable I:

$$I = \frac{E_0 - \sqrt{{E_0}^2 - 4R_{int}P_{batt}}}{2R_{int}} \tag{38}$$

Thus, the SOC evolution in time will be calculated as:

$$SOC = \int \frac{I}{C_0} dt \tag{39}$$

The battery has limits in terms of maximum currents that can be handled safely. All currents outside those limits are cut to the limit value, therefore cutting also the power in demanding conditions. The limit in charging, which is much more stringent, will have an impact on the regenerative braking effectiveness.

The battery model has no dependence on the cell temperature, since no data were available in this sense. However, it is well known that the efficiency of the battery at low temperature drops dramatically, as explained in Chapter 1.6, so that a Battery Management System (BMS) is usually present on a BEV. At low temperatures, the main function of the BMS is to heat up the battery to its optimal temperature operating range, which for Lithium-Ion batteries is around 20-40°C.

A simple BMS model is developed, based on experimental data coming from a real-world application. The heating element is assumed to be a PTC resistor working at constant power $P_{PTC,b}$. The heating requirements are expressed in terms of total energy to be delivered $E_{PTC,req}$: the coldest the ambient temperature, the higher the energy required. In particular, the energy to be delivered is assumed to be linearly variable in the interval $-10 \div 10°C$, as shown in the Figure 21.

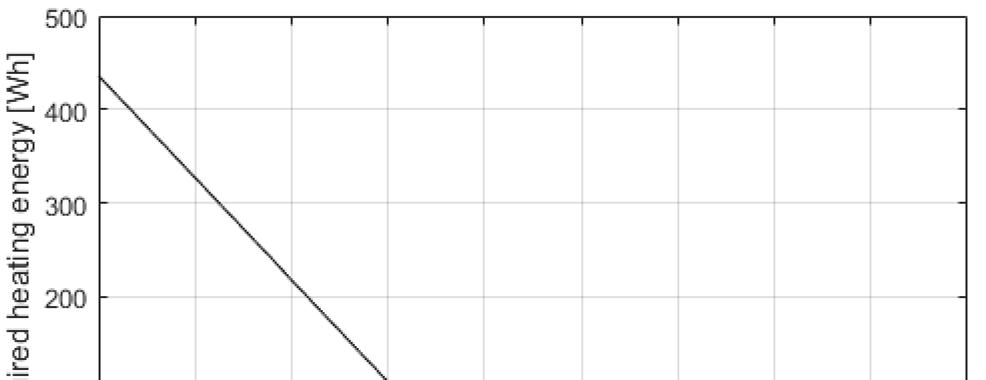

Figure 21. Energy requirement for battery heating for different ambient temperatures

Being power and energy known, it is easy to calculate how long the BMS will heat up the PTC resistor:

$$t = \frac{E_{PTC,req}}{P_{PTC,b}} \tag{40}$$

3.8 GENERIC AUXILIARIES MODEL

In this model, all the other accessories and auxiliaries not considered before are present, such as radiator fan, ECU fan, battery and motor coolant pumps, dashboard and cabin lights, EPS, etc. A part of these auxiliaries will be always running and adsorb a constant power, while another one will be variable and depend on some operating conditions. The main dependency has been found to be the external temperature, which influences mainly the power required by the fans and pumps. An empirical law for the power required by those auxiliaries has been set, based on experimental data. It is shown in Figure 22.

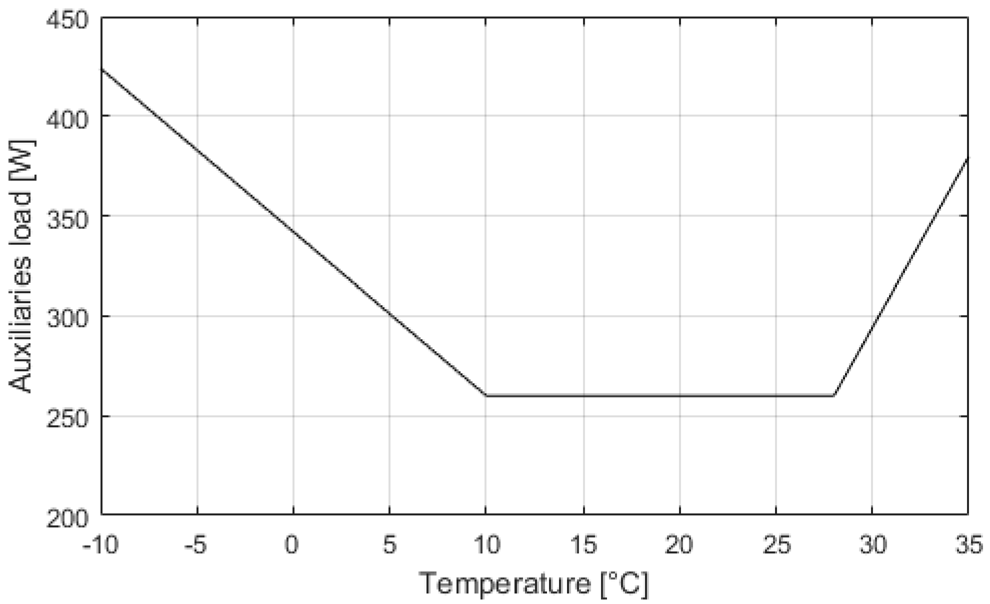

Figure 22. Auxiliaries load as a function of ambient temperature

3.9 LIGHTS MODEL

A separate model with respect to the generic accessories' one has been created for the lights, in order to take into account the dependence of the adsorbed power with respect to the daily hour, which is one of the characteristics of the cycle. The power requirements, of course, depend on the type, style and dimensions of the lights installed on the vehicle. In this thesis, after some literature and market research [22], the values in Table 7 were used. In particular, the considered components are

- For travels in the light: Daytime Running Lamp (DRL), tail light, stop light[11], license plate light.
- For travels in the dark: Low Beam, tail light, stop light, license plate light.

[11] Stop lights should only illuminate when braking. Making reference to the mission described in Chapter 3.11, the braking accounts for 34% of the running time. Then, the average value of power adsorbed by stop lights is 34% of their rated power.

For traditional lighting system, the power required in the two conditions is, respectively, 45W and 100W. For LED lighting system, those values become 15W and 69W.

Function	Power per lamp (W)	
	Traditional system	LED system
DRL, dedicated	22.9	11.4
Low beam	56.2	54.0
High beam	63.9	34.4
Parking/position	7.4	1.7
Turn signal, front	26.8	6.9
Side marker, front	4.8	1.7
Stop	26.5	5.6
Tail	7.2	1.4
CHMSL	17.7	3.0
Turn signal, rear	26.8	6.9
Side marker, rear	4.8	1.7
Backup/reverse	17.7	5.2
Licence plate	4.8	0.5

Table 7. Power adsorption of vehicle lights

3.10 REGENERATIVE BRAKING

All of the equations presented before were implicitly assuming to be in the traction case, where the motor is providing useful torque to the wheels. In the case of braking, the powers calculated with the kinematic approach are negatives and some of the equations previously presented modify slightly, since the efficiencies will act in the reverse path, from wheels to the motor. In particular Eq. 34 becomes

$$P_{em} = P_{traction}\eta_{tra} \tag{34.1}$$

The same happens for Eq. 36, which becomes

$$P_{batt} = P_{em}\eta_{em} \tag{36.1}$$

The negative power coming from the wheels during braking can be used to recharge the battery, as it can easily be understood by Eq. 36.1: this strategy is called regenerative braking and it’s intrinsic to the electric powertrain, whose motor can reverse its operation and work as a generator. Usually, the power required for braking is ensured by the electric motor and by mechanical brakes, which work together in order to guarantee maximum braking performance and vehicle stability. In particular, when the electric motor is present on just one axis of the vehicle, it has to be taken into account that some braking should come also from the other axis: this has great importance when the electrified axis is the rear one, since braking all on rear axle has pejorative effects on the stability of the vehicle.

In this work, a 100% braking by front-axle motor is considered. The only limit, after which mechanical braking intervenes to guarantee the extra braking requirement, is the one of the charging currents towards the battery: the motor will brake just as much as not to overcome that limit.

3.11 MISSION

The vehicle model will be simulated in two different conditions: homologation and real driving.

"Homologation driving" is characterized by running on test cycles such as FTP75, NEDC and WLTP at standard temperature ($23°C$) , with all auxiliaries off (including air conditioning, battery heater and lights) and with fixed test mass. The speed profiles of those cycles are shown in Figure 23. This first set of simulation is important since it guarantees that the vehicle model is able to give results in line with the ones declared by manufacturers for similar BEVs. Also, it will function as a reference for the following simulations.

"Real driving" means that the vehicle model runs on a mission which is characteristic of its real-world average use, which is usually much more demanding than type-approval conditions. This is due to many factors:

- driving style more dynamic, with a higher number of strong accelerations and decelerations;
- running mass variable, depending on the number of passengers and their luggage;
- road unevenness, that causes additional load not taken into account in the case of type-approval running;
- accessories and auxiliaries utilization, which in standard conditions ($T = 23°C$) are not needed. Instead at high or low temperatures air-conditioning, nowadays available virtually on all the sold cars, is usually provided. Moreover, at low temperature conditions, the battery of a BEV should be heated up, in order to have it working in its optimal range. Among the accessories, also the lights should be mentioned, which are instead kept off during type-approval running.

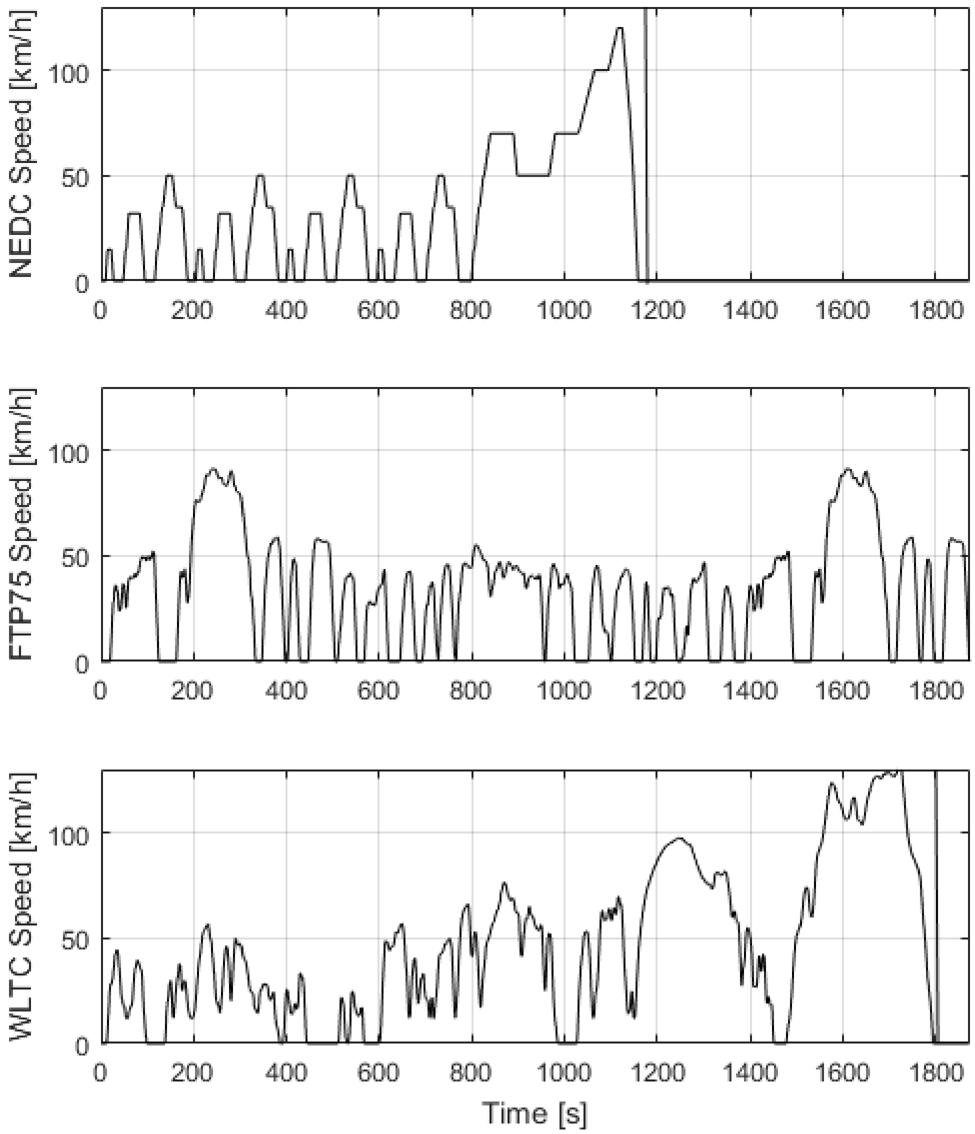

Figure 23. NEDC, FTP75 and WLTC speed profiles

For the sake of this thesis a “realistic” mission is generated taking into account the previous points, except for the road incline, which has not been considered. In the following it is explained how the mission is generated. The mission is made by a number of cycles which are characterized by the following flags: speed profile, daily hour, ambient temperature, number of passengers and battery state of charge.

Speed profile

The speed profile can be of two types: urban and extra-urban. Instead, no highway condition is considered, since highway-speed driving is usually not among the targets of an A-segment BEV, such as the one object of study in this thesis. Arthemis cycles are adopted, since they are thought to be representative of urban (AUDC) and extraurban (ARDC) conditions. They are shown in Figure 24. Arthemis cycles speed profile. In

Table 8 their main characteristic, compared with the one of FTP45, NEDC and WLTP cycles are shown.

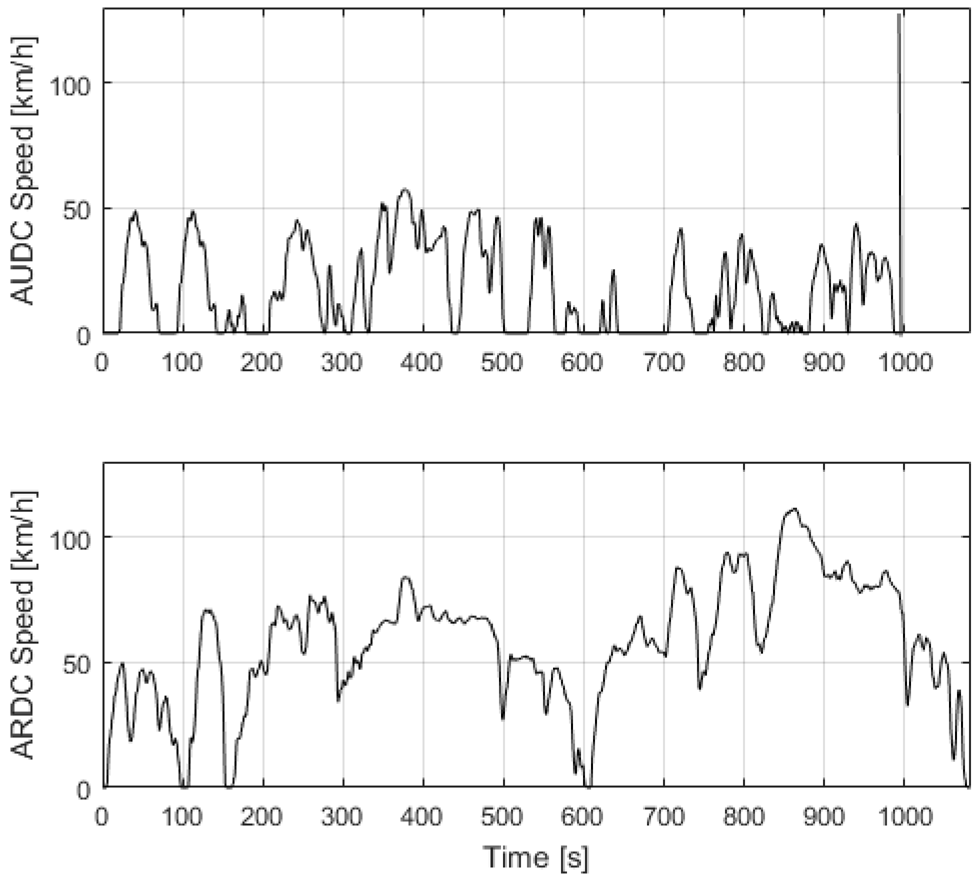

Figure 24. Arthemis cycles speed profiles

	units	NEDC	FTP75	WLTC	AUDC	ARDC
Duration	s	1180	1875	1801	994	1083
Distance	km	11.01	17.77	23.27	4.87	17.27
Max speed	km/h	120	91.25	131.3	57.7	111.5
Mean speed	km/h	33.60	34.11	46.51	17.64	57.41
Max acceleration	m/s^2	1.04	1.48	1.67	2.86	2.36
Max deceleration	m/s^2	-1.39	-1.48	-1.5	-3.14	-4.08
Stop phase	%	24.83	19.09	13.05	28.47	3.14
Acceleration phase	%	20.93	39.41	43.81	34.61	41.46
Braking phase	%	14.66	33.76	39.48	30.18	39.34
Constant driving phase	%	39.58	7.73	3.66	6.74	16.07

Table 8. Main characteristics of the NEDC, FTP75, WLTC, AUDC and ARDC cycles

It is evident that the Arthemis cycles are much more dynamic with respect to all the type approval ones, even considering WLTC which is already quite demanding. In particular, it is important to observe that the magnitude of acceleration and deceleration, which ranges from 2 to 3 times more than the ones on type approval. This is important because it makes the power request more sensitive to vehicle mass.

The urban speed profile flag has a probability to be assigned of 70%, versus a probability of 30% for the extra-urban speed profile. The speed profile determines the mechanical load, in terms of speed and torque, at the wheels.

Daily hour

This flag can be also of two types: daily or night driving. The first condition corresponds to driving with plenty of light, while the second one corresponds to driving in the dark. The first possibility has a probability to be assigned of 80%, and, of course, the second has a probability of 20%. The daily hour flag determines which is the load on the lighting system.

Number of passengers

The number of passengers can either be one, two or three, with probabilities respectively of 70%, 20% and 10%. It impacts directly on the vehicle weight and on the metabolic load inside the vehicle cabin.

Ambient temperature

The ambient temperature is not a discrete flag, such as the first three. It can assume a value in a given interval with uniform probability. The interval to be considered depends strongly on the city where the vehicle is run. This is due to the fact that, even in the same country, different cities can experience very different temperatures during the year. In our case, taking into account the Turin area temperature evolution in year 2017, as shown in Figure 25, the interval has been set to $-2 \div 30°C$. The ambient temperature determines mainly the load of the air conditioning system, but also the one of the battery heater, in case of cold conditions.

Battery state of charge

The SOC at the beginning of each cycle is also randomized in a given interval, which was assumed to be between 40 and 90%. The SOC influences directly the battery model parameters and, then, its efficiency.

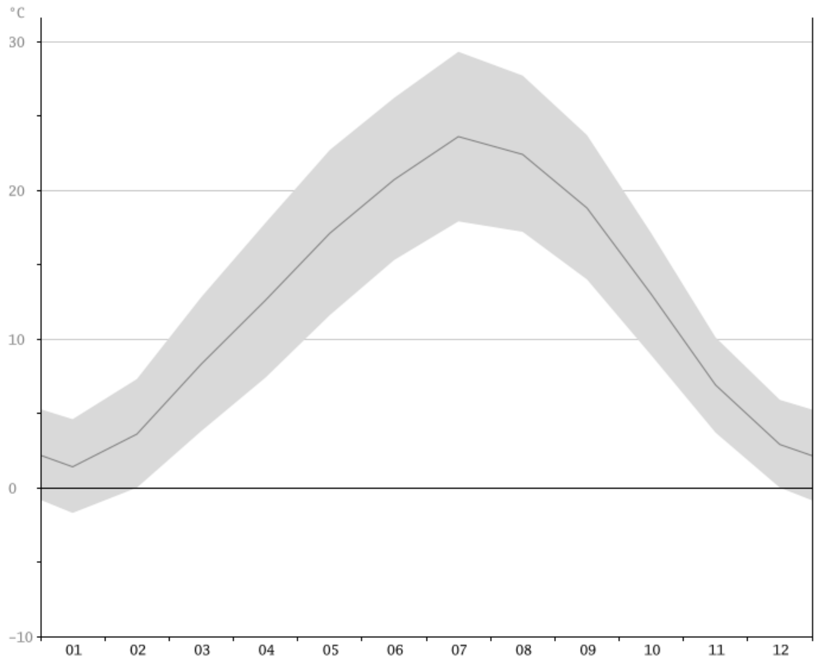

Figure 25. Historical temperature series for year 2017 regarding the city area of Turin.
Source: ClimateData

In Figure 26 can be observed part of the mission with four cycles and their flags.

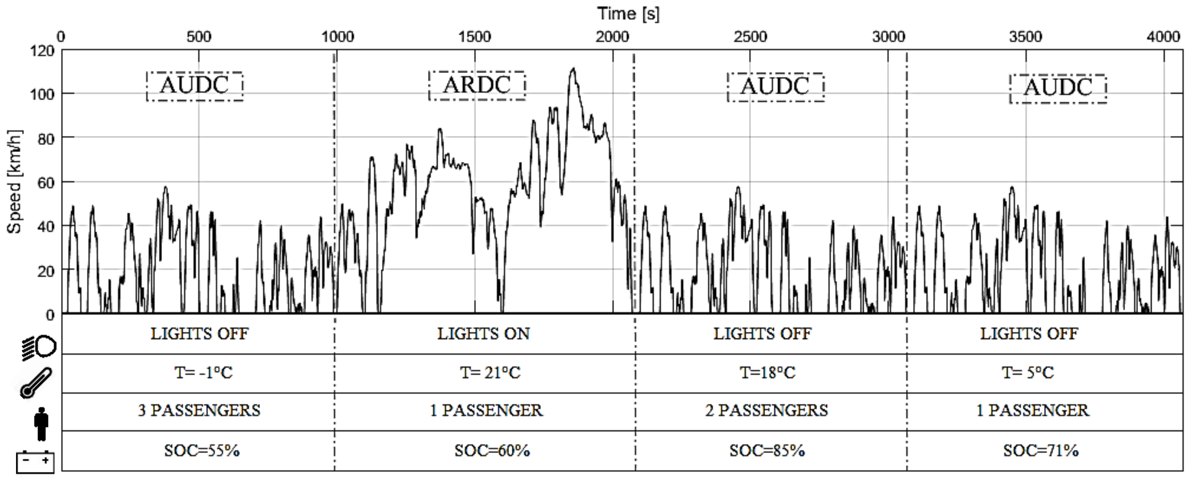

Figure 26. Mission with some of its cycles and their characteristics

4.1 MODEL TUNING

4.1 INTRODUCTION

The models introduced in the previous Chapter 3 were either theoretical or experimental. In both cases, however, they contained a large amount of assumptions, simplifications and data related to other applications: this makes the results shift with respect to the experimental ones of the considered vehicle, which is an A-segment Battery Electric Vehicle. A tuning of the parameters adopted in the models is necessary in order to get results comparable with the experimental ones, which are known at least for type-approval conditions.

The most important model to be tuned is the thermal model of the cabin and of the heating and cooling systems. This is true for two reasons: first of all, the thermal model is the one with the highest number of uncertainties and assumptions not linked to the real vehicle; secondly, the air conditioning load is thought to be one of the main ones in determining the final energy consumption of the vehicle. Two different tunings are made for the heating and cooling conditions, which are assumed to be performed by two different systems, namely a PTC resistor and a Heat Ventilation Air Conditioning (HVAC).

After the model set-up, the simulation is run on the main type-approval cycles and in different ambient conditions. Results are recorded and compared with the ones available inside the company: a satisfying correlation is registered, and the program is validated.

4.2 THERMAL TUNING

The thermal model of the vehicle cabin is described in Chapter 3.3. Eq. 17 is a differential equation that, given a boundary condition (namely the initial temperature), is able to describe the system evolution in time. Eq. 21, 23, 27 represent the expressions of the thermal loads. Eq. 28 is applied in order to calculate the electrical power required to the battery, either by the air conditioning compressor or by the PTC cabin heater. The following system summarizes the entire model:

$$\begin{cases} TM\dfrac{dT}{dt} = \dot{Q}_{amb} + \dot{Q}_{sol} + \dot{Q}_{AC} \\ \dot{Q}_{AC} = k_P\left(T - T_{obj}\right) + k_I\displaystyle\int \left(T - T_{obj}\right))dt \\ \dot{Q}_{amb} = (C_1 + C_2 + C_3)(T - T_{amb}) \\ C_i = \dfrac{1}{R_{cd,i}} + \dfrac{1}{R_{cv,i}} \\ P_{electric} = \dfrac{\dot{Q}_{AC}}{COP} \end{cases} \tag{41}$$

However, all the parameters featuring in the model are taken by literature (such as the convection coefficient, the *COP*), estimated by best guess (such as the PI coefficients) or calculated by a mixed approach (such as the thermal mass and geometric dimensions). In Table 9 first guess parameters are shown.

$R_{cv,i} = \dfrac{1}{hA_i}\ with\ h = 0.6 + 6.64\sqrt{V}$
$R_{cd,i} = \sum_k \dfrac{s_{i,k}}{k_{i,k}\,A_i}$
$TM = 75000$
$k_P = 500$
$k_I = 1$
$COP_{cooling} = 2.33\ ;COP_{heating} = 1$

Table 9. First-guess parameters for the vehicle thermal model

In order to have significant results, it was decided to tune the model with respect to a real application, for which cool-down and heat-up test results were available. The tuning has to be made separately for the two conditions because two different systems are adopted: an HVAC system for cooling and a PTC resistor for heating. Tuning conditions are without passengers and without ventilation (the corresponding loads are null).

4.2.1 COOL-DOWN TUNING

Table 10 shows the cool-down test conditions.

Cycle	NEDC
Initial cabin temperature	$T_0 = 36\ °C$
Ambient temperature	$T_{amb} = 35°C$
Target temperature	$T_{obj} = 22°C$

Table 10. Cool-down test conditions

Cabin temperature[12] and compressor power are recorded and their evolution is shown in Figure 27. In the same figure are represented also the simulated temperature and compressor power profiles, based on the model and parameters value described above. In the case of cooling a maximum evaporator load $\dot{Q}_{AC} = 5500W$ has been considered.

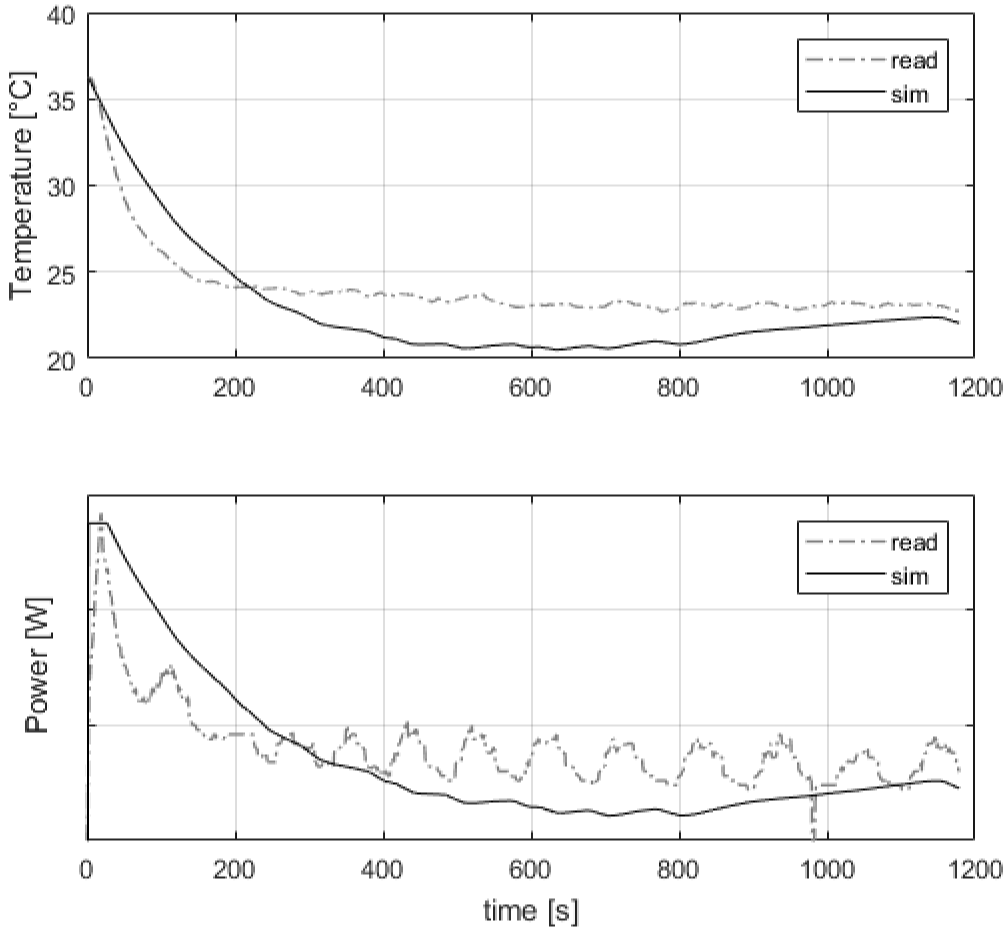

Figure 27. Cool-down test results before thermal tuning.

[12] The measured cabin temperature is intended as an average temperature at the locations of the heads of the front row occupants.

It can be noticed that the simulation accuracy is not good, even if the general behavior is similar to the real one, being the curves of both real and simulated values in the form of decreasing exponentials. Table 11 reports all the parameters subjected to tuning.

$R_{cv,i} = \frac{1}{hA_i}$ $with\ h = \beta_1 + \beta_2\sqrt{V}$
$R_{cd,i} = \beta_3 \sum_k \frac{s_{i,k}}{k_{i,k}\,A_i}$
$TM = \beta_4$
$k_P = \beta_5$
$k_I = \beta_6$
$COP_{cooling} = \beta_7$

Table 11. Tuning parameters.

The parameters β_i are varied discretely around their starting value. A grid of possible combinations will be generated and the tuning is made by a grid-search of the minimum error of both the temperature and compressor power profiles. In particular, starting from the Mean Square Error (MSQ) of both the profiles:

$$\begin{cases} MSE_T = \frac{\sum_{i=1}^{n}\left(T_{sim,i} - T_{exp,i}\right)^2}{n} \\ MSE_P = \frac{\sum_{i=1}^{n}\left(P_{sim,i} - P_{exp,i}\right)^2}{n} \end{cases} \tag{42}$$

the total error will be defined as a combination of the two:

$$ERR = k_1 MSE_T + k_2 MSE_P \tag{43}$$

where k_1 and k_2 are two coefficients which will take into account the fact that the intrinsic error of the power profile is always bigger than the one of temperature. Indeed the experimental profile of the compressor power, as can be seen from Figure 27, it's quite dynamic, due to its working principle based on an ON-OFF strategy. Instead, simulated profile is much smoother, since the air conditioning system has not been modeled in detail, but only with an average COP coefficient. Therefore, the values adopted are:

$$k_1 = 1$$
$$k_2 = 10^{-5}$$

The new parameters of the thermal model, at the end of the tuning process, are shown in Table 12, while Figure 28 reports the new temperature and power profiles compared with the experimental ones. It is evident graphically that the model represents with much more detail the real system behavior. Mathematically, the mean square errors of temperature and power, normalized to their average square value, will be respectively 0.009% and 5.97% .

β_1	48
β_2	1
β_3	1
β_4	36250
β_5	500
β_6	0.55
β_7	2.33

Table 12. Cool-down tuned parameters.

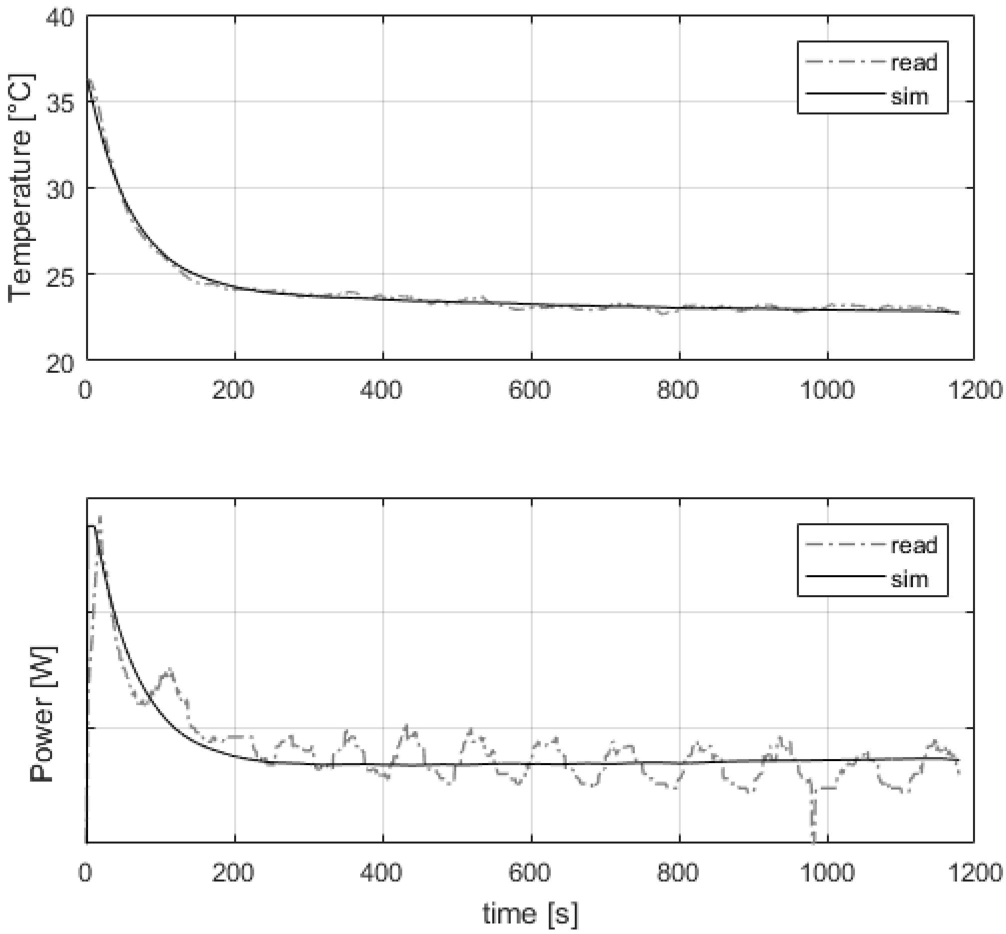

Figure 28. Cool-down results after tuning of thermal parameters.

The average compressor power simulated by the thermal model after the tuning of the parameters has a discrepancy of only 0.25% with respect to the experimental value. This is probably the most important result of the tuning, since it has a direct impact on the energy consumption. Also, the average compressor power for an experimental test in the same condition with the addition of a solar load is available. Also in this case the discrepancy of the average compressor power is small, in the order of 0.53%. The model is sufficiently precise to be used for further simulations.

4.2.2 HEAT-UP TUNING

The tuning in heat-up conditions is exactly specular to the cool-down one already shown. It has to be taken into account that the heating system is based on a PTC resistor. The COP of the system has to be searched in a range less than unity. Test conditions are shown in Table 13:

Cycle	NEDC
Initial cabin temperature	$T_0 = -4\ °C$
Ambient temperature	$T_{amb} = -10°C$
Target temperature	$T_{obj} = 24°C$

Table 13. Heat-up test conditions.

Figure 29 shows the experimental results and the ones simulated before system tuning. Figure 30 shows, instead, the result after tuning. Table 14 reports the parameters of the thermal model after tuning.

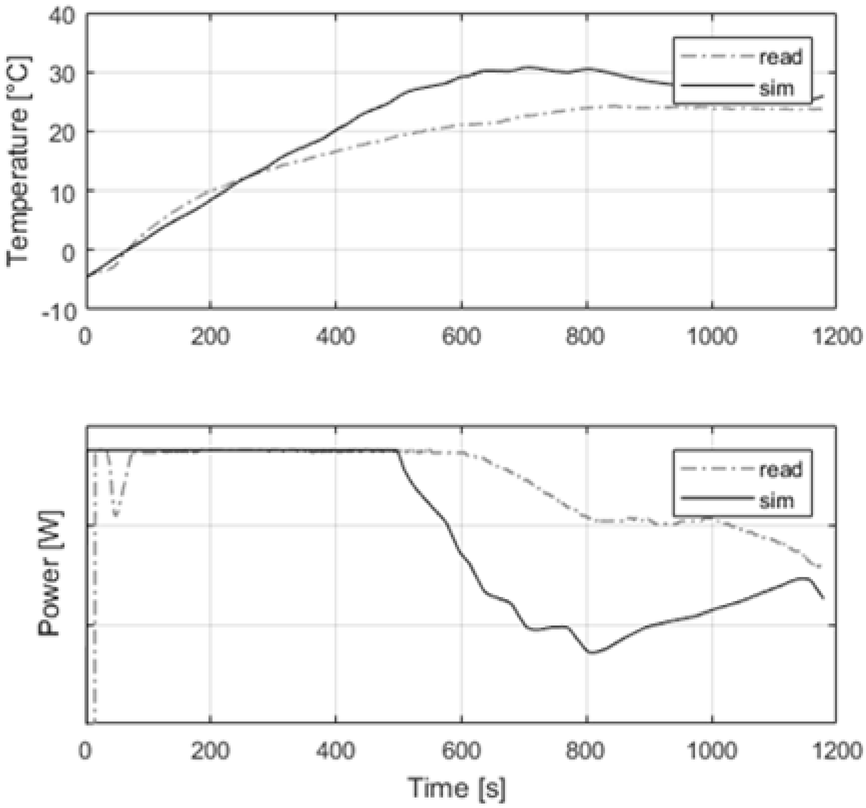

Figure 29. Heat-up results before thermal tuning.

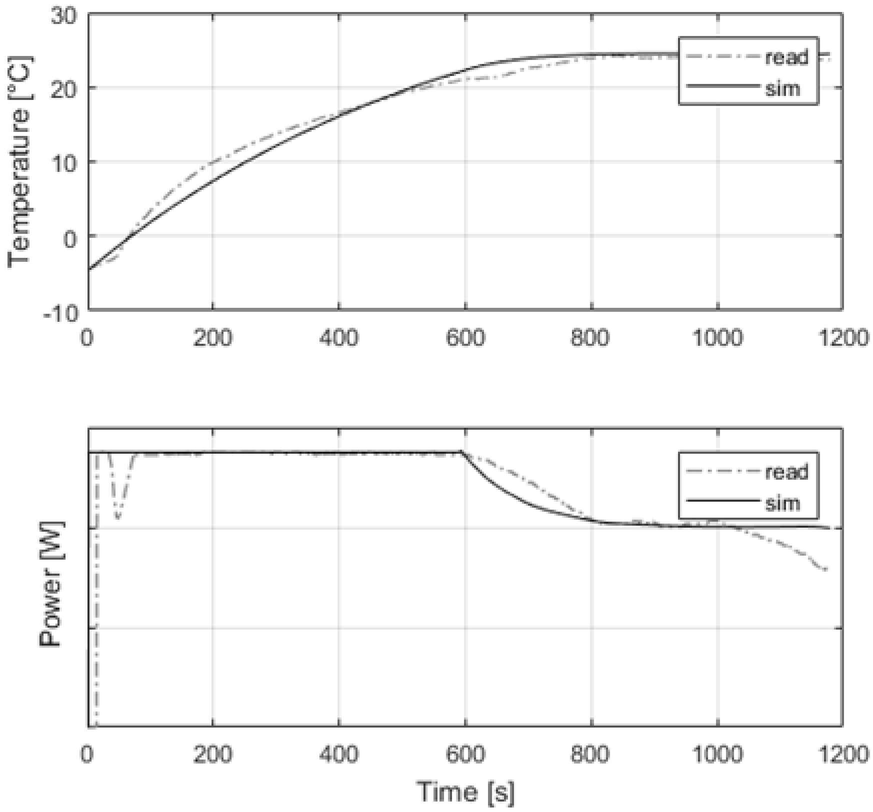

Figure 30. Heat-up results after thermal tuning.

β_1	30
β_2	0.33
β_3	1
β_4	50000
β_5	500
β_6	0.45
β_7	0.8

Table 14. Heat-up tuned parameters.

We can notice that the experimental trace of the compressor power, during the test, shows three main phases:

- 100% working for the first 600 seconds;
- Lower power adsorption in the interval 600-1000s;
- Even lower adsorption for the remaining time.

The model isn't able to represent this behavior, which is probably due to some ventilation or heating strategy adopted during the testing. The MSE of temperature and electric power, normalized with respect to their mean values, are respectively 0.47% and 1.71%.

Even if the model isn't able to predict exactly the power profile, the most important thing is that it is able to predict the average power, which has a direct impact on the energy consumption. In particular, the discrepancy obtained at the end of the tuning process, is in the order of 0.66%: this is considered sufficiently accurate to the purpose of this thesis.

4.3 RESULTS ON TYPE-APPROVAL CYCLES

The model is run on the NEDC in various ambient conditions, in order to check the impact of different parameters on the energy consumption and range. Moreover, type approval test results will work as a reference to the ones obtained on the "real" mission. In addition to that, also FTP75 and WLTC are tested. Table 15 summarizes all the test conditions and the simulated energy consumption[13]. Moreover, given the battery rated capacity $E_{C,0} = 24kWh$, also the projected range will be calculated as:

$$range = \frac{E_{C,0}}{cons} \tag{44}$$

TEST CONDITIONS							RESULTS	
Cycle	Temperature	Air Conditioning	Solar Radiation	Number of passengers	Initial SOC	Lights	Energy consumption	Range (~)
NEDC	23°C	OFF	0W	1	0.65	OFF	152 Wh/km +0% (REF)	158 km
NEDC	35°C	ON	0W	1	0.65	OFF	182 Wh/km +20.06%	131 km
NEDC	35°C	ON	900W	1	0.65	OFF	194 Wh/km +27.47%	124 km
NEDC	-10°C	OFF	0W	1	0.65	OFF	204 Wh/km +34.18%	118 km
NEDC	-10°C	ON	0W	1	0.65	OFF	344 Wh/km +125.78%	70 km
FTP75	23°C	OFF	0W	1	0.65	OFF	149 Wh/km -2.10%	161 km
WLTC	23°C	OFF	0W	1	0.65	OFF	177 Wh/km +16.65%	135 km

Table 15. Results of the simulation over type-approval cycles.

Taking as reference the simulated fuel consumption on the NEDC at 23°C, the following considerations about the table can be made:

[13] They all include a charger efficiency of η=0.85.

- Ambient conditions impact on the energy consumption due mainly to the power adsorbed by the air conditioning compressor, by the cabin heater and by the battery heater. However their impact is not uniform: for example in hot conditions, the registered increment in energy consumption is 20% and 27%, respectively for the cases without and with solar load radiation. Instead, in cold conditions the consumption rises much more, since both battery heating and cabin heating are based on the Joule effect, i.e. on energy dissipation. This is why at -10°C an increment of 34% is registered only considering the battery heater and of 126% considering also the cabin heater. This last number means that the consumption is more than double of the reference one, and, correspondingly, the range will be more than halved;
- The FTP75 cycle doesn't show much difference in results with respect to the NEDC, even if it's more dynamic. This is due to the fact that the energy required by stronger accelerations is in part compensated by the energy recovered with stronger decelerations.
- The WLTC shows to be more demanding than the other test cycles, with a consumption increment of 14% with respect to the reference condition.

All the results given in the table are simulated ones. They're compared with the experimental ones in the same conditions and the values order of magnitude correspond in all conditions. Therefore, the program is validated on type-approval cycles and ready to be used on the realistic mission. The results on the mission will be compared with the ones of the cycles in order to understand whether the impact of the auxiliaries is the same noted on type-approval simulation.

5. OPTIMIZATION OF THE TRANSMISSION

5.1 INTRODUCTION

The A-segment vehicle considered in this work has a single-speed transmission. This is due to the fact that electric motors working torque characteristic is already close to the ideal curve, with a wide constant power range. Moreover, electric motors have no start-up problems, they don't idle and the maximum speed is quite high. Therefore, motor speed adaptation to the road requirements is not necessary as it could be in an ICE, where the speed working range (in which power and torque are high enough) is much more limited. This is the reason why all the major electric vehicles actually on the market do not equip a gearbox.

In these conditions an optimization of the final-drive ratio, which is the only parameter of the transmission, is essential. Indeed, it will determine how the speed and forces at vehicle level translate on motor speed and torque: when changing its value, the operating point on the motor for a given vehicle condition will change as well. The objective of the optimization is to shift as much as possible all operating points towards high efficiency areas, in order to minimize energy consumption. The final drive-ratio is, therefore, optimized for both type-approval cycles and for the mission's cycles.

Having two possible gear ratios available, i.e. having a two-speed gearbox, increases the possibility of moving more operating points towards the high-efficiency area of the motor map. Therefore the impact of having an optimized two-speed gearbox is assessed in terms of energy consumption on the mission.

Finally, the optimization of a two-speed transmission is done also for the WLTP cycle, which is the one to which regulations are referring from 2017. A comparison between the two conditions (on-cycle and on-mission) is conducted in order to understand if they converge towards the same transmission, or if a compromise solution between the two could be found.

5.2 OPTIMIZATION OF THE FINAL DRIVE RATIO

5.2.1 OPTIMIZATION OVER THE TYPE-APPROVAL CYCLES

Starting from the speed and torque at the wheels, the final drive ratio defines which are the electric motor operating points (in terms of speed and torque) over the motor efficiency map, as expressed by Eq. 33, 35. Thus, the motor average efficiency directly depends on the final drive ratio and, therefore, an impact over the energy consumption is to be expected.

The final drive ratio has an upper limit, given by the fact that the operating points should never go beyond the maximum motor speed, even at maximum vehicle speed. In particular, this limit is:

$$tau_{fin,max} = \frac{rpm_{max} r_d}{V_{max}} \approx 10.17$$

where $rpm_{max} = 12000rpm$ is the maximum motor speed, $V_{max} = 130\ km/h$ is the maximum vehicle speed and $r_d = 0.292$ is the rolling radius. To be safe, we will take as limit $tau_{fin,max} = 10.1$.

As a reference, the average engine efficiency and the energy consumption over NEDC, FTP75 and WLTC cycles are calculated for a range of final drive ratio $7 \div 10.1$ and shown in Figure 31. Table 16 shows the final drive ratio minimizing the consumption, the minimum consumption and compares the latter with the one of the non-optimized final drive ratio.

CYCLE	OPTIMAL FINAL DRIVE	OPTIMAL CONSUMPTION	CONSUMPTION WITH NON OPTIMIZED FINAL DRIVE	DIFFERENCE
	$[-]$	$[Wh/km]$	$[Wh/km]$	[%]
NEDC	7.80	151	152	-0.76
FTP75	9.4	149	149	-0.00
WLTC	7.2	175	178	-1.62

Table 16. Optimization of the final drive for NEDC, FTP75 and WLTC.

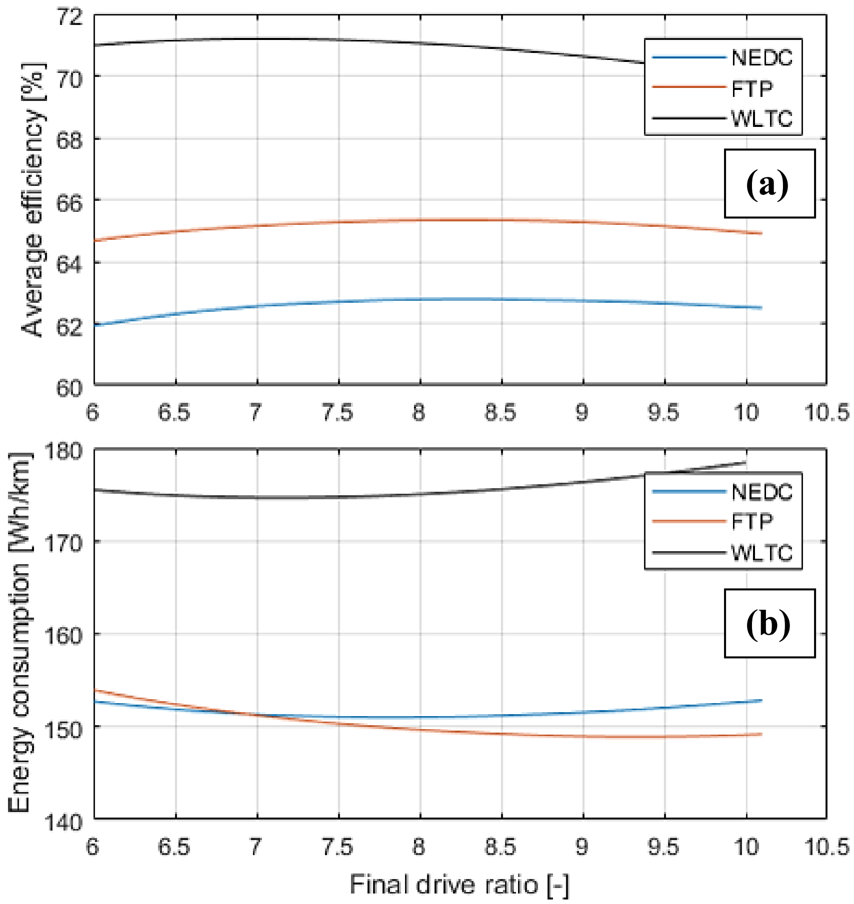

Figure 31. Impact of the final drive ratio on (a) average motor efficiency and (b) energy consumption for different type approval cycles.

The first thing to be noted is that the two conditions of maximum average motor efficiency and minimum energy consumption are not obtained for the same final drive ratio. This is because the average efficiency is not a complete indicator, not taking into account the transmitted power associated to the efficiency of each operating point. A weighted average, where the weight is the efficiency of the operating point, would be, instead, much more significant. Therefore, the real optimum is found in the condition minimizing energy consumption.

For what concerns the numeric result of the simulation, the initial value of final drive ratio is optimized for driving over FTP75 cycle. Instead, for what concerns NEDC a much smaller value of final drive ratio, $\tau_{fin} = 7.8$, would be the best solution, with an energy consumption reduction of -0.76%. The reduction of the final drive ratio for WLTC down to $\tau_{fin} = 7.2$ has an even stronger impact on the energy consumption, with a reduction of -1.62%.

5.2.2 OPTIMIZATION OVER THE REAL MISSION

For what concerns the real mission, just the variables of speed profile and number of passengers will be considered, while all the others will be neglected. Indeed, those two are the only ones for which the final drive ratio has an impact on consumption, while the impact of temperature, state of charge and lights on consumption is independent from the final drive ratio.

There are two possible cycles and three possible numbers of passengers, so there are six possible combinations. A simulation for each of these will be made in order to calculate the final drive ratio minimizing consumption, reporting them in Table 17. Figure 32 shows, instead, the AUDC and ARDC consumption as a function of the final drive ratio for the three levels of passengers[14].

CYCLE	NUMBER OF PASSENGERS	OPTIMAL FINAL DRIVE RATIO	OPTIMAL CONSUMPTION	CONSUMPTION WITH NON OPTIMIZED SINGLE-SPEED	DIFFERENCE
	$[-]$	$[-]$	$[Wh/km]$	$[Wh/km]$	[%]
AUDC	1	10.10	197	198	-0.57
AUDC	2	10.10	207	208	-0.59
AUDC	3	10.10	217	218	-0.62
ARDC	1	7.50	161	162	-0.86
ARDC	2	7.70	166	168	-0.77
ARDC	3	7.80	172	173	-0.64

Table 17. Optimization of the final drive for AUDC and ARDC and different passenger loads.

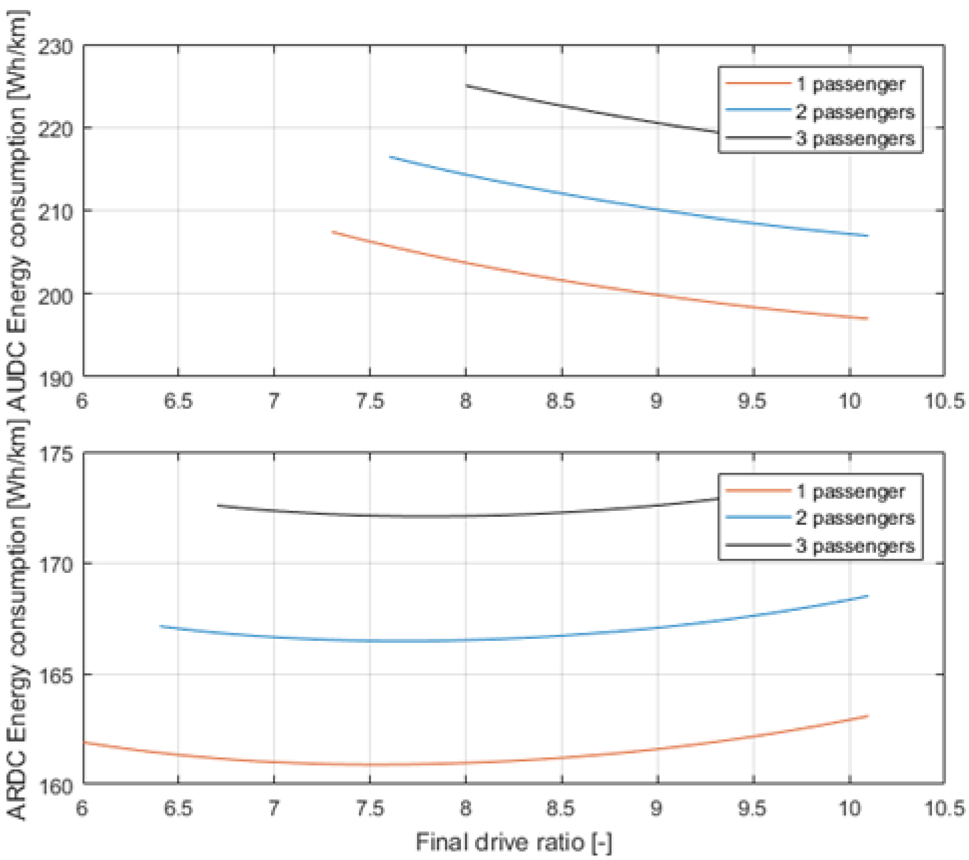

Figure 32. Energy consumption of AUDC and ARDC for different passengers number as a function of final drive ratio.

[14] Some of the simulations with low final drive ratios are discarded, since they lead to overcoming the maximum electric machine torque.

AUDC minimizes its consumption for high final drive ratios: actually simulation is conducted only up to the maximum final drive ratio limit defined before, while the actual minimum would be found for values even larger. This is due to the fact that its low speeds (always smaller than $53\ km/h$) make the operating points lay always in the low motor speed range, which has low efficiency. A higher ratio could shift the points towards higher speeds and efficiencies.

ARDC minimum, instead, is found for a final drive ratio smaller than the initial one. This is because the high speeds (up to $120\ km/h$) make the operating points lay in the high speed zone of the map which, just like the low speed one, has lower efficiency. Therefore the optimum is found in the opposite direction with respect to the one followed for AUDC.

The consumptions found in the previous simulations are combined based on the percentages of utilization over the mission. This means that, for AUDC, the considered consumption is calculated as a weighted average of the three cases of one passenger (weight 70%), two passengers (20%) and three passengers (10%). For ARDC the same holds. The total consumption is calculated as a weighted average of the AUDC one (weight 70%) and ARDC one (weight 30%). In Figure 33 the combined consumption over the mission as a function of the final drive ratio is shown. It's possible to see that the minimum consumption is achieved at maximum final drive ratio: the result is understandable since AUDC has stronger weight with respect to ARDC. The consumptions with non-optimized final drive and $\tau_{\mathrm{fin}} = 10.10$ are respectively $191\ \mathrm{Wh/km}$ and $190\ \mathrm{Wh/km}$: the optimized final drive ratio would guarantee an energy saving of just 0.3%, which, in terms of range, is an increment of only $0.37\ \mathrm{km}$. This means that an optimization of the final drive ratio would bring minor benefits on the vehicle in real driving. A possibility to be analyzed would be the introduction of a gearbox with a very long first gear (large reduction ratio) to be used at low speeds, and a second gear able to ensure the vehicle top speed requirement without exceeding electric machine maximum speed.

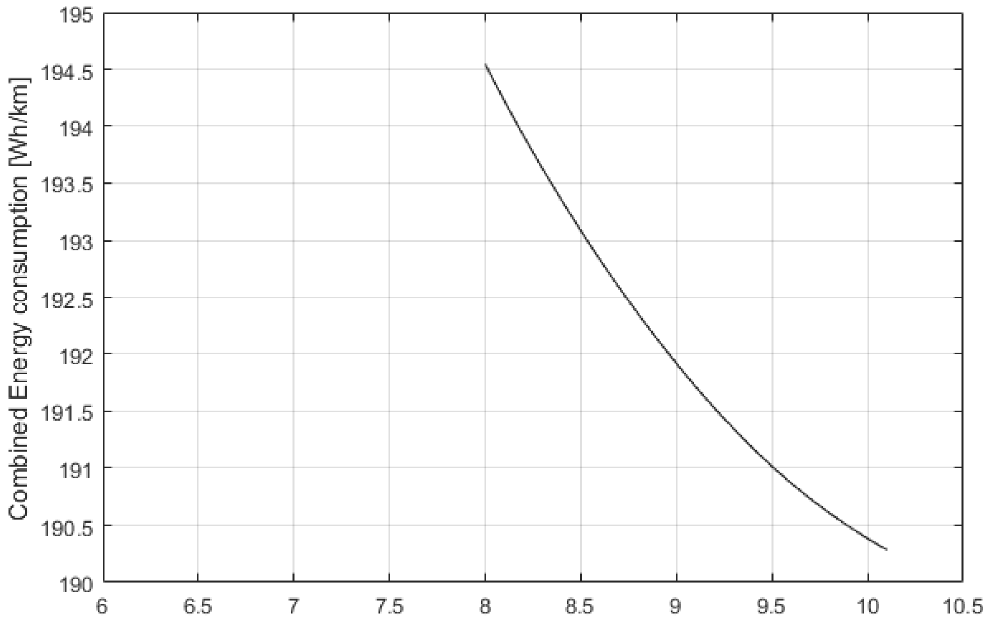

Figure 33. Combined energy consumption over the mission cycles.

5.4 TWO SPEED GEARBOX OPTIMIZATION OVER MISSION CYCLES

Previous considerations led to the possibility of introducing a two-speed gearbox, such as to have a very short[15] first gear to be used in low speed / low load conditions, such as city driving, and a longer second gear able to guarantee the wanted vehicle top speed. In particular, it was observed that AUDC could minimize the energy consumption adopting a final drive ratio exceeding the limit which guarantees top speed requirements. Figure 34 shows that the final drive ratio minimizing energy consumption for the AUDC cycle (with one passenger), is $\tau_{fin} = 14.40$. The energy consumption would be $193.31\ Wh/km$, with a saving of 2.43% with respect to the energy consumption obtained with the non-optimized final-drive ratio.

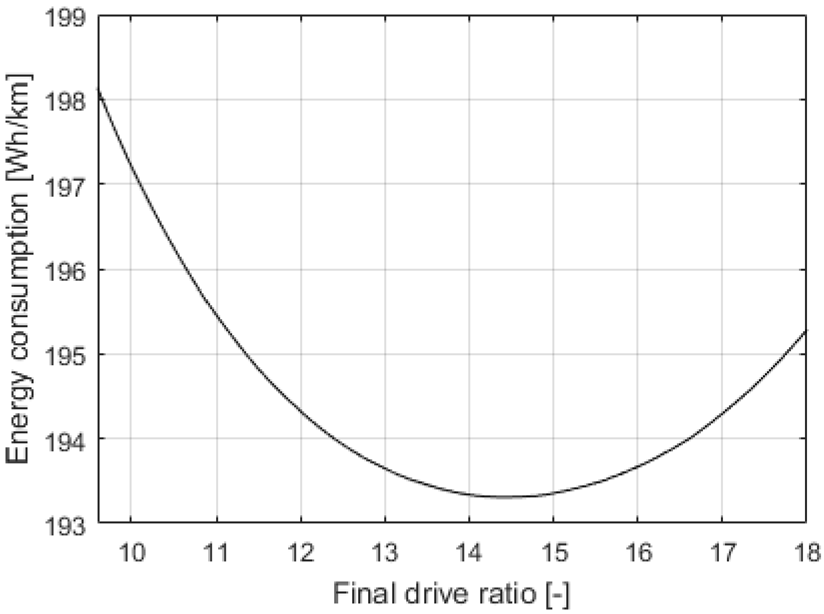

Figure 34. AUDC energy consumption for short final-drive ratios.

Introducing a two-speed gearbox would lead to even better results, since some points could be optimized with the first gear, some others with the second. For each added gear an improvement smaller and smaller in energy consumption could be obtained, while complexity, cost and shifting inefficiency rise quickly. That is why just a two-speed gearbox is studied in this thesis. In particular, the total second gear ratio (including final drive) is fixed to $\tau_{t,2} = 9.6$, which was the ratio of the final drive minimizing FTP75 consumption: this gear is the one able to guarantee top speed and to be used at high loads and high speeds. Instead, the first gear ratio is optimized with a grid search over the range $13 \div 25$. It is assumed that, in each interval $\Delta t = 1s$, the gear which ensures the best motor efficiency is chosen; moreover, ideal gear shift hypothesis is adopted:

[15] "Short" gear means that the reduction ratio (output speed divided by input speed) is high, so that the torque multiplication is high. Of course "long" gear has the opposite meaning.

- the gear shift is instantaneous;
- no torque loss happens during gear shift;
- no limitations in how often gear shift happens.

The results of the simulation for different first gear ratios are shown in Figure 35.

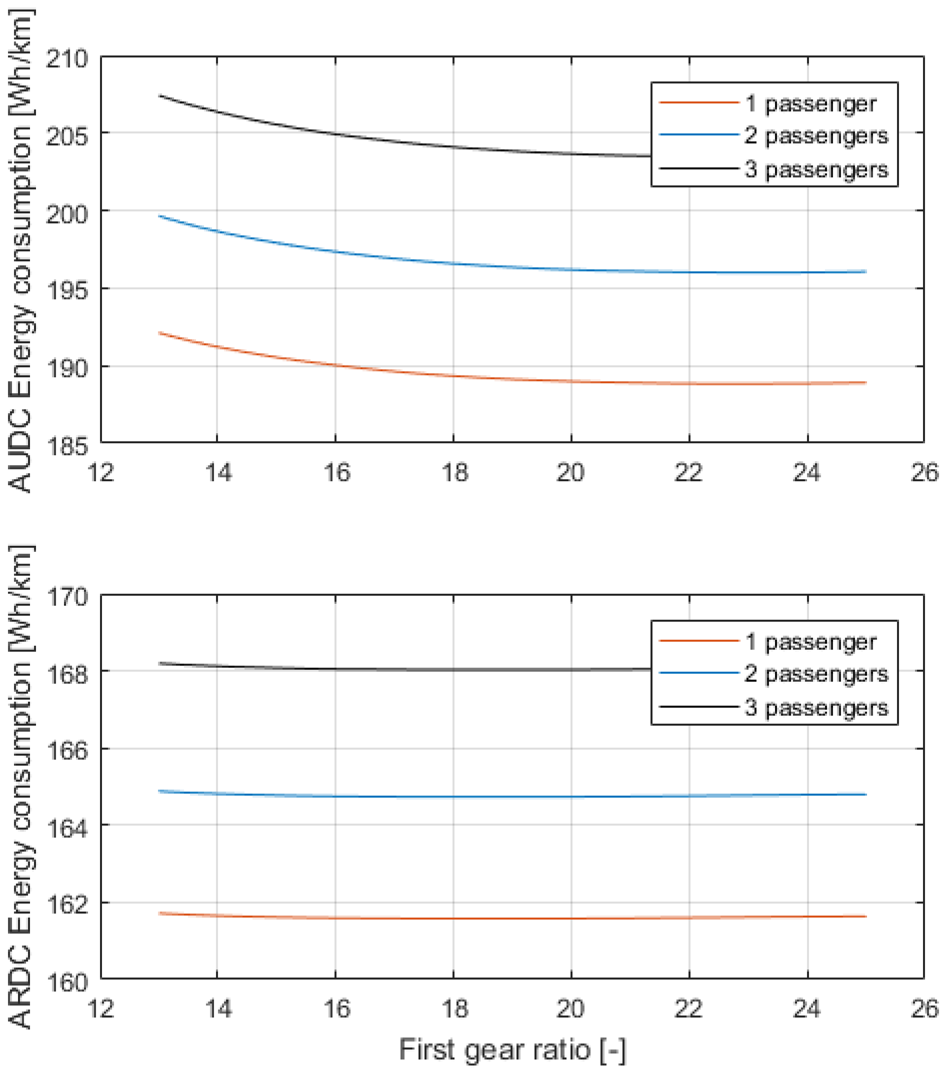

Figure 35. Energy consumption of AUDC and ARDC with different passengers' number and for varying first gear ratio (second gear ratio fixed to $\tau_{t,2} = 9.6$)

It can be observed that AUDC benefits from very large final drive ratio, with the minimum being at around $\tau_{t,1} \approx 23$ for the three conditions. Instead, the value of first gear ratio has not a strong impact on the ARDC, since the gearbox would be anyway in second gear for the greatest part of the cycle. The average consumption, combined as explained in the previous Chapter 5.3.2, behaves as shown in Figure 36 when the first gear ratio changes.

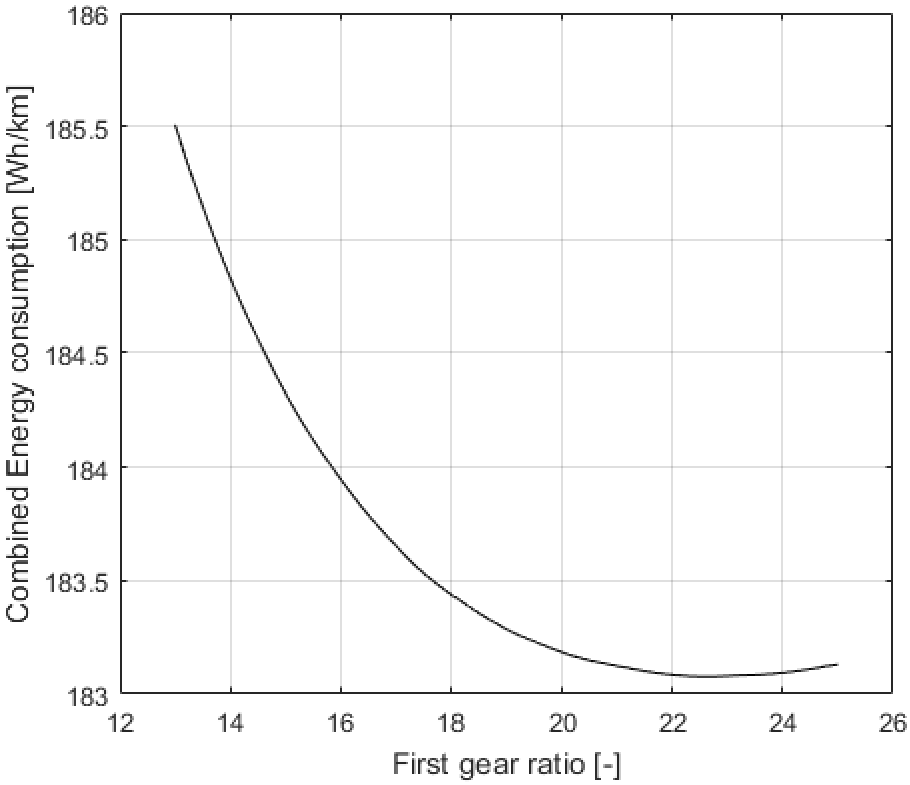

Figure 36. Combined energy consumption over mission cycles for varying first gear ratio.

The minimum energy consumption of

$$183\ Wh/km$$

is obtained with the optimal first gear ratio of $\tau_{t,1} \approx 22.50$. If compared with the energy consumption of $191\ \mathrm{Wh/km}$ obtained with the single-speed transmission reference case, the energy saving is of 4.08%. In particular, in terms of range, it passes from $125.74\ km$ to $131.09\ km$. The increment is of $5.35\ km$. The behavior of the combined energy consumption shown in Figure 36 follows almost identically the one of the AUDC cycles shown in Figure 35, proving once again that ARDC impact is minor. In order to understand why the optimization works, the operating points in the reference single-speed transmission case and in the case of optimized two-speed transmission are shown in Figure 37. It is evident that the second configuration is much more able to shift more operating points towards higher efficiency areas of the electric machine.

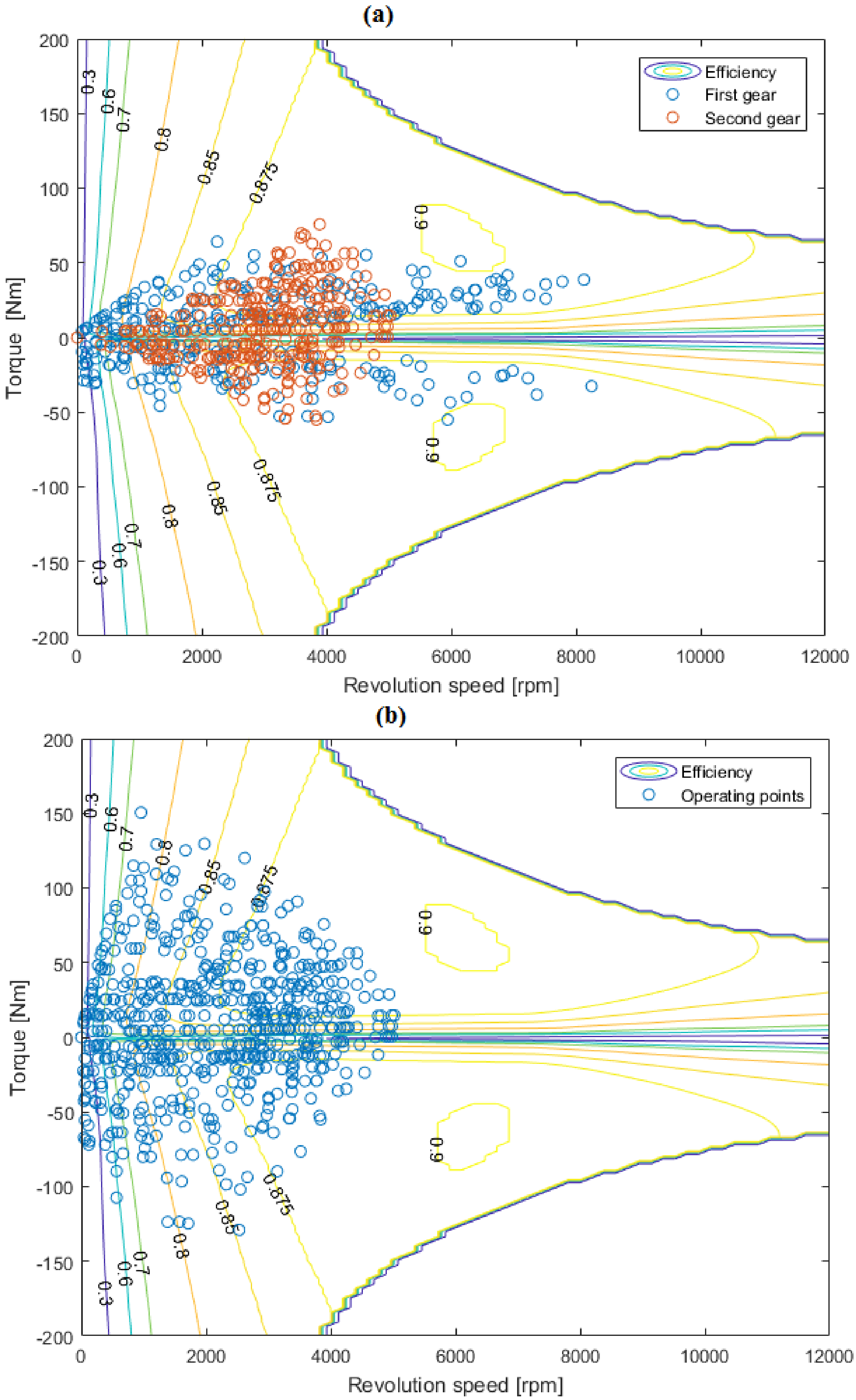

Figure 37. Operating points over the e-machine efficiency map for (a) two-speed gearbox case and (b) non-optimized single-speed transmission case.

An optimization on both the gear ratios is also conducted. The optimal gear ratios are $\tau_{t,1} \approx 20.50$ and $\tau_{t,2} \approx 8.00$, as shown in Figure 38. However the optimal energy consumption is only slightly lower than 183 Wh/km which is better than the previous one (only first gear optimized) by only 0.17%. From now on, when referring to the optimal two-speed configuration, we will refer to the case with $\tau_{t,1} \approx 22.50$ and $\tau_{t,2} \approx 9.6$.

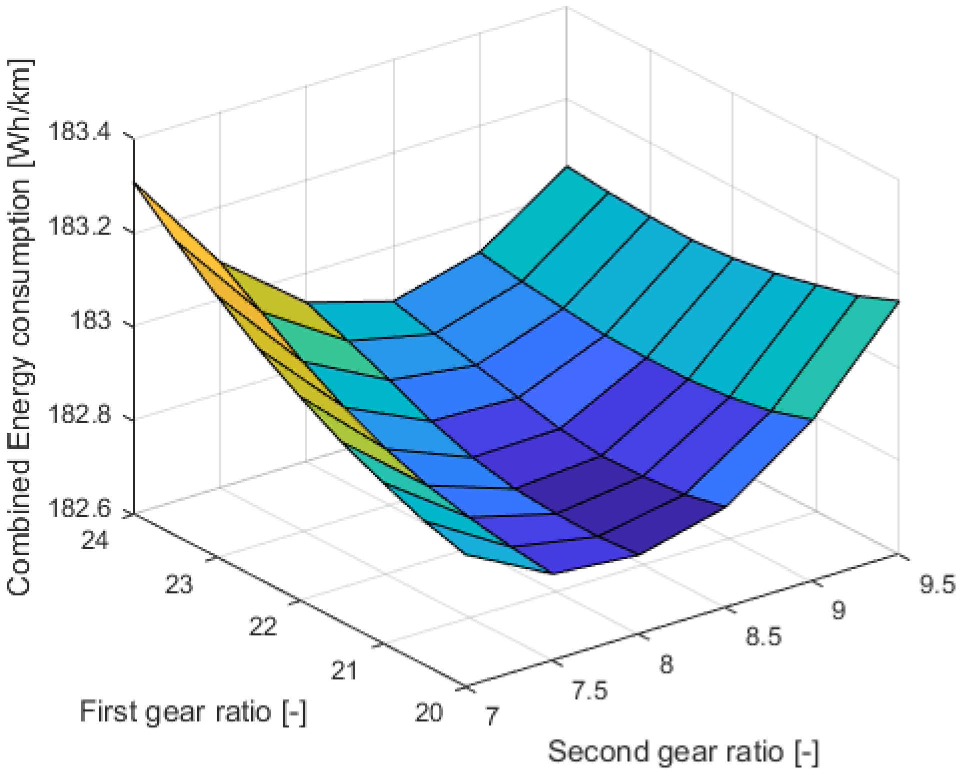

Figure 38. Combined energy consumption on the mission cycles for varying first and second gear ratios.

5.5 TWO SPEED GEARBOX OPTIMIZATION OVER WLTP CYCLE

An optimization of the first gear is also made when running on WLTP cycle, since this is the cycle adopted for homologation starting from 2017. Indeed, even if the main aim of this Chapter is the optimization on the real mission, a look to the type-approval results should always be given, since regulations still don't take into account real driving. Figure 39 shows the energy consumption on WLTC as a function of the first gear ratio. The optimal ratio is $\tau_{t,1} \approx 18.00$, with an energy consumption of 177 Wh/km. A configuration with $\tau_{t,1} \approx 22.50$, instead, leads to a consumption only slightly higher than the previous one. This means that the optimization of the first gear over the real mission provides a configuration which is good enough also for type approval.

For what concerns the cycle per se, the energy saving with respect to the reference single-speed case, for which the consumption was around 178 Wh/km, is just of 0.3%.

This is due to the fact that WLTC would benefit much more from a reduction of the second gear ratio than from an increase of the first gear one. This is easily understandable when looking at Table 15. Therefore an optimization of both gear ratios is conducted in order to find the best solution. In this case the optimal configuration would be $\tau_{t,1} \approx 20.50$ and $\tau_{t,2} \approx 8.00$, as shown in Figure 40, with an energy consumption of $172\ Wh/km$, that, with comparison to the reference one obtained with a non-optimized single-speed transmission, provides a saving of 3.37%. The two values of gear ratios are practically identical to the ones optimizing the real mission energy consumption. So it can be asserted that the optimization on the mission doesn't have a negative impact on the type-approval cycle consumption.

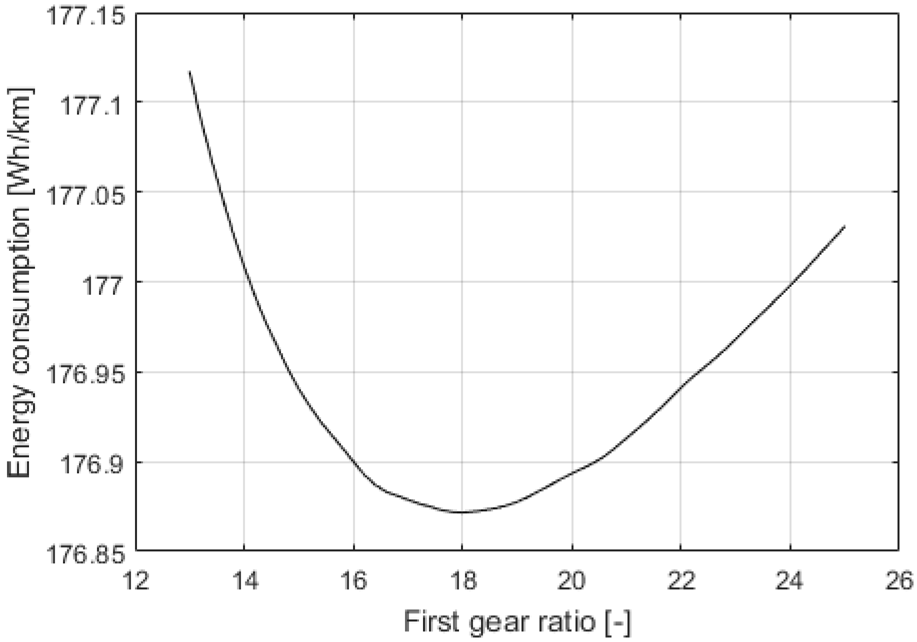

Figure 39. WLTC energy consumption for varying first gear ratio (second gear ratio fixed to $\tau_{t,2} = 9.6$)

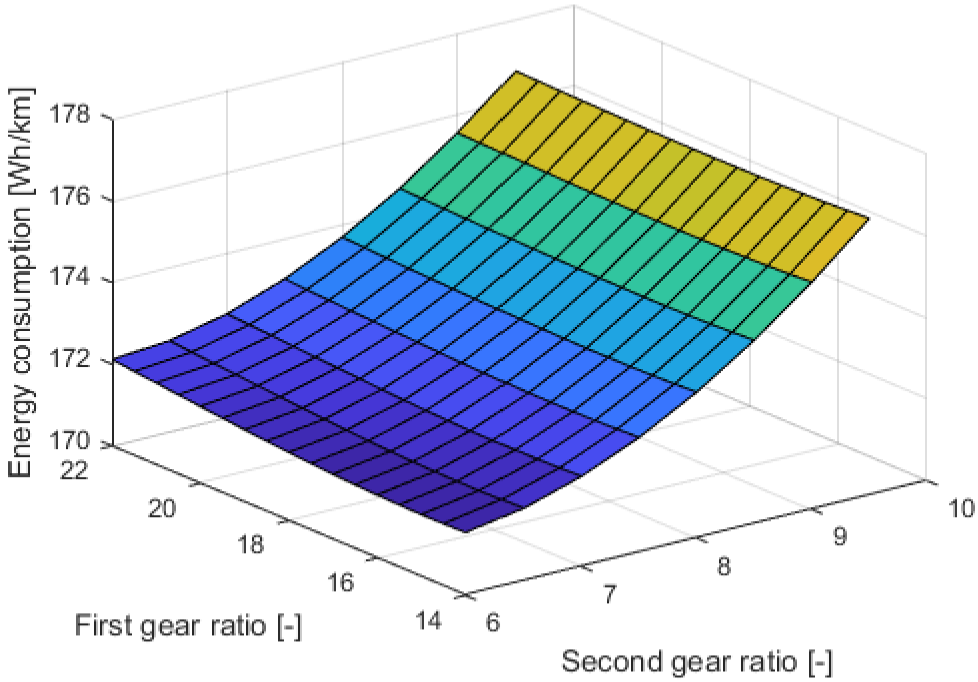

Figure 40. WLTC energy consumption for varying first and second gear ratios.

6. SIMULATION AND RESULTS ON THE REAL MISSION

6.1 INTRODUCTION

At this stage of the work the program is well tuned and is able to reproduce experimental results in terms of energy consumption on type-approval cycles, both in standard conditions and in cool-down / heat-up conditions. Moreover, optimal transmission parameters are available and ready to be tested on the cycles, both for the cases of single-speed and two-speed gearbox transmission.

Therefore the program is run on a mission made of 1000 cycles. The simulation times are reduced thanks to a number of actions on the Matlab® code. The program is able to give as output the evolution, for each cycle of the mission, of its main operating parameters.

A great increase in energy consumption with respect to standard type-approval conditions is registered. Therefore, an energetic analysis is conducted in order to understand which the conditions impacting the most on the final result are.

The program is then run with the optimized two-speed gearbox, in order to understand how the impact expected after the discussion in previous chapter translates in real-world conditions.

Finally, an analysis on what is the impact of the limit in charging of the battery is conducted. It will help to understand that its influence on the final energy consumption result is not negligible, in particular in the real-driving conditions, where decelerations are harder than on type-approval driving.

6.2 SIMULATION ON THE "REAL" MISSION

The software is run on the "real" mission, as defined in Chapter 3.11, made of 1000 cycles. The first run is conducted with the non-optimized single-speed transmission. The result in terms of energy consumption is

$$238\ Wh/km$$

which translates in a range (for a $24kWh$ battery) of $101\ km$. The vehicle has covered a distance of $8524\ km$ in about $283\ h$, with an average speed of about $30\ km/h$. The total energy required at the power grid is $1720\ kWh$.

6.2.1 SIMULATION OUTPUTS

For each cycle of the mission the software is able to give the evolution of the main operating parameters, such as the power at each point of the powertrain, the currents in the battery and its SOC, the power adsorbed by each auxiliary or accessory, the cumulated energy and covered distance, etc. As a reference, the results of the first cycle are shown: its conditions are the ones presented in Table 18.

CYCLE	LIGHTS	TEMPERATURE	NUMBER OF PASSENGERS	INITIAL SOC
AUDC	ON	$5.1°C$	3	52.84%

Table 18. Initial conditions of the first cycle of the realistic mission

The consumption in this particular cycle is $417\ Wh/km$.

In the following Figure 41÷Figure 44 the evolution of the main operating parameters.

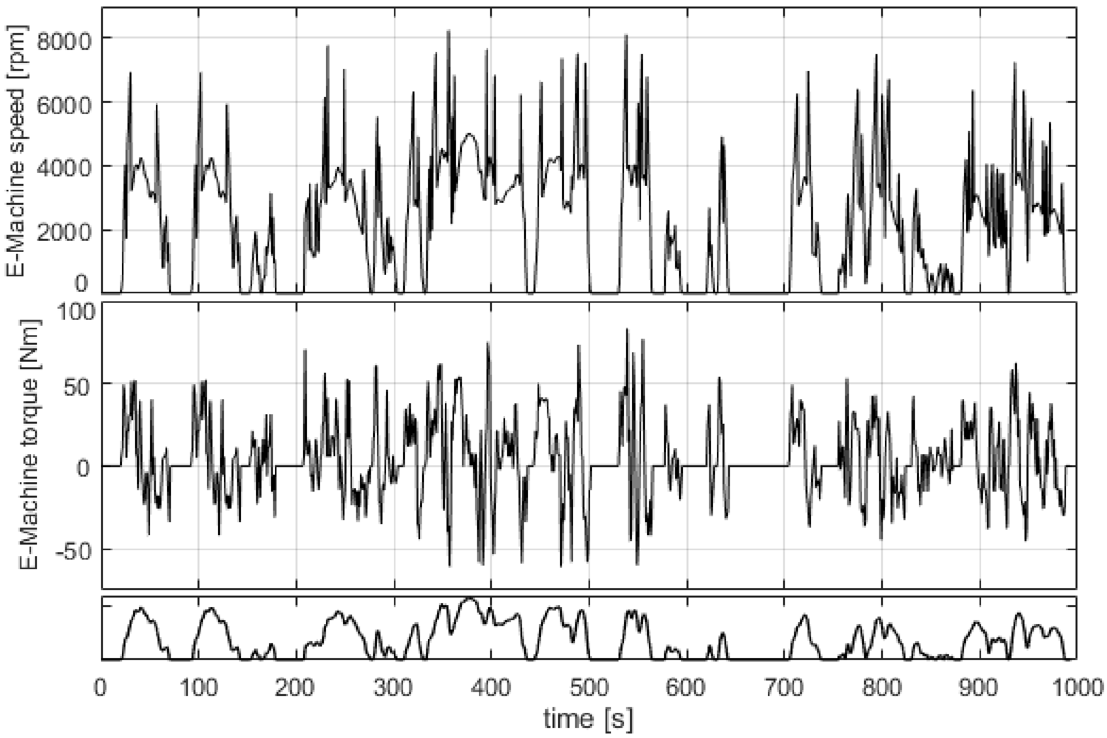

Figure 41. E-machine torque and speed evolution.

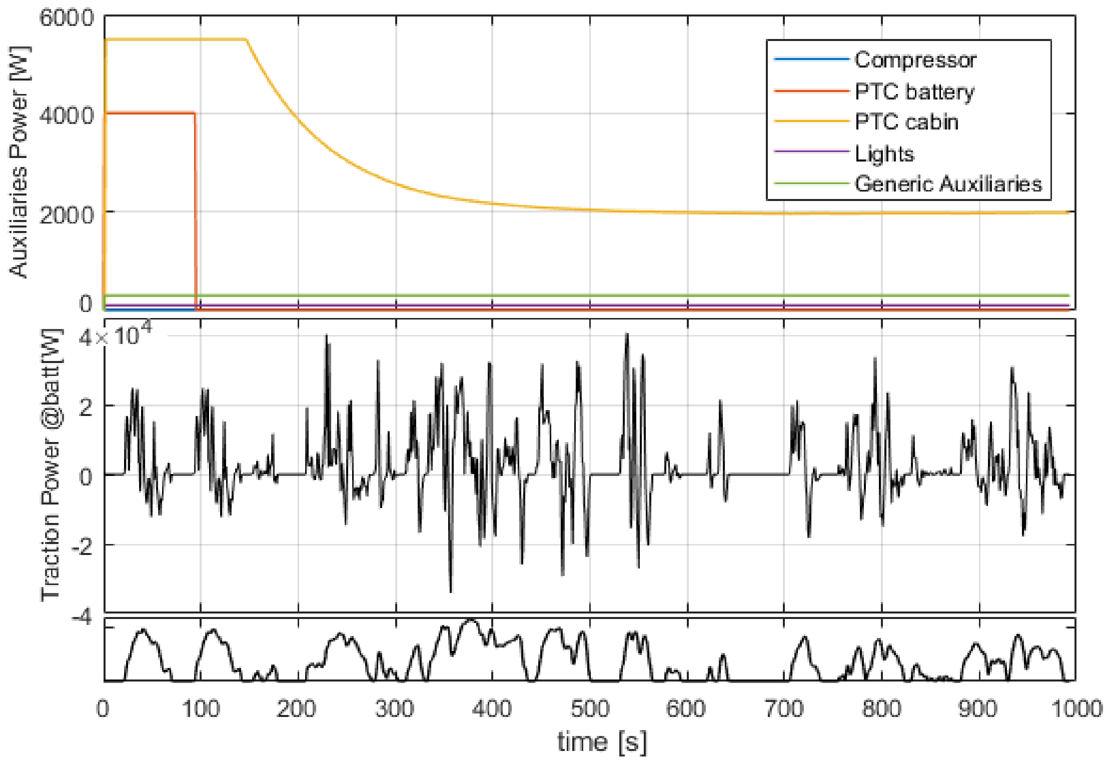

Figure 42. Auxiliaries and traction power evolution.

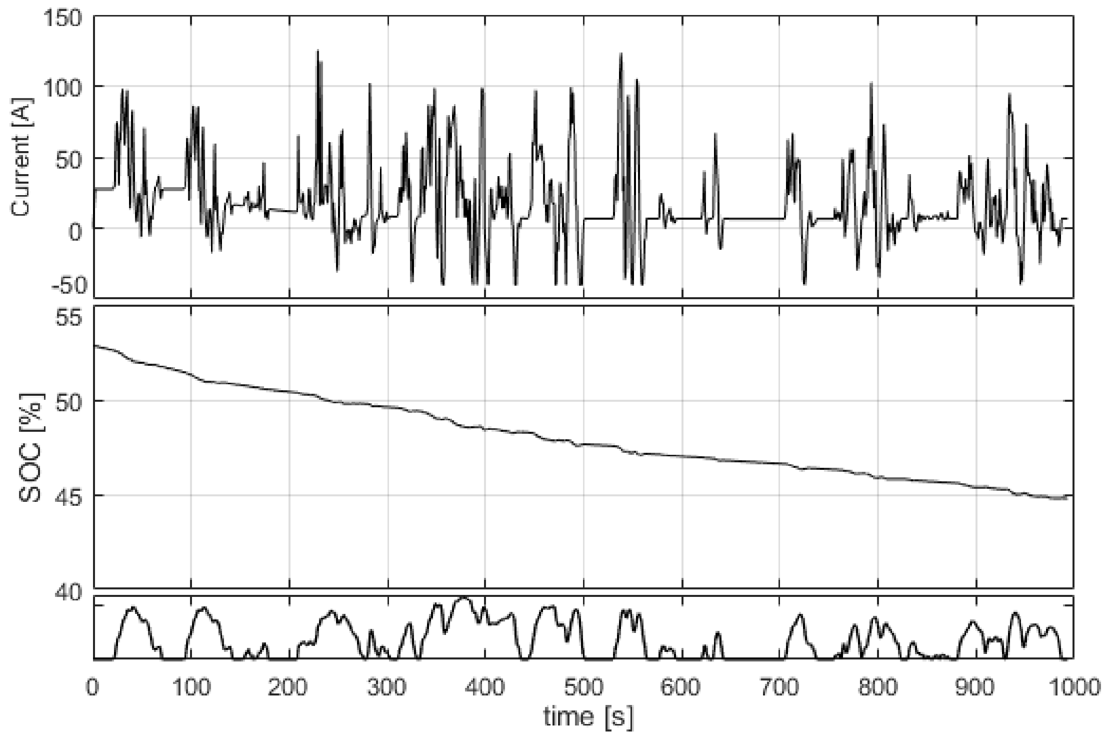

Figure 43. Current and SOC evolution.

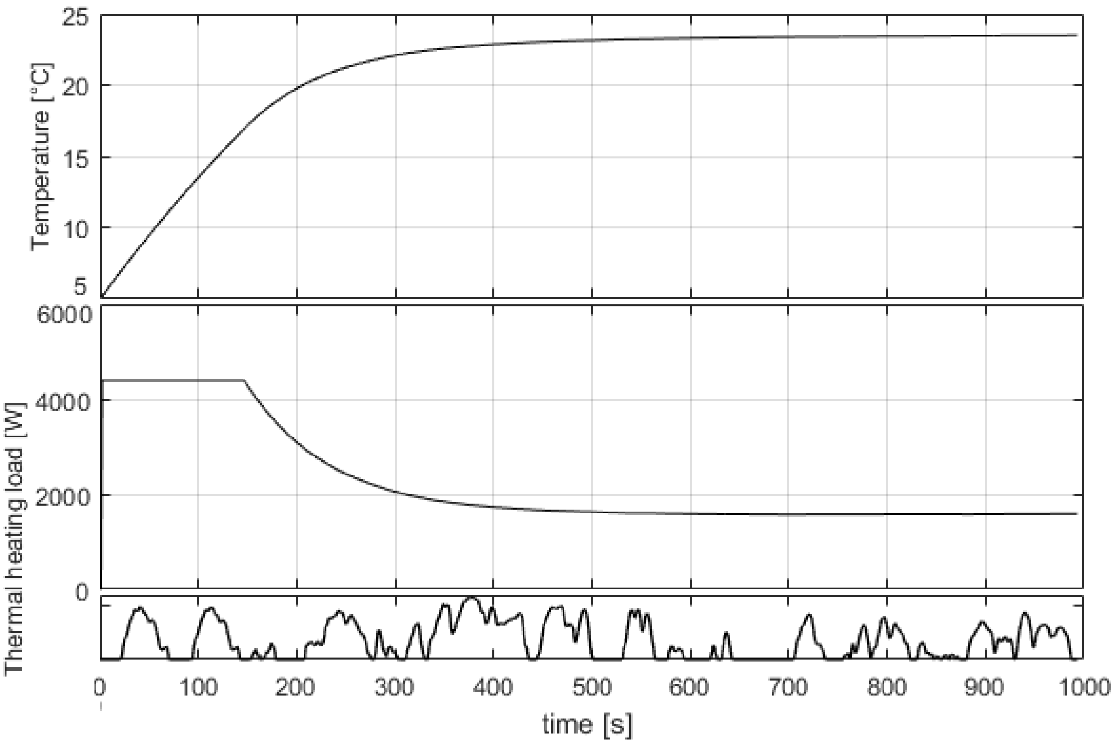

Figure 44. Cabin temperature and thermal heating load evolution.

6.2.2 OPTIMIZATION OF THE CODE

The program is based on a "`for`" loop which explores all the different cycles of the mission. Inside the loop, the initial conditions are read from a matrix which contains the information for each cycle of the mission. After the set-up of the corresponding initial conditions, the cycle is initialized. A second "`for`" loop will develop the kinematic analysis of the vehicle on the cycle and run the models for the auxiliaries. The total simulation cycle was found to be around $3000s$, with about two thirds of the time imputable to the "`interp2`" function, which is interpolating the 2D e-machine efficiency map in order to get the efficiency for each torque and speed condition.

However, the motor operating points positioning on the map depends just on two of the cycle characteristic, which are the cycle type (AUDC or ARDC) and the number of passengers (one, two or three). This means that there are only six possible operating points evolutions and, as a consequence, only six possible efficiencies evolutions. Therefore, those evolutions are simply calculated one time before running the program, so that the "`interp2`" function has only to be called for six cycles, and not for 1000. Then, the evolution corresponding to the cycle conditions of speed profile and number of passengers is simply recalled inside the cycle. The result in terms of simulation time is very good, since it goes down to around $900s$.

Last step is the possibility of make more processors, when available, work in parallel, using the "`parfor`" function. This doesn't allow saving all the parameters evolution of each cycle, since some of the cycles are run on a processor different from the one on which the program Workshop is running. However, the simulation time reduction is outstanding, allowing simulating all the 1000 cycles in only around $360s$. The times summaries generated by the program for each step of the code optimization are shown in Figure 45.

Profile Summary

Generated 19-Feb-2018 15:11:03 using performance time.

Function Name	Calls	Total Time	Self Time*	Total Time Plot (dark band = self time)
number1	1	2969.190 s	118.315 s	
interp2	1020768	1966.671 s	894.572 s	
interp1	2043536	876.401 s	716.765 s	
polyfun\private\compactgridformat	1020768	473.214 s	423.855 s	
polyfun\private\checkmonotonic	1020768	244.016 s	127.474 s	
interp2>makegriddedinterp	1020768	153.995 s	153.995 s	
interp1>reshapeAndSortXandV	2043536	119.198 s	77.148 s	
pol...te\checkmonotonic>makemonotonic	2041536	116.541 s	116.541 s	
polyfun\private\methodandextrapval	1020768	115.302 s	115.302 s	

Profile Summary

Generated 19-Feb-2018 17:16:15 using performance time.

Function Name	Calls	Total Time	Self Time*	Total Time Plot (dark band = self time)
number3	1	914.962 s	70.399 s	
interp1	2044426	826.787 s	684.338 s	
interp1>reshapeAndSortXandV	2044426	105.387 s	68.297 s	
interp1>reshapeValuesV	2044426	37.090 s	37.090 s	
interp1>parseinputs	2044426	37.062 s	37.062 s	
xlsread	9	17.734 s	0.147 s	
iofun\private\xlsreadCOM	9	16.493 s	2.247 s	
iofun\private\xlsreadCOM>segmentedRead	9	5.522 s	5.325 s	

Profile Summary

Generated 11-Mar-2018 10:54:28 using performance time.

Function Name	Calls	Total Time	Self Time*	Total Time Plot (dark band = self time)
number3mo1d	1	365.034 s	1.075 s	
parallel_function	1	356.103 s	0.238 s	
parallel_function>distributed_execution	1	295.767 s	0.036 s	
...>remoteparfor.getCompleteIntervals	5	295.620 s	0.381 s	
java.util.concurrent.LinkedBlockingQueue (Java method)	298	294.833 s	294.833 s	
...arfor>remoteparfor.tryRemoteParfor	1	59.760 s	0.015 s	
pctTryCreatePoolIfNecessary	1	59.745 s	0.061 s	
...rayManager.getOrAutoCreateWithCleanup	1	59.684 s	0.095 s	
parpool	1	52.817 s	0.057 s	

Figure 45. Optimization steps of the program code in terms of simulation times.

6.2.3 ENERGETIC ANALYSIS

Table 19 shows a comparison of the main performances results (energy consumption and range), with the ones obtained over the three main type-approval cycles in standard conditions.

CYCLE	ENERGY CONSUMPTION	$cons_{real}$ $/cons_{cycle}$	RANGE	$range_{real}$ $/range_{cycle}$
	$[Wh/km]$	$[-]$	$[km]$	$[-]$
MISSION	238	1 (REF)	101	1 (REF)
NEDC	152	1.56	158	0.64
FTP75	149	1.60	161	0.63
WLTC	177	1.35	135	0.75

Table 19. Comparison between results on mission and type-approval conditions.

All the type approval cycles consumptions are lower with respect to the one obtained on the real mission. In particular, real driving consumption is around 60% higher than the one calculated over NEDC and FTP75. WLTC is more demanding, as observed in Chapter 3.11, but real driving consumption is still 35% higher than the one on this cycle. The increase in energy consumption is not only due to the more demanding cycles adopted, but also to the other variables that the mission has introduced and to the usage of auxiliaries and accessories. The temperature will be the main parameter impacting on the consumption: this is assessed with an analysis of the percentage of energy consumed over the total consumption in three different conditions:

- COLD, in the range $T_{amb} < 10°C$, which is the working range of the battery and cabin heaters;
- INTERMEDIATE, in the range $10°C < T_{amb} < 25°C$, in which no auxiliaries except generic ones are used;
- HOT, in the range $T_{amb} > 25°C$, in which air conditioning is on.

Figure 46 reports the percentage of occurrence of each of these conditions and the relative percentage of energy related to the cycles. Figure 47 shows instead the average consumption in each of those conditions and compares it with the average consumption on the whole mission.

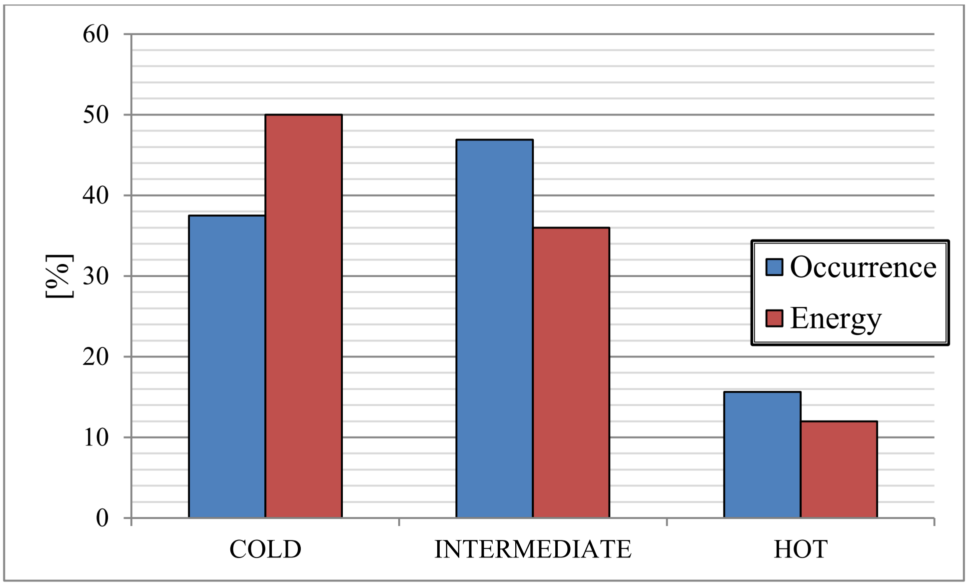

Figure 46. Occurrence and energy distribution for cold, intermediate and hot conditions.

Even if the intermediate condition occurs the most, 47% of the times, it has only a minor impact on the consumption, since the related energy is only 37% of the total. Cold condition is by far the largest contribute to the total energy, with a share of 51% compared to 37% of occurrence. Finally, hot condition impact is 13% with an occurrence of 16%.

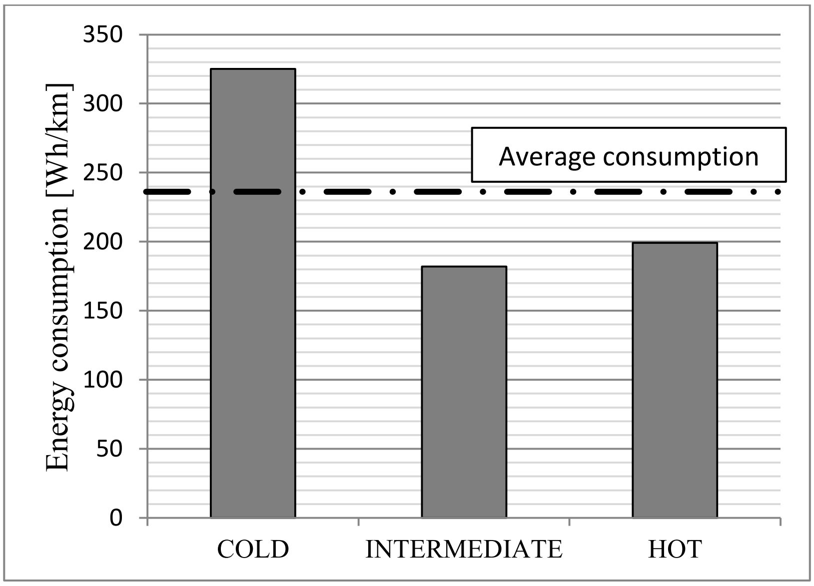

Figure 47. Average consumption on cold, intermediate and hot conditions.

Translating the numbers from energy to energy consumption, the scenario is even clearer. The average energy consumption in intermediate conditions is $182\ Wh/km$, while in hot conditions it jumps to $199\ Wh/km$. However the worst case is the one in cold conditions, where the average energy consumption is $325\ Wh/km$. Figure 48 shows the same results in terms of average ranges in the three conditions. Cold condition is critical, leading to an average range of only $73.84\ km$. These results are not unexpected, since already in Chapter 4.3 the effect of temperature on the driving cycles led to similar results.

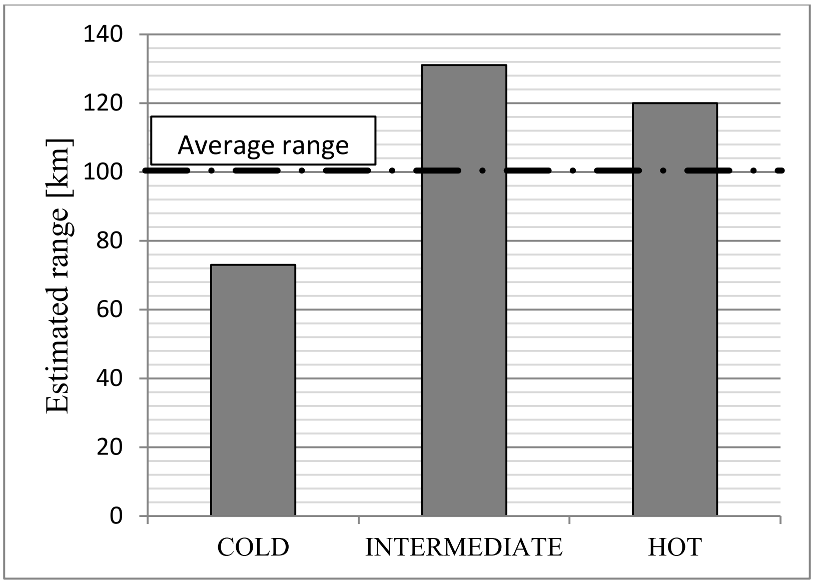

Figure 48. Average range for cold, intermediate and hot conditions.

6.3 SIMULATION WITH TWO-SPEED GEARBOX

The simulation is run with the two-speed gearbox following the analysis of Chapter 5, so with gear ratios $\tau_{t,1} \approx 22.50$ and $\tau_{t,2} \approx 9.6$. The result is

$$234\ Wh/km$$

which compared to the $238\ Wh/km$ obtained with the single-speed transmission, leads to an energy saving of 1.83%, as shown in Figure 49. The extra range that can be provided is $2km$ since we pass from $101km$ to $103\ km$.

The benefit is not as pronounced as it was when optimizing considering only the cycles because in this case there's the contribution of the auxiliaries, which is independent from the final drive ratio, to both the cases of gearbox / no gearbox. Then an increase in efficiency of the e-machine has a lower impact.

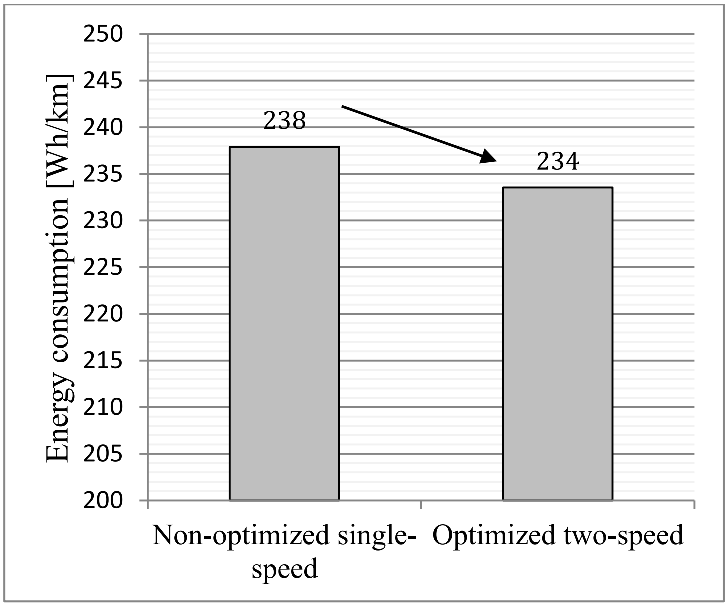

Figure 49. Energy consumption saving adopting an optimized two-speed gearbox.

6.4 BATTERY LIMIT IN RECHARGING

As already exposed in Chapter 3.7, the battery has a limit in charging which could potentially cut off the current coming from regenerative braking, reducing the BEV efficiency. As an example, Figure 50 shows the current[16] provided by the battery when running on NEDC, while Figure 51 highlights the cutting area.

[16] The current is normalized with respect to the maximum current that the battery can handle safely in charging

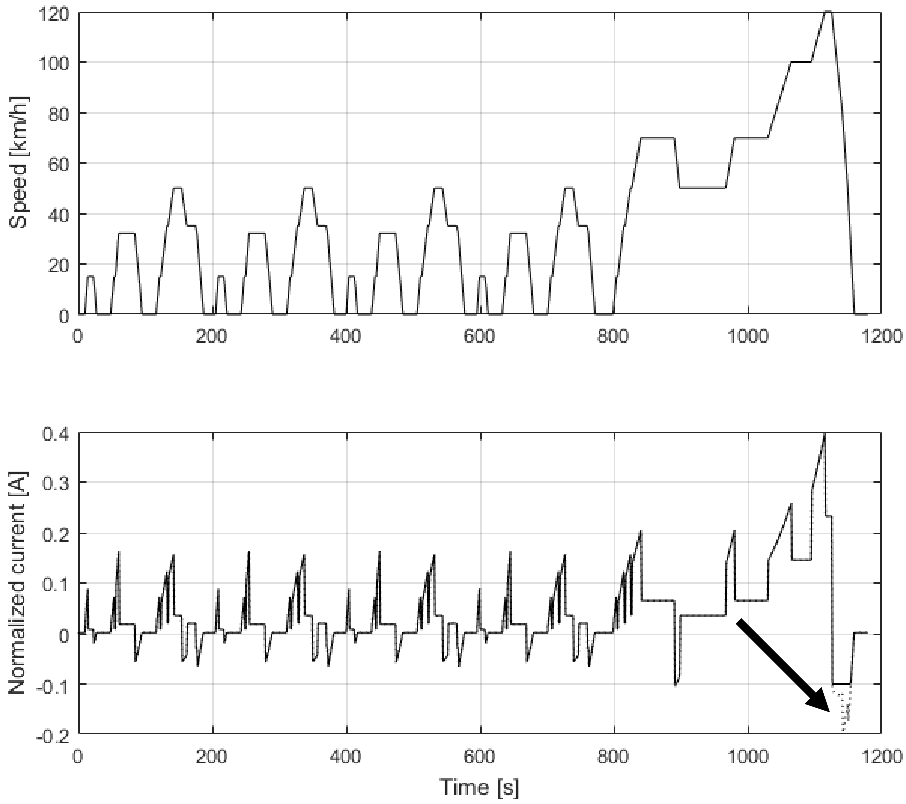

Figure 50. NEDC current exchanged by the battery.

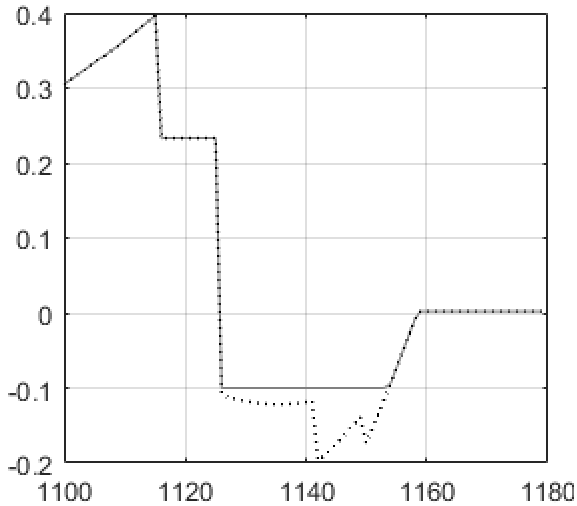

Figure 51. Highlight of cut recharging current on NEDC.

A sensitivity analysis of the energy consumption with respect to the value of this limit is conducted, in order to understand which the impact of the parameter is. In particular, the analysis is conducted on all type approval cycles, on AUDC and ARDC cycles and on the realistic mission. Results are presented in Table 20. All values are in Wh/km, while the differences are referred to the non-optimized single-speed transmission case.

	NEDC	FTP75	WLTC	AUDC	ARDC	MISSION
NORMAL LIMIT	152	149	177	198	162	238
	+0% (REF)	+0% (REF)	+0% (REF)	+0% (REF)	+0% (REF)	+0% (REF)
+33% LIMIT	150	146	175	192	159	234
	-1.43%	-1.91%	-1.20%	-3.18%	-1.98%	-1.67%
+66% LIMIT	149	145	174	189	157	232
	-2.03%	-2.44%	-1.73%	-4.76%	-3.36%	-2.65%
+100% LIMIT	149	145	174	187	155	230
	-2.23%	-2.50%	-1.95%	-5.49%	-4.19%	-3.18%
NO LIMIT	149	145	174	186	153	228
	-2.24%	-2.50%	-1.99%	-5.94%	-5.85%	-3.98%

Table 20. Influence of the battery limit in charging on different driving cycles and on the mission.

The main results are those referred to the WLTP cycle and to the mission, since the first one is important for homologation reasons, while the second gives information about real-world driving conditions. For what concerns the type-approval cycle, the impact is not too strong, with a maximum energy saving in the order of 2% when no limit in charging to the battery is applied. This translates in an additional range of around 3 km. For what concerns the mission, instead, being the Arthemis cycles more dynamic, the limit increase has a stronger impact, with possible savings up to 6% both for AUDC and ARDC. However the maximum energy saving on the mission, obtained when no limit to the current in recharging is applied, is only of 3.98%. In particular, in this condition, the range would increase of 4 km with respect to the initial one. The greater savings on AUDC and ARDC do not transpose fully on the mission due to the presence of auxiliaries, whose energy consumption is independent from the limit in charging.

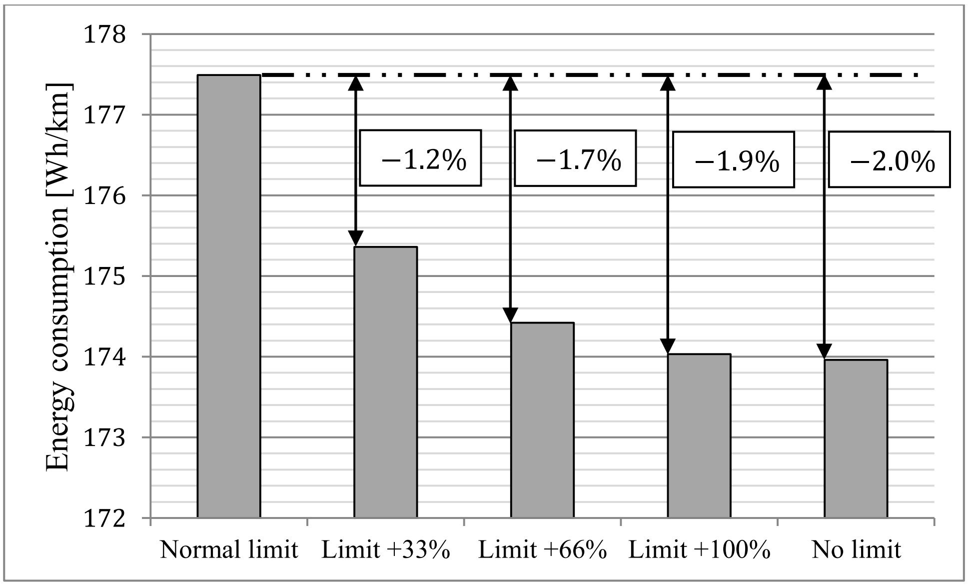

Figure 52. Influence of battery limit in charging on energy consumption on WLTC.

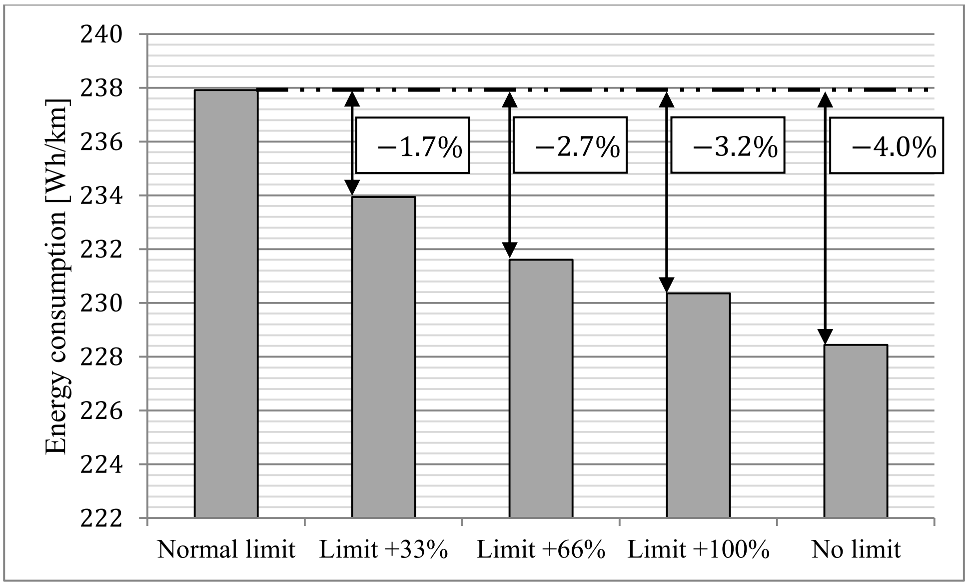

Figure 53. Influence of battery limit in charging on energy consumption on the mission.

CONCLUSIONS

The work has highlighted that the electric range of the vehicle is strongly related to the environment conditions that affect the performances of the auxiliaries systems for the passengers comfort.

It has been demonstrated that cold condition is the most critical one for a low-segment Battery Electric Vehicle, especially when equipping a cabin heater based on PTC resistor technology, with the estimated range of the vehicle that could easily be halved.

Considering an annual mission, the vehicle autonomy can have an important reduction, from 25% up to 40%, with respect to the values achievable in standard type-approval.

Also, the impact of an optimization of the transmission, either single-speed or equipping a two-speed gearbox, has been shown to be contained for type-approval cycles (-3.4% on WLTC) and almost negligible for real-driving (-1.8%). Similar considerations can be made for the sensitivity analysis on the battery limit in recharging, whose maximum saving in real-driving is contained (-4%).

On the basis of the analysis carried out it is evident that, for this typology of low segment BEV, it’s more important focusing on the vehicle energy management optimization than on the powertrain configuration.

The potentiality of the MATLAB® code developed in the thesis, based on simplified models of a Battery Electric Vehicle, has allowed to produce energy consumption results that match the experimental ones, with very low simulation times.

This makes this type of program, once tuned, a very powerful tool for at least two reasons: first of all, it can show criticalities of the vehicle system and of its components; secondly, a number of analyses can be carried out in order to optimize a component or to check the sensitivity of the entire system on the component. Most importantly, all of this can be done in an acceptable amount of time.

The range of still unexplored possibilities for this code is large. Just to name a few: sensitivity analysis to the motor size and type, sensitivity analysis to the efficiency of the air conditioning system, evaluation of the adoption of a heat-pump for heating, integration of a detailed thermal model of the battery and of its conditioning system. Moreover, cost models could be added in order to get the initial cost of each vehicle configuration and the operating cost of the vehicle when running on the mission.

LIST OF FIGURES

LIST OF TABLES

BIBLIOGRAPHY

[1] *"EV Auxiliary Systems Impacts", Advanced Vehicle Testing Activity, INL*

[2] *Notes of the course "Electric and Hybrid Propulsion Systems" by prof. Vittorio Ravello, a.y. 2016/2017*

[3] *"Modern Electric, Hybrid Electric and Fuel Cell Vehicles", M. Ehsani, Y. Gao, A. Emadi, CRC Press, 2010*

[4] *"Uno sguardo all'aria", ARPA Piemonte, 2016*

[5] *"Too low to be true? How to measure fuel consumption and* CO_2 *emission of plug-in hybrid vehicles, today and in the future", I. Riemersma, P. Mock, ICCT, 2017*

[6] *"Passenger Vehicle Technology: U.S. CAFE and GHG standards", J. German, ICCT, 2014*

[7] *"Measurement of noise from electrical vehicles and internal combustion engine vehicles under urban driving conditions", L.M. Iversen, COMPETT*

[8] *"2012 DOW Vehicle Technologies Program Review", N. Karditsas, Cobasys, 2012*

[9] *"Lithium-ion Battery Costs and Market", C. Curry, Bloomberg New Energy Finance, 2017*

[10] *https://electrek.co/2016/04/26/tesla-model-3-battery-pack-cost-kwh/*

[11] *"Electrifying insights: How automakers can drive electrified vehicle sales and profitability", McKinsey&Company, 2017*

[12] *http://www.lithiummine.com/lithium-mining-and-environmental-impact*

[13] *"Motor Vehicle Dynamics: modeling and simulation", G. Genta, World Scientific Publishing, 1997*

[14] *"Evaluation of thermal conditions inside a vehicle cabin", T. Orzechowski, Z. Skrobacki, EDP Sciences, 2016*

[15] *"Comprehensive Modeling of Vehicle Air Conditioning Loads Using Heat Balance Method", M.A. Fayazbakhsh, M. Bahrami, SAE International, 2013*

[16] *"The development and validation of a thermal model for the cabin of a vehicle", D. Marcos et al., Applied Thermal Engineering, 2014*

[17] *"Cooling Load Calculation and Thermal Modeling for Vehicle by MATLAB", O. Abdulsalam, B. Santoso, D. Aries, International Journal of Innovative Research in Science Engineering and Technology, 2015*

[18] *"A Novel Concept of Air-Conditioner-Integrated Electric Vehicle for the Future Smart Community", T. Nakagawa, Y. Notoji, S. Shibata, Heat Transfer Engineering, 2016*

[19] *"Thermodynamical Modeling of a Car Cabin", L. Moller, L. Sorensen, Chalmers University of Technology, 2011*

[20] *"ASHRAE Handbook – Fundamentals", Different authors, 2017*

[21] *"Impact of Vehicle Air-Conditioning on Fuel Economy, Tailpipe Emissions, and Electric Vehicle Range", R. Farrington, J. Rugh, National Renewable Energy Laboratory, 2000*

[22] *"LEDs and Power Consumption of Exterior Automotive Lighting: Implications for Gasoline and Electric Vehicles", B. Schoettle, M. Sivak, Y. Fujiyama, UMTRI, 2008*

ACKNOWLEDGMENTS

I would like to thank all the people who allowed this project to be developed and who followed each step of the same. In particular, I would like to mention Ing. Alessandro Piu and Ing. Diego Caporali, whose professional guidance was essential in order to work on the right rails towards the final goal.

Also, I would like to thank all my loved ones, my family and friends, who supported me during these years, encouraged me when it was needed and celebrated with me in good moments.

"Whatever you do in this life, it's not legendary,
unless your friends are there to see it."